Positron Emission Tomography in colorectal cancer using 3'-[18F] Fluoro-3'-deoxythymidine: a clinical and biological study

A thesis submitted to the University of London for the Degree of Doctor of Medicine

by

Daren Leslie Francis MBBS, FRCS

March 2004

Institute of Nuclear Medicine and Department of Surgery
Royal Free and University College Medical School

University of London

UMI Number: U602785

UMI U602785

Abstract

The success of Positron Emmission Tomography (PET) in oncological imaging is based on the fact that malignancy leads to an alteration in cellular biochemical reactions. PET tracers, used for detecting malignancies, are synthetic positron emitting analogues of molecules involved in these metabolic processes. The recent development of the thymidine analogue [^{18}F]3'-deoxy-3'-fluorothymidine (FLT) targets the salvage pathway of DNA synthesis and it is thought to have the potential to visualise cellular proliferation.

The aim of this thesis was to investigate the potential clinical use of FLT in colorectal cancer (CRC).

FLT pharmacokinetics in patients with CRC were mapped, and methodologies for the quantitative analysis of *in vivo* FLT uptake were defined; subsequently the accuracy of semi-quantitative indices (SUVs) was assessed. FLT uptake was compared to that of the established glucose analogue radiotracer [^{18}F]fluoro-2-deoxy-D-glucose FDG (calculated using SUVs), in patients with primary and/or metastatic disease. Both FLT and FDG were compared with Ki67 immunohistochemistry in the same patients to determine whether PET can quantify cellular proliferation *in vivo*. FLT was also used to assess response to cytotoxic drug treatment 5-Fluorouracil (5FU) in cultured CRC cells.

Semi-quantitation in the form of SUVs allowed an accurate interpretation of the uptake rate of the tracer. FLT PET provides acceptable imaging of primary colorectal tumours, but there are inherent difficulties in diagnosing the presence of liver metastases, secondary to the hepatic metabolism of the tracer. There was excellent correlation between FLT SUVs and Ki67 immunohistochemistry (R=0.8), which can be interpreted as a true reflection of the proliferative rate of colorectal cancer tissue. *In vitro*, cell killing caused by exposure to 5FU resulted in increased FLT uptake, with excellent correlation (R = 0.9).

FLT PET could in the future contribute to a non-invasive method of *in vivo* grading of malignancy and be used to predict early response to adjuvant chemotherapy.

Contents

Chapter 1
Introduction

Chapter 2
General materials and methods

Chapter 3
Characterisation of *in vivo* FLT uptake in colorectal cancer

Chapter 4
Potential clinical role of FLT in imaging colorectal cancer

Chapter 5
Quantifying cellular proliferation in colorectal cancer: a comparison of FDG and FLT PET with immunohistochemistry

Chapter 6
Monitoring response to 5-Fluorouracil chemotherapy *in vitro* using FLT

Chapter 7

Conclusion

Appendices and bibliography

Statement of originality

I hereby declare that the studies described and presented in this thesis are the original work of the author. This work has led to the publication of original papers which are listed in Appendix J (Publications arising from thesis).

Image reconstruction was performed by qualified radiographers at the Institute of Nuclear Medicine. Radiochemical HPLC analysis was performed by the radiochemist at the Institute of Nuclear Medicine and the Kinetic modelling using JAVA based software PMOD (Biomedical Image Quantification & Kinetic Modelling software) was carried out by a physicist. MIB-1 Immunohistochemical staining was performed with the help of the technicians in the immunocytochemistry laboratory at University College London Hospital.

All clinical studies in this thesis were performed in accordance with protocols approved by the Ethics Committees of University College London and University College London Hospitals NHS Trust, after obtaining informed patient consent.

This thesis has not been submitted to any other university for consideration for a higher degree.

Daren Francis 2004

Acknowledgements

List of figures

List of tables

List of abbreviations

AA	Abdominal aorta
ACF	Aberrant crypt foci
AJCC	American Joint Committee on Cancer
APC	Adenomatous polyposis coli
ARSAC	Administration of Radioactive substances
CDKs	Cyclin-dependant kinases
CLM	Colorectal liver metastases
CRC	Colorectal cancer
CT	Computerised Tomography
DAR	Differential absorption ratio
DCBE	Double contrast barium enema
DMEM	Dulbecco's modified eagles medium
DMSO	Dimethyl sulfoxide
DNA	Deoxyribose nucleic acid
dTDP	Deoxythymidine diphosphate
dTMP	Thymidine monophosphate
dTTP	Deoxythymidine triphosphate
dUMP	Deoxyuridine monophosphate
DUR	Differential uptake ratio
EDTA	Ethylenediamine tetracetate
EGF	External growth factors
EORTC	European Organisation for the Research and Treatment of Cancer
FAP	Familial adenomatous polyposis
FCS	Foetal calf serum
FDG	$[^{18}F]$ fluoro-2-deoxy-D-glucose
FLT	$[^{18}F]$3'-deoxy-3'-fluorothymidine.
FLTMP	FLT monophosphate
5-FdUMP	5-Fluorodeoxyuridine monophosphate
5FU	5-Fluorouracil
5-FUTP	5-Fluorouridine triphosphate
GLUT	Glucose transporter protein
^{3}H-Tdr	Tritiated thymidine
H&E	Haematoxylin and Eosin
HCL	Hydrochloric acid
HIV	Human immunodeficiency virus
HNPCC	Hereditary non-polyposis colorectal cancer
HPLC	High performance lquid chromatography
LI	Labelling Index
MDT	Multidisciplinary team
MRI	Magnetic Resonance Imaging
MSI	Microsatellite Instability
NICE	National Institute for Clinical Excellence
NLR	Non linear regression
NPV	Negative predictive value

PBS	Phosphate buffered saline
PET	Positron Emission Tomography.
PPV	Positive predictive value
ROI	Region of interest
SD	Standard deviation
SUV	Standardised uptake value
TA	Thoracic aorta
TAC	Time activity curve
TBS	Tris buffered saline
TK	Thymidine Kinase
TNM	Tumour, Nodes, Metastases
TS	Thymidylate Synthase
UCL	University College London
UCLH	University College London Hospitals
UICC	Union Internationale Contre le Cancer
UTP	Uridine triphosphate

CHAPTER 1

Introduction

1.1 Colorectal cancer

1.1.1 Impact on deaths in the United Kingdom

Life expectancy at birth in the UK increased during the last century from 48.5yrs to 75.5yrs for men and 52.4yrs to 80.3yrs for women. When UK government used broadly defined causes of death and published the mortality data for the calendar year 1998, the leading cause of mortality, accounting for 40.8% of deaths, was circulatory disease, with neoplasms accounting for 24.9%, respiratory diseases 16.4%, digestive diseases 3.8% and others 14.1%.

More than one in three people in England will develop cancer at some stage in their lives. One in four will die of cancer. This means that, every year, over 200,000 people are diagnosed with cancer, and around 120,000 people die from the disease (Office of National Statistics, Mortality Statistics: cause, England and Wales 2000). In the UK, as treatment of ischaemic heart disease improves and the general population ages, trends show that cancer will become the leading cause of death within the next 10 years.

The most common cancer for men in terms of mortality is lung cancer followed by prostate cancer and colorectal cancer, and for women is lung cancer followed by breast cancer and colorectal cancer. Lung cancer is the cancer most commonly associated with smoking with over 80% of all lung cancer deaths caused by smoking (The UK Smoking Epidemic: Deaths in 1995. Health Education Authority, 1998). It follows that for non-smokers, considering both sexes, colorectal cancer (CRC) is the leading cause of cancer death in the UK.

1.1.2 Aetiology

CRC arises following the accumulation of multiple mutations within the cell, which allow it to escape the growth regulatory control mechanisms and acquire characteristics which allow invasion. It is well established that a high proportion of CRC arise from pre-existing benign adenomatous polyps. Work by Muto et al in 1975 first established the progression from adenoma to carcinoma and suggested that cancers overtake adenomatous tissue as they invade the bowel wall (Muto et al., 1975). A model describing the specific genetic changes occurring during the colorectal adenoma carcinoma development was originally described by Fearon and Vogelstein (Fearon and Vogelstein, 1990; Vogelstein et al., 1988). This model known as the "Vogelgram" is illustrated in figure 1.1. It demonstrates the cumulative effect of either loss of genes suppressing growth or mutational overexpression of genes promoting growth, leading to the development of cancer.
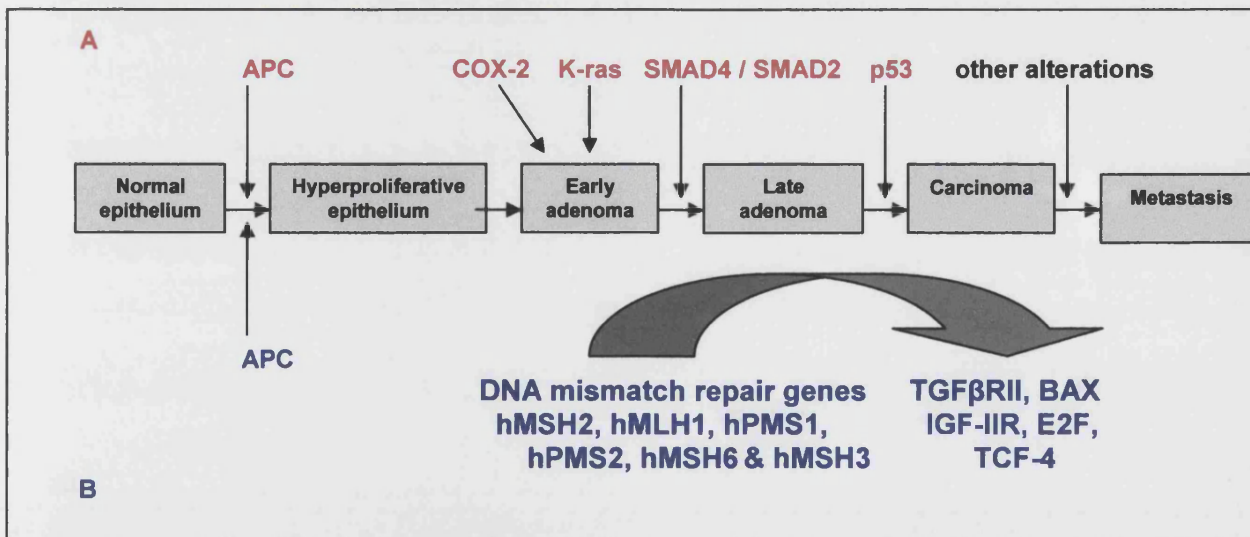
Figure 1.1 Diagram of the key genetic events in colorectal cancer tumourigenesis. Two major pathways are currently accepted: **A** and **B**. The genetic events of the traditional adenoma-carcinoma sequence, which 85% of tumours follow, are illustrated in **A** (Vogelgram). The remaining 15% of tumours follow path **B** and exhibit microsatellite instability due to an alteration in a DNA mismatch repair gene. *APC = adenomatous polyposis coli, tumour suppressor gene; COX-2 = Cyclo-oxygenase-2; K-ras = oncogene; SMAD 4/2 =*

signaling molecules in the anti-proliferative TGF-β pathway; p53 = tumour suppressor gene; TGFβRII = transforming growth factor-β receptor class II; BAX = apoptosis regulator molecule; IGF-IIR= insulin-like growth factor receptor class II; E2F = cell cycle regulated transcription factor; TCF-4 = T-cell factor 4, transcription factor.

i) Familial adenomatous polyposis

Earlier work into Familial Adenomatous Polyposis (FAP) an inherited syndrome in which hundreds of colorectal adenomas develop and colorectal cancer is inevitable, localised a gene on chromosome 5q21-22 responsible for the syndrome (Bodmer et al., 1987). Vogelstein proposed that alterations in this gene caused hyperproliferation preceding adenoma formation. He hypothesised that allelic loss at chromosome 5q was enough to produce hyperproliferation which when associated with alteration of a second gene is enough to initiate sporadic adenomas. In 1991 this gene became characterised and is known as the APC (adenomatous polyposis coli) gene (Kinzler et al., 1991).

The vast majority of sporadic colorectal cancers are thought to be initiated by changes in the APC gene and, together with FAP cancers, accumulate the genetic changes shown in the Vogelgram which result in the adenoma-carcinoma progression.

ii) Hereditary non –polyposis colorectal cancer and microsatellite instability

Hereditary non-polyposis colorectal cancer (HNPCC) is a syndrome characterised by the lack of colonic polyposis. It was identified following work by Lynch into families presenting with colonic adenomas at an early age without the presence of multiple colonic adenomas (Lynch et al., 1966; Lynch and Krush, 1971). In 1993 colorectal cancers from patients with HNPCC and a subset of sporadically occurring disease were noted to have a unique type of genetic abnormality, first known as replication errors and subsequently as

microsatellite instability (MSI). Microsatellites are short segments of repetitive DNA bases that are scattered throughout the genome. MSI is defined as "a change of any length due to either insertions or deletions of repeating units in a microsatellite within a tumour compared to normal tissue" (Boland et al., 1998) and results from a failure of the cell to repair errors made during DNA replication. When a group of intranuclear proteins known as the mismatch repair system-which is responsible for removing these errors-fails, then MSI develops and genes with a lot of microsatellites are particulary susceptable to alteration.

Cancers demonstrating MSI develop using an alternative genetic pathway to that described by Vogelstein and this is reflected in the clinical presentation of the tumour.

HNPCC and sporadically occurring CRC have similar histological features and show a tendency to present on the right hand side of the colon, with approximately two thirds of HNPCC being detected proximal to the splenic flexure.

iii) Enviromental factors

External factors are contributory to colorectal tumourigenesis. This is demonstrated by migrant studies showing varying incidence of this disease around the world. Wynder et al highlighted a higher incidence of colon cancer in second generation Japanese immigrants to California and Hawaii than Japanese in Japan (Wynder and Reddy, 1974).

Increseased intake of dietary fibre was previously thought to be associated with lower rates of CRC as demonstrated by Howe et al in a meta analysis of 13 studies (Howe et al., 1992). Although contradictory evidence is now emerging from recent studies by Fuchs, Alberts, Schatzkin and their colleagues, which have shown no benefit or protective

effect from dietary fibre (Alberts et al., 2000; Fuchs et al., 1999; Schatzkin et al., 2000). There is currently no explanation to this discrepancy.

Other contributory factors have been thought to be associated with vitamin intake. Dietary supplementation of folic acid has been shown to be associated with the reduction of rectal mucosal proliferation indices in patients with adenomas (Khosraviani et al., 2002). Evidence also exists that red meat has the potential to be a definite risk factor (Potter, 1999) in addition to a high body mass index in the presence of low levels of physical activity (Slattery et al., 1997) and increased alcohol intake (summarised in Potter 1999 #462).

Recent developments have highlighted the potential of non-dietary chemo protective agents. The findings of polyp regression associated with non-steroidal anti inflammatory drug (NSAID) ingestion in patients with FAP (Giardiello et al., 1993; Labayle et al., 1991) led to theories regarding an increase in cell death mediated through inhibition of the enzyme cyclooxygenase (COX) (Piazza et al., 1995). Further work has demonstrated that lack of the COX-2 isoform in mice corresponded to a reduction in tumours (Williams et al., 1999). The overexpression of this enzyme in human CRC tissue has led to suggestions that the inhibition of COX-2 may lead to the retardation of colon cancer development (Sano et al., 1995).

1.2 Staging of colorectal cancer

1.2.1 Background

Once a tumour becomes invasive, it can extend through the layers of the colonic wall and invade adjacent structures. Lymphatic, haematogenous and peritoneal spread may also occur. The disease process is staged both clinically and pathologically. The stage of the disease at presentation may be a reflection not only of the rate of growth and extension of the tumour but also of the type of tumour and the tumour host relationship. International agreement on a system of classification is needed in order that groups of patients can be compared. It also serves to aid in the selection of primary and adjuvant therapy, estimation of prognosis, assistance in the evaluation of the results of treatment, facilitation of exchange of information and contribution to the continuing investigation of CRC (American Joint Commmittee on Cancer, 2002).

1.2.2 Clinical staging

This assessment is based on a full history and physical examination with either sigmoidoscopy or colonoscopy with biopsy. The presence of extra colonic metastases is demonstrated using radiological techniques such as chest x-ray, ultrasound, computerised tomography (CT), magnetic resonance imaging (MRI), in addition to Positron Emission Tomography.

1.2.3 Radiological staging

There has been dramatic evolution in the radiology of CRC over the past twenty years. In the 1980's CRC was diagnosed using Barium enema and its liver metastases

were visualised with ultrasound and incremental CT. Now there is a definite difference in the imaging approach. This section addresses the conventional imaging modalities excluding Positron Emission Tomography.

i) Barium enema

The malignant potential of a polyp is estimated using four determinants; size, presence or absence of a stalk, architecture and cellular atypia. Barium enema examination is capable of determining the first three and therefore detects both adenomas and carcinomas. Obviously the fourth cannot be assessed.

Two types of examination exist; single and double contrast barium enema (DCBE) the latter being more appropriate in those individuals who are physically able to co-operate, and also have a high probability of colonic disease. DCBE has been shown to depict polyps less than 1cm in size better than the single contrast technique (Gelfand, 1997; Smith, 1997). The reported sensitivities for CRC are between 62 -100% (de Zwart et al., 2001; Ott, 2000). Barium enema is a technique which examines the entire colon, a useful adjunct when it is used as a screening tool considering that 5% of patients have a synchronous tumour and more than one third have additional polyps (Levine et al., 2000).

ii) Ultrasound

Transabdominal U/S is generally not used for the detection of primary CRC although it has had a role in the detection of colorectal liver metastases. Trans rectal ultrasound does have an established role in the staging of rectal cancer as it can distinguish between the various layers of the rectal wall (Heriot et al., 1999; Rifkin et al.,

1989). This allows attempts at T staging as described in section 1.2.3 with reported accuracies of between 67-93% (Beynon, 1989)

iii) Magnetic resonance imaging (MRI)

MRI is most useful in CRC located in the rectosigmoid, because image quality is only minimally degraded by respiratory motion and peristalsis in this relatively fixed part of the colon.

MRI used to be acquired using a body or external surface coil but more recently endoluminal or phased array coils are used. The images created with endoluminal coils allow detailed visualisation of both tumour and rectal wall courtesy of the high resolution, although because of the limited field of view it is difficult to evaluate the mesorectum and surrounding pelvic structures. Phased array coils allow a larger field of view to be imaged although spatial resolution is lost.

The superior demonstration of rectal wall layers achieved by endoluminal MRI does not improve staging accuracy of rectal cancer compared with phased array MRI (Blomqvist et al., 1997). Beets-Tan and colleagues found that the clinically more important circumferential resection margin in rectal (section 1.3.2) can be predicted very accurately and consistently with phased array MRI (Beets-Tan et al., 2001).

iv) Virtual colonoscopy

Virtual colonoscopy or CT colonography uses helical CT to generate high resolution, two dimensional axial images of the abdomen and pelvis. In addition three dimensional images can be constructed from the data obtained. The advantages of virtual

colonoscopy are its ability to provide a full structural evaluation of the colon with high patient acceptance and safety.

The indications for virtual colonoscopy include screening for polyps, incomplete or failed colonoscopy and the assessment of the proximal colon in a distal obstructing lesion (Pijl et al., 2002).

v) Computerised Tomography

In the 1970s, CT images were acquired by sequentially scanning single slices (Hounsfield, 1995). The introduction of spiral scanning in 1989 led to faster volume coverage than sequential slice by slice scanning in addition to increased 3D resolution. In spiral scanning, the patient is transported continuously through the field of measurement while the x-ray tube and the detector rotate continuously. Relative to the patient, the X-ray focus travels on a spiral path allowing continuous data sampling along the axis of table motion and thus the long axis of the patient (Kalender et al., 1990).

The principles of image reconstruction are similar for both sequential and spiral CT although in spiral CT a single slice is reconstructed from the spiral volume data set which allows images to be reconstructed from any arbitary position along the long axis of the patient.

Since the end of the 1990s, rotation times of 0.5s and multirow detectors have become available, making CT a universal imaging modality for all organs.

CT imaging of CRC

CT has an established role in the imaging of CRC. It has been successfully utilised in the assessment of local infiltration of the tumour with the previously encountered problems with lower stage tumours being overcome by the advent of high resolution spiral CT (Harvey et al., 1998).

The detection of malignant lymph node metastases is based upon the size criteria and the arbitary figure of 1cm has been given to delineate malignant disease. However, this has been shown many times not to be the case. Rodriguez-Bigas demonstrated that malignant cells exist in nodes less than 1cm and nodes even greater than 3cm have been shown to be benign (Rodriguez-Bigas et al., 1996).

Previously CT has been shown to be inaccurate in the detection of liver metastases (Steele, Jr. et al., 1991). Later studies have utilised the different blood supply of the metastases and the normal liver parenchyma. The use of intravenous contrast coupled with the rapid acquisition times of spiral CT has partially addressed this problem and reported sensitivities of 68-79% (Paul et al., 1994; Zerhouni et al., 1996).

CT has performed poorly in the detection of recurrent extrahepatic disease. The reason for this is its inability to differentiate between benign, fibrotic tissue resulting from surgery and /or radiotherapy and malignant tumour recurrence. The reliance on change in tumour morphology without any other tissue characteristics makes dealing with indeterminate tissue masses within the abdomen very difficult. Although modern spiral CT is more accurate than non-spiral CT (Mendez et al., 1993), MRI is establishing itself as the more accurate morphological imaging tool (Brown et al., 2003b; Brown et al., 2003a; Holzer et al., 2003).

CT has played a significant role in tumour imaging over the last two decades, as it is widely available and clinicians are sufficiently experienced to perform and interpret the investigation. The problems of this cross sectional imaging modality in terms of both intra and extra hepatic recurrent disease have been highlighted above. In view of this the role of functional imaging in CRC is addressed in the following section.

1.2.4 Pathologic staging

Full staging of CRC follows surgical exploration, tumour and regional lymph node resection which provides tissue for pathological assessment. In the early 1930's Sir Cuthbert Duke devised a pathological staging system for CRC (Dukes, 1932) (table 1.1) which was later modified in 1954 into the modified Astler-Coller classification (Astler and Coller, 1954). In the 1980's following close collaboration between the International Union against Cancer (UICC) and the American Joint Committee on Cancer (AJCC), the Tumour, Nodes, Metastases (TNM) system of pathological staging was introduced (table 1.2) the importance of which became internationally accepted in the 1990's. Today in the UK, the AJCC-TNM is used in conjunction with the Dukes and modified Astler-Coller classification to pathologically group stage CRC (table 1.3).

Stage	Definition	% of Cases	5-Year Survival
A	Confined to bowel wall	10	97%
B	Extended through bowel wall, but no lymph node involvement	35	80%
C1	Lymph node involvement, apical node disease-free	30	65%
C2	Apical lymph node involved		35%
D	Distant metastases	25	5%

Table 1.1 Dukes staging and classification. Stage D has been added to Dukes' original classification. % of Cases represents the percentage of cases with that stage at diagnosis at first presentation.

Classification	Definition of TNM classification
Primary Tumour (T)	
TX	Primary tumour cannot be assessed.
T0	No evidence of primary tumour.
T_{is}	Carcinoma in situ.
T1	Tumour invades the submucosa.
T2	Tumour invades mucularis mucosa.
T3	Tumour invades through muscularis mucosa into subserosa or into nonperitonealised pericolic or perirectal tissues.
T4	Tumour directly invades other organs or structures or perforates visceral peritoneum
Lymph Nodes (N)	
NX	Regional lymph nodes cannot be assessed
N0	No regional lymph node metastases
N1	Metastases in 1 -3 regional lymph nodes
N2	Metastases in ≥ 4 regional lymph nodes
Distant Metastases (M)	
MX	Presence of distant metastases cannot be assessed
M0	No distant metastases
M1	Distant metastases

Table 1.2 Modified TNM classification system for the staging of colorectal cancer.

Stage	T	N	M	Dukes	Modified Astler-Coller
0	T_{is}	N0	M0	-	-
I	T1	N0	M0	A	A
	T2	N0	M0	A	B1
IIA	T3	N0	M0	B	B2
IIB	T4	N0	M0	B	B3
IIIA	T1-T2	N1	M0	C	C1
IIIB	T3-T4	N1	M0	C	C2/C3
IIIC	Any T	N2	M0	C	C1/C2/C3
IV	Any T	Any N	M1	-	D

Table 1.3 Group staging of colorectal cancer.

1.2.5 Histological grade

The histological grade is the qualitative assessment of the differentiation of the tumour expressed as the extent with which a tumour resembles the normal tissue and is graded as follows:

GX Grade cannot be assessed

G1 Well differentiated

G2 Moderately differentiated

G3 Poorly differentiated

G4 Undifferentiated

The terms "low" and "high" grade are employed for G1-G2 and G3-G4 tumours respectively because it has been suggested this may be associated with outcome independently of TNM stage group for CRC (Newland et al., 1981).

1.2.6 Other prognostic factors

Currently other independent prognostic factors used in patient management and well supported in the literature are histological types, where small cell and signet ring cancers have a less favourable outcome (Jass and Sobin, 1989). Extramural venous invasion has been shown to be a poor prognostic marker (Talbot et al., 1981) and submucosal vascular invasion arising in adenomas is associated with a higher risk of regional lymph node involvement (Fenoglio-Preiser and Hutter, 1985).

The intra-tumoural expression of specific molecules like p27 (Belluco et al., 1999; Loda et al., 1997), DNA microsatellite instability (Wright et al., 2000) and thymidylate

synthase (Takenoue et al., 2000) have potential to act as prognostic indicators but need to

be evaluated further before they are routinely included in the staging process.

1.3 Treatment

1.3.1 Curative colonic surgery

Curative surgery for cancer of the colon comprises of a segmental resection of the primary lesion based on its arterial blood supply. This procedure should also include dissection of the regional lymph nodes, which acts as an accurate staging procedure for determining whether adjuvunct chemotherapy will be of benefit (1995). Extended lymphadenectomy to the para-aortic nodes and initial ligation of the vascular pedicle were previously thought to confer survival advantages, but this does not appear to be the case (Sugarbaker and Corlew, 1982; Wiggers et al., 1988). In all cases a thorough inspection of the peritoneal cavity is carried out looking for synchronous tumours and metastatic disease. Synchronous tumours occur in 1.5 – 7.5% of all cases (Davison and Stern, 1995) and completion colectomy should be carried out. Based on evidence from progression of polyps into invasive cancers a case can also be made for completion colectomy once any existing polyps are removed and histopathologically evaluated. Usually this information is available pre-operatively, but in certain cases, such as a stenosing primary CRC that does not allow the passage of the colonoscope, the finding may be intraoperative. It is essential to obtain histological diagnosis before the conversion of a segmental resection into a radical colectomy. It has also been suggested that these same principles apply to patients with HNPCC, who have a 45% risk of developing a metachronous cancer within 10 years (Lynch, 1996). The optimal result of surgical treatment should result in tumour free resection margins, both longitudinal and circumferential as well as maintenance of intestinal continuity. It is possible to perform *en bloc* resections with curative intent if the tumour is invading adjacent organs.

34

1.3.2 Curative rectal surgery

At diagnosis, most rectal tumours have already spread beyond the rectal wall, either by direct extension or lymphatic spread, and require radical resection. The overwhelming evidence now available regarding the lateral spread of rectal tumours into the mesorectal tissues requires an *en bloc* removal of the cancer with the surrounding mesorectal fat habouring the blood vessels and lymphatics (known as the mesorectum) (Heald and Ryall, 1986). Involvement of the lateral or circumferential resection margin is strongly correlated with the later development of local recurrence. It is now accepted by most surgeons that a total mesorectal excision should be attempted in all cases. A margin of at least 1-2cm of normal rectal tissue distal to the tumour should be included to reduce the risk of anastomotic recurrence. As with colon cancer, any adhesion to adjacent organs should be resected *en bloc* with the rectum. Restoration of intestinal continuity is an important but secondary consideration. It should only be attempted if a well perfused, tension free anastomosis can be performed. When the cancer is so low that the 2cm margin cannot be obtained without compromising the sphincter function, the entire rectum and anus should be removed. This is known as an abdominal perineal resection and in this case a permanent colostomy is created.

1.3.3 Recurrent disease

There is a standard pattern to the presentation of recurrent CRC. The sites include:

i)   Liver >30%

ii)   Lung and locoregional disease 20-25%

iii)   Other intraabdominal sites 15-20%

iv)   Elsewhere 10%

Approximately half of the patients who have undergone surgery for CRC will develop recurrent disease within 3 years of initial resection. In up to 30% of cases recurrences following treatment of primary CRC is localised and therefore suitable for curative resection (Turk, 1993). Ogunbiyi et al has also demonstrated that a significant disease free interval can be produced by aggressive therapy on appropriately selected cases of recurrent rectal cancer (Ogunbiyi et al., 1997b).

1.3.4 Management of colorectal liver metastases

Metastases localised to the liver alone occur in approximately half of all patients presenting with metastatic disease. Liver resection is the only curative option. Investigation of patients with liver metastases should determine whether the disease is resectable and the criteria usually employed are; lesions confined to a single lobe, no extrahepatic metastases, patient fit to undergo major surgery, non-jaundiced with good liver function. Five year survival rates following resection now range between 25% and 39%, with a median survival between 28 and 40 months in most large series. Reported ten year actual survival rates have also been documented in a few studies ranging between 20 and 26% of patients (Fusai and Davidson, 2003).

Strategies employed for unresectable colorectal liver metastases (CLM) include downstaging using neo-adjuvant chemotherapy (most commonly 5FU-leucovorin-oxaliplatin) which is delivered either intravenously or via the hepatic artery. Adam et al published results of a study of 701 patients with unresectable liver metastases who underwent neoadjuvant chemotherapy; of this group 13.5% were found to be resectable

on reevaluation and underwent potentially curative resection with overall five year survival rates of 35% from the time of resection (Adam et al., 2001). Currently the European organisation for the research and treatment of cancer (EORTC) is carrying out a randomised phase III trial comparing the effectiveness of surgery with or without combination chemotherapy in treating patients who have colorectal liver metastases.

Portal vein embolisation has been used in cases where the liver tumour is resectable but surgery is contraindicated, because the anticipated liver remnant is too small. This technique produces atrophy of the affected lobe and compensatory hypertrophy of the future liver remnant. Azouly et al have showed an increase in resectability rate of 19% of such patients (Azoulay et al., 2000). In patients with bilobar disease a two staged procedure can be undertaken allowing liver regeneration following the initial resection; and the second stage can only be undertaken if clear margins can be achieved and there is no evidence of disease progression.

Local ablative techniques like radio frequency ablation act as an alternative to systemic chemotherapy. This technique uses heat generated from a radio frequency electrode which is inserted into the target hepatic lesion under Ultrasound, CT or MRI control. Radiofrequency ablation can be administered at open surgery, laparoscopy or percutaneously (Oshowo et al., 2003).

1.4 Chemotherapy

1.4.1 Background

As discussed above, the primary treatment of CRC is surgical resection, but over half of all patients will eventually die of metastatic disease. Approximately 80% of patients with colon cancer present with localised disease and are suitable for curative resection. However despite attempted curative surgery, patients have a significant probability of disease relapse and cancer related death. Over the past few decades there has been much interest in adjuvant therapeutic approaches that would eliminate microscopic disease and thereby prevent recurrence.

Once CRC has metastasised , the average survival duration without chemotherapy is only 3-9 months. Two thirds of patients well enough to participate in clinical trials, and randomised to best supportive treatment, die within 1 year (Simmonds, 2000). Systemic chemotherapy is rarely curative in such patients except, sometimes, where metastatic disease is confined to the liver and potentially resectable after chemotherapy.

The chemotherapeutic drug developments for advanced CRC in chronological order are as follows:

1960s 5-Fluorouracil (5FU)

1980s Modulated 5FU

1990's Infusional 5FU

Newer cytotoxic agents   Oxaliplatin
                                     Raltitrexed
                                     Irinitecan
                                     Oral fluoropyrimidines

2000 Agents acting on novel targets/molecular markers.

1.4.2 5-Fluorouracil

For the past 40 years 5-Fluorouracil (5FU) has been the mainstay of drug therapy for metastatic CRC. 5FU belongs to the group of anti-cancer drugs known as the 'antimetabolites'. These are drugs that interfere with normal cellular function, particularly the synthesis of DNA and hence cellular replication (Midgley and Kerr, 1999).

5FU is a pyrimidine analogue that resembles the bases uracil and thymidine. The drug penetrates rapidly into cells, where it is converted intracellularly by the enzymes which normally act on uracil and thymidine converting them into nucleoside forms. It interferes with the ribonucleotide and deoxynucleotide synthesis pathways after phosphorylation which leads to the active fluorinated nucleotides 5-fluorouridine triphosphate (5FUTP) and 5-fluorodeoxyuridine monophosphate (5-FdUMP). 5FUTP can be incorporated into RNA in place of uridine triphosphate (UTP), leading to inhibition of the nuclear processing of ribosomal and messenger RNA and may cause other errors of base pairing during transcription of RNA (Glazer and Lloyd, 1982). 5-FdUMP inhibits irreversibly the enzyme thymidylate synthase (TS), this leads to depletion of thymidine monophosphate (dTMP) which is required for DNA synthesis, thus conferring a degree of S phase specificity on the drug. These two mechanisms for the toxicity of 5FU are shown in figure 1.2.
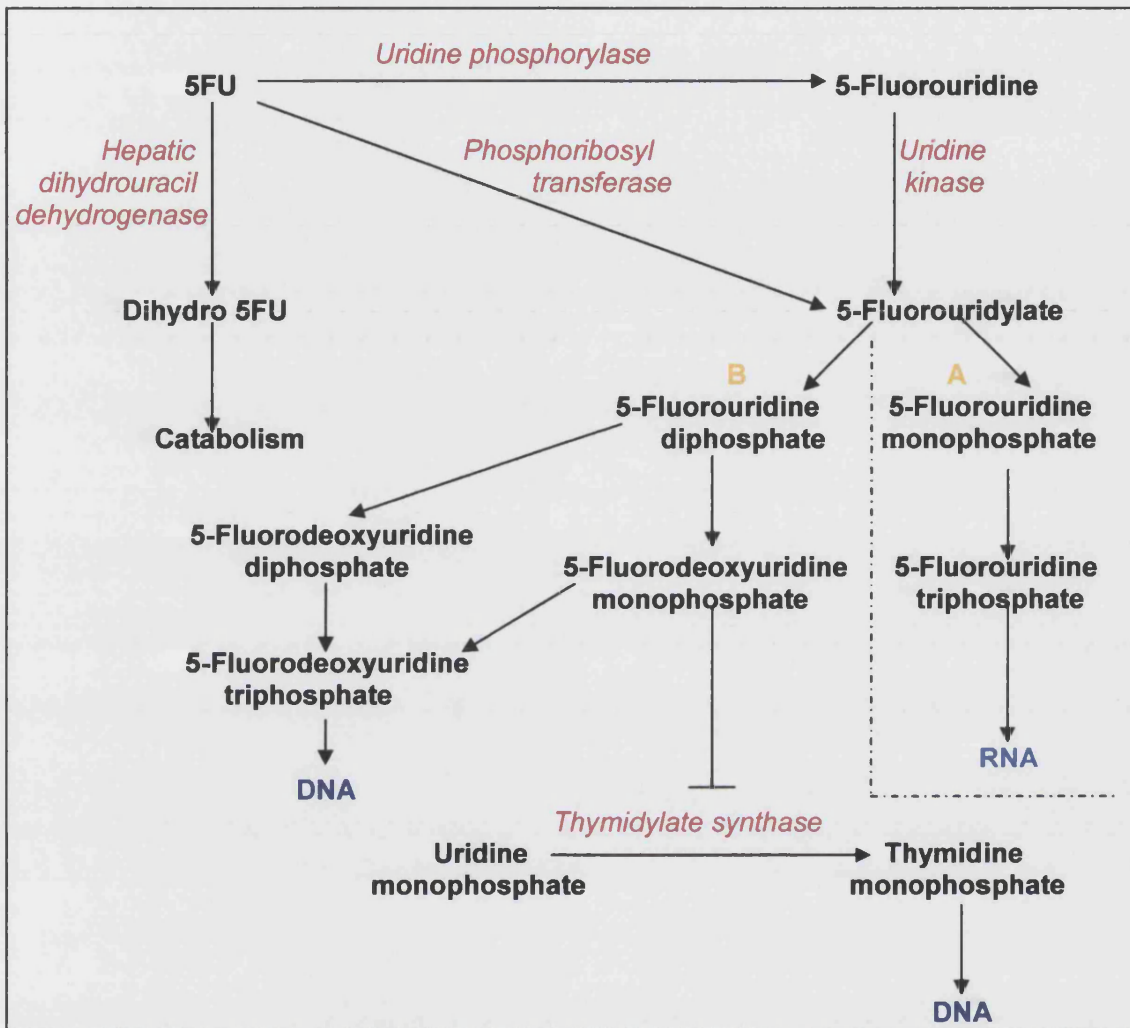
Figure 1.2 Metabolism and activation of 5-fluorouracil. Upon uptake by cells, 5-fluorouracil (5FU) is metabolised via two separate pathways: A and B. A represents the ribonucleotide synthesis pathway, in which 5FU is converted to 5- fluorouridine monophosphate, then to 5-fluorouridine triphosphate and finally incorporated into RNA. B represents the deoxynucleotide synthesis pathway, where 5FU exerts two independent effects. It may become metabolised to 5-fluorodeoxyuridine triphosphate and then incorporated directly into genomic DNA, with potentially cytotoxic results. Alternatively, 5FU may become metabolised to 5-fluorodeoxyuridine monophosphate which inhibits thymidylate synthase, an enzyme important in DNA synthesis.

The co-administration of folinic acid potentiates the inhibition of TS by 5FU and increases response rate (Piedbois et al., 1992) and is now a component of most 5FU based regimens used in both the adjuvant and metastatic contexts. Data exists supporting the

40

use of infusional 5FU where response rate is undoubtedly higher, time to progression longer, but survival only minimally extended (Woolmark et al., 1998).

Adjuvant therapy in those patients with Dukes B CRC remains controversial, despite two large studies addressing this issue, IMPACT B2 and NSABP (Erlichman et al., 1999; Mamounas et al., 1999). The former study pooled results from five trials including 1,006 patients with Dukes B2 colon cancer and provided no evidence for the routine use of 5FU/Leucovorin as routine adjuvant treatment in this group. Likewise the NSABP trial used results from four trials comparing the relative efficacy of adjuvant chemotherapy in patients with Dukes B and C disease. Although the results suggested that patients with Dukes B disease benefited from adjuvant chemotherapy and should be presented with this treatment option, the number of patients with Dukes B was too limited to rule out a difference in treatment effect according to staging. In addition this trial also collectively looked at the studies by creating two comparison groups; the first group consisted of all patients receiving the better of the two treatments in each of the four trials, and the second group consisted of patients receiving the inferior treatment. This allowed a pooling of the results of 1,565 patients with Dukes B cancer and a reduction in mortality and recurrence when adjuvant therapy was used. It must be noted however that not all the trials looked at within this study used an observation arm and the methodology used in the pooling of results for these separate trials in which the treatment received varied widely is unconventional. These results should therefore be interpreted with an element of caution. Recently Taal et al published the results of a prospective trial on behalf of the Netherlands Adjuvant Colorectal Cancer Project (NACCP) randomising 1029 patients with Dukes B or C colorectal cancer to receiving twelve months 5FU plus

levamisole or no further treatment following curative surgery (Taal et al., 2001). This showed a 19% reduction in death among those patients with Dukes B CRC.

The large randomised controlled trial conducted by Quasar found that the inclusion of levamisole and high dose folinic acid to 5FU and standard dose folinic acid did not delay recurrence or improve survival (Gray et al., 2000).

The jury is still out in the value of adjuvant chemotherapy for the treatment of Dukes B CRC. In real terms a small treatment difference can only be reliably detected with many more patients. To detect an absolute risk reduction of 4% at 5 years with a 90% power, 4,700 patients are required (Taal et al., 2001). The general consensus in the oncological world is that in patients with Dukes B CRC and no other medical contraindications, adjuvant treatment with 6 months of 5FU/Leucovorin could be offered after careful discussion with the patient, who must be aware that such additional treatment is not definitely proven and that any benefit is likely to be small. It must also be remembered that that there is a group of patients with high risk characteristics (poorly differentiated tumours, venous or lymphatic invasion) to whom adjuvant chemotherapy can be reasonably offered.

1.4.3 State-of-the-art chemotherapy

A brief summary of the more recent drugs is offered as a detailed explanation falls outside the remit of this thesis.

Irinitecan disrupts cell division and is licensed for first line treatment in patients with advanced CRC in combination with 5FU and folinic acid and as a second line monotherapy when 5FU based treatment has failed. In randomised controlled trials it has

increased tumour response rate and extended both progression free and median survival when used in combination (Douillard et al., 2000; Saltz et al., 2000). Its role as a second line montherapy when 5FU has failed has also shown positive results (Cunningham et al., 1998).

Oxaliplatin is a platinum compound which inhibits DNA replication by forming cross links (Culy et al., 2000). Randomised trials involving the use of oxaliplatin in combination with 5FU/folinic acid as first line treatment have shown significant improvement in tumour response and progression free survival (de Gramont et al., 2000; Giacchetti et al., 2000).

Raltitrexed inhibits TS and is indicated as a montherapy for palliative treatment when 5FU is not tolerated or inappropriate and has shown comparable results to 5FU regimens (Cocconi et al., 1998; Cunningham et al., 1996).

Two oral fluoropyrimidines are marketed in the UK, Capecitabine and Tegafur, these are closely linked to 5FU and are more convenient for patients. Large randomised trials have shown that they are effective in the treatment of metastatic CRC (Hoff et al., 2001; Van Cutsem et al., 2001) with potential pharmacoeconomic advantages (Hoff and Pazdur, 1998).

The National Institute for Clinical Excellence (NICE) has recently published recommendations on the use in the NHS of irinotecan, oxaliplatin and raltitrexed in patients with advanced CRC (NICE 2002). It has advocated the use of irinitecan as a second line monotherapy following failure of first line 5FU based treatment and only advises the use of combination oxaliplatin plus 5FU in patients with CLM confined to the liver where chemotherapeutic shrinkage would allow possible curative resection.

Interestingly NICE advises against both irinitecan and oxaliplatin being used as first line chemotherapeutic agents until further evidence is provided from the Medical Research Council FOCUS trial. This has received much criticism amongst UK cancer specialists who contest the interpretation of the trial results in addition to the cost analysis (Saunders and Valle, 2002).

1.4.4 Future perspectives of chemotherapy

In recent years the options for chemotherapy in CRC have expanded enormously. The development of multiple agents with differing mechanisms of action that can be used to good effect on their own or in combination with 5FU regimens has made defining the ultimate correct schedule for different patients even more of a challenge. Encouragingly the new regimens have been shown to be as or more effective than 5FU when used in combination or as a monotherapy. The development of prognostic factors and refinement of predictive testing will aid in allowing the optimisation of the large range of options available and accurately determine how likely a patient is to benefit from specific drug treatments.

1.5 Positron Emission Tomography

1.5.1 Background

Positron emission tomography (PET) is a functional imaging technique, in which tracer compounds labelled with positron-emitting radionuclides are injected into the subject of the study. There is a fundamental difference between the underlying mechanism of image production between clinical radiology and PET. Clinical radiology uses instrumentation to induce signal changes and then detects the effects, whereas in the case of PET, instrumentation detects the signal *but* the radioligand used is the source of the signal.

PET uses radioligands, also known as *tracers* to produce images. Positron emitting isotopes known as radionuclides (^{15}O, ^{13}N, ^{11}C, ^{18}F) are incorporated into a large number of biological compounds to create radioligands (or tracer molecules) for studying normal and pathophysiological processes. The radionuclide used has an unstable nuclei which decays by the emission of a positron. This behaves in a similar way to an electron but has a positive charge. The result of this decay is that the emitted positron having travelled a short distance in human tissue (~1mm) collides with an electron and undergoes mutual annihilation which results in the production of energy in the form of two 511KeV photons or γ rays travelling in opposite directions . If these γ rays are emitted at $180°$ to each other, they are detected simultaneously by the PET scanner, a term known as 'coincidence detection' and an image of original radionulide distribution can be reconstructed.

For further information regarding the components of a PET facility, including cyclotrons and scanner types see appendix A. Also, this appendix covers the physics of annihilation coincidence detection and attenuation correction, necessary for image processing.

1.5.2 Imaging sequences

i) Whole body image sequences

In the case of CRC the disease has the potential to metastasise to most areas of the body, hence whole body PET scans are routinely performed. The axial field of view of the majority of PET scanners is 14.5cm, so subsequently larger areas of the body can only be imaged by moving the patient couch through the gantry. To complete a wholebody scan the patient is moved through the scanner.

ii) Dynamic image sequences

In many studies, one is interested not in the static distribution of the tracer at one particular time but in the rate at which the activity enters and leaves a particular region. It is in these types of research cases that dynamic imaging is employed and a series of images over time are acquired. Factors of clinical interest which can be measured using this technique are peak tracer activity within an organ, the time occurrence of peak activity, the rate of activity uptake in the organ and the rate of clearance of activity.

In dynamic data sets, each image in the series is acquired over a short space of time and so only yields a small number of counts in each serial image. If a single image of a dynamic sequence is displayed it invariably contains considerable statistical noise

which in turn makes the identification of anatomical structures even more difficult. To analyse a set of dynamic images, a region of interest (ROI, section 2.4.2) is placed over the image with the best anatomical detail and then copied onto the remaining images. This enables the computation of a time activity curve (TAC) where uptake of the tracer within the ROI can be mapped as a function of time (count rate v. time). In addition, the data from the TAC allows further quantitative analysis to be performed.

1.5.3 Biological basis of FDG-PET

"If the carcinoma problem is attacked in its relation to the physiology of metabolism, the first question is: In what way does the metabolism of growing tissue differ from the metabolism of resting tissue?" *Otto Warburg 1924*

In 1924 this fundamental question was posed by the German biochemist Otto Warburg. From a series of observations based on a rat model and later confirmed on human cancer cell lines he concluded that the predominant form of glucose metabolism in tumour cells is glycolysis (Warburg, 1931). Tumours have increased demands of ATP which is derived from glycolysis. This is due to two factors; cancer cells are by definition rapidly replicating cells and secondly these cells are not efficient in the production of ATP via the Krebs cycle. This leads to a 19-fold increase in glucose consumption per mole of ATP produced. The reason for this is two fold, firstly neoplastic degeneration of tumour cells is associated with a loss of efficient production of ATP and secondly there is activation of the glucose reliant hexose monophosphate pathway providing the backbone for the DNA and RNA synthesis required in growing tumours (Weber, 1977a; Weber,

1977b). The increased demands of the malignant cell are in some way met by the increased number of various membrane glucose transporters (Flier et al., 1987; Hatanaka, 1974). A major early marker of cellular malignant transformation is the activation of the gene coding for the glucose transporter GLUT 1 (Hiraki et al., 1988).

1.5.4 [18F] 2–fluoro-2 deoxy-D-glucose

The application of the above principles led to the development of [18F]2-fluoro-2-deoxy-D-glucose (FDG). In this tracer the 18F is substituted for the hydroxyl group in the 2- position.

FDG is transported into cancer cells by the GLUT1 facilitative glucose transporter molecules. Once inside the cell phosphorylation occurs by the enzyme hexokinase to form FDG-6-phosphate. This is a polar molecule hence does not cross the cell membrane well and becomes metabolically trapped. Although FDG-6-phosphate can be converted back to FDG by the enzyme glucose-6-phosphatase, this is a slow reaction by an enzyme which is present in very small amounts in cancer cells. Following trapping, radioactive decay occurs by positron emission.

In the evaluation of FDG images normal uptake can be seen in the brain, heart, kidneys and urinary tract (see figure 1.3). The brain has a high physiological glucose metabolism, whilst myocardial uptake is seen as a consequence of insulin sensitive glucose transporters (GLUT4). Uptake of FDG by the myocardium is variable although generally uptake is decreased in the fasting state and increased in the presence of insulin. This is also seen in the skeletal muscle. The effects of fasting on the uptake of FDG has

48

led to oncological PET studies being carried out following several hours of fasting to reduce insulin levels and hence physiological uptake (Wahl et al., 1991).

Competitive inhibition of FDG uptake by glucose in tumour tissue is an additional reason for optimal scanning to be carried out in the fasting state.
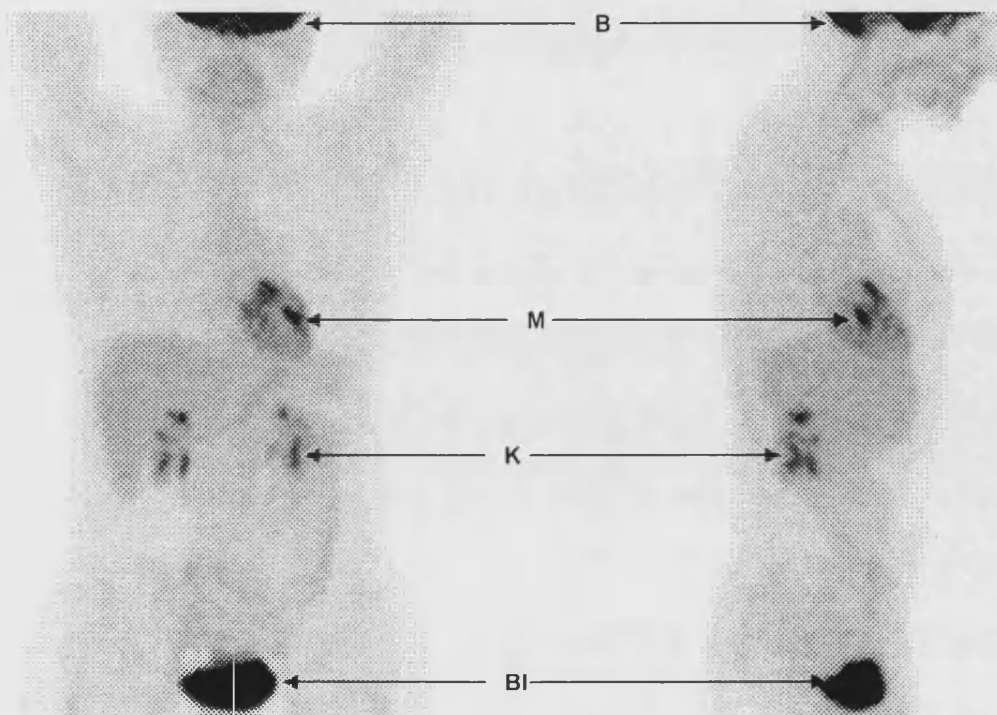
Figure 1.3 Normal physiological uptake of FDG. High uptake is seen in the brain (B), in addition to the myocardium (M). Renal excretion can be seen via the kidneys (K) into the bladder (BI).

1.6   PET in colorectal cancer imaging

1.6.1 Primary disease

i) Screening

Other than the study by Yasuda and colleagues (Yasuda et al., 2000) there is little substantial published data for the use of FDG-PET in screening for asymptomatic CRC. This study of 3165 patients demonstrated an unacceptable false positive and negative rate. Further considering the availability of PET and current costs – two important contributory factors - this technique is currently unsuitable for unselected screening programmes.

PET's role in the detection of colonic polyps has been investigated. Drenth et al validated pre malignant colonic abnormalities using FDG-PET with endoscopy findings. In a cohort of 39 patients, PET had a sensitivity and specificity of 74% and 84% when compared with the gold standard of colonoscopy, making it a useful adjunct in the non-invasive follow up of patients with CRC (Drenth et al., 2001). Incidental colonic uptake of FDG was investigated by Tatlidil et al in a retrospective study of 27 patients without a history of CRC referred for FDG-PET studies. In this study high FDG uptake correlated with at least a 79% chance of histological analysis at the same site being abnormal, making colonoscopy a reasonable next step for those patients displaying abnormal high FDG uptake within the colon (Tatlidil et al., 2002).

However, there may be value in detecting polyps on reconstructed CT images and matching this data to the metabolic signal using the new imaging modality of PET/CT.

ii) Symptomatic disease

A PET positive rate of over 95% has been reported in the diagnosis of primary

CRC in symptomatic individuals (Mukai et al., 2000) . However, endoscopy and barium

enema detect over 90% of CRCs while being significantly cheaper and more widely

available than PET. CT colonography is beginning to make a clinical impact (section

1.5.4). PET is, therefore, unlikely to play a significant role in diagnosing primary CRC,

although its use as a targeted screening investigation in high risk groups is yet to be fully

evaluated.

1.6.2 Pre-operative staging

Pre operative staging investigations allow all foci of cancer to be treated by an

appropriate combination of surgical excision, chemotherapy and radiotherapy so as to

minimise the chance of recurrence.

i) Local infiltration

CT is widely used to stage primary CRC and is an accurate method of assessing

local infiltration especially in advanced tumours (sensitivity 55% - 70%) (Balthazar,

1991; Zerhouni et al., 1996). Conventional and endoluminal MRI are reportedly more

accurate for rectal cancers as is endoanal ultrasound (USS) (Hildebrandt and Feifel, 1995;

Napoleon et al., 1991). Many studies have compared FDG-PET and CT in the staging of

primary CRC. Abdel-Nabi found in 48 patients that PET had a higher sensitivity and

specificity than CT (Abdel-Nabi et al., 1998) and similar results were demonstrated in a

smaller study of 16 patients by Falk et al (Falk et al., 1994). This showed that although

PET had a increased sensitivity for the pre-operative staging of primary CRC, CT had a higher specificity. In addition to detecting malignant lymphadenopathy, synchronous tumours can also be detected using FDG-PET as demonstrated in Pin's case report (Pin et al., 2000) FDG-PET does not, however, give accurate information regarding local infiltration and it is this which might be a key area in which PET/CT comes into its own.

ii) Involvement of lymph nodes and extrahepatic intraabdominal spread

Standard pre-operative evaluation, using size criteria, lymph node involvement and extrahepatic, intraabdominal spread with CT and MR has been shown to be inadequate by a number of studies (Freeny et al., 1986; Guinet et al., 1988; Thompson et al., 1986). These studies report accuracy for CT ranging between 25-73% (overall sensitivity is 45%) with a 40% sensitivity for MRI. Laparoscopy with or without USS may further improve the accuracy of staging although this is invasive and information is not available prior to definitive surgery. Immunoscintigraphy (radiolabelled antibodies) is significantly more sensitive for pelvic and intraabdominal disease when compared to CT and this technique has potentially useful clinical applications (Veroux et al., 1999). Lymphoscintigraphy can also play some role in the detection of the sentinel node.

The studies mentioned earlier in this section also comment on the assessment of lymph node involvement and extrahepatic intraabdominal spread. In Falk's study of 16 patients, he demonstrated that FDG-PET was superior to CT for staging (positive predictive value (PPV) 93% and negative predictive value (NPV) 50% for FDG-PET versus PPV of 100% and NPV of 27% for CT. The study by Abdel-Nabi et al is more interesting

because it showed no difference between the modalities for detection of lymph nodes (sensitivity of 29% for both) (Abdel-Nabi et al., 1998). Mukai and colleagues again showed the limited value of PET in the detection of metastases to regional lymph nodes surrounding the primary lesion by reporting sensitivities of 22.2% (2/9) for lymph node detection with specificity of 86.7% (13/15) (Mukai et al., 2000).

Metastases to the liver

Liver metastases are found in 10-25% of patients at the time of operation for their primary CRC and 25% are candidates for resection (Adson, 1987). CT is the imaging modality most frequently used in the staging of primary CRC and has a reported sensitivity of 72% and specificity of 99% with MR having similar results (Freeny et al., 1986; Rummeny et al., 1992).However, published data also shows that CT failed to demonstrate lesions in 7% and underestimated the number of lobes involved in 33% of cases (Ferrucci, 1990; Steele, Jr. et al., 1991). Immunoscintigraphy using Indium-111-labelled anti-CEA antibodies has shown promise (Patt et al., 1990), but specificity and poor spatial resolution can be a problem when compared to FDG-PET. Again in Abdel-Nabi's study the detection of liver metastases by FDG-PET was shown to be superior to CT (sensitivities of 88% versus 38%), although this study was not controlled and PET reporters were not blinded to CT reports (Abdel-Nabi et al., 1998).

1.6.3 Recurrent disease

i) Detection of local recurrence

Following treatment of primary CRC, patients undergo surveillance of varying intensity in order to detect recurrence. In up to 30% of cases the recurrence is localised and therefore suitable for curative resection especially if radical surgery is performed (Turk PS, 1993). In order to avoid unnecessary morbidity and mortality appropriate selection of patients is essential.

MR remains the optimum morphological imaging modality although there were early reports questioning the ability of MR to distinguish recurrent tumour from benign fibrotic changes (de Lange et al., 1989). Even so, CT remains the most frequently used option when detecting recurrence and suffers similar drawbacks when evaluating "scar" tissue. Immunoscintigraphy has been shown to be superior than CT for differentiating scar from tumour in the pelvis (Doerr et al., 1991; Lunniss et al., 1999). However, Libutti's recent prospective study of twenty eight patients comparing PET with CEA scan and blind second look laparotomy, revealed that FDG-PET scanning is superior to anti-CEA immunoscintigraphy and could predict those patients with recurrent disease most likely to benefit from laparotomy (Libutti et al., 2001).

Several authors have confirmed the value of measuring the metabolic activity of a tissue mass through FDG-PET in order to differentiate between malignant local recurrence and scar tissue (Ito et al., 1997; Schlag et al., 1989; Strauss et al., 1989). In a study by Schiepers and colleagues (Schatzkin et al., 2000) accuracy for disease in the pelvis was 95% with FDG-PET against 65% with CT (Schiepers et al., 1995). Takeuchi et al also reported impressive results for the accuracy of PET for diagnosis of pelvic

recurrence when compared to both CT and MR with 15 of the 16 histologically proven recurrences imaged positively (Takeuchi et al., 1999). More recent studies have reported similar findings (Flamen et al., 1999; Valk et al., 1999). In fact Valk and colleagues demonstrated sensitivity and specificity of 93% and 98% respectively with FDG-PET compared to 69% and 96% in the 115 patients with available CT's. This led to a cost saving of approximately US$ 3000 per pre-operaitve study through the avoidance of surgical intervention. To date our own prospective experience comparing PET with CT in the detection of locally recurrent disease also demonstrated increased accuracy using PET with a sensitivity of 100% and specificity of 86% compared to 75% and 100% for CT (Arulampalam et al., 2001). Whiteford's review of 105 patient records of which 70 had locoregional recurrence also confirmed the superiority of PET when compared to CT plus colonoscopy with sensitivities of 90% and 70% respectively (Whiteford et al., 2000).

ii) Evaluating a rising CEA

Evaluating patients who present with an isolated elevation of CEA with minimal symptoms and normal imaging is ideally suited to PET and PET/CT. Flanagan et al showed that in 17 out of 22 patients PET was abnormal and recurrence was confirmed by tissue sampling and/or follow up. PET had a PPV of 89% and NPV of 100% (Flanagan et al., 1998). A PPV of 89% was also demonstrated by Flamen's group with a sensitivity of 79% in a cohort of 50 consecutive patients with an elevated CEA with completely normal or equivical conventional diagnostic work up (Flamen et al., 2001). The superior accuracy of PET over CEA has also been discussed by Simo's group who looked at 58

patients referred for FDG PET because of an elevated CEA. PET detected recurrence leading to a major management change in 34 (58%) of the cohort. Of this group 18 underwent curative surgery and 16 were treated with systemic therapy (Simo et al., 2002). In Zervos's study, of the 15 patients with an increasing CEA level and normal diagnostic imaging, 14 were found to have abnormal PET scans, 9 of these underwent surgical exploration with curative intent. This study also looked at 4 patients with symptoms of recurrent CRC but a normal CEA level and non diagnostic conventional imaging but positive PET scans. Three of the four were found to have no evidence of recurrence at surgery, the results of PET scans in these types of patients should therefore be interpreted with caution (Zervos et al., 2001).

iii) Evaluation of the extent of disease

The evaluation of patients with suspected recurrent CRC aims to differentiate isolated resectable disease from disseminated metastases allowing appropriate patient selection for surgical intervention and increasing the chance of disease free survival. FDG-PET is more accurate than CT for the purpose of evaluating the extent of recurrent CRC as shown by both Ogunbiyi and Vitola (Ogunbiyi et al., 1997a; Vitola et al., 1996). The usefulness of PET in diagnosing peritoneal recurrence of CRC has been investigated by Tanaka et al in a retrospective review of 23 patients (Tanaka et al., 2002). PET was found to have a sensitivity of 88% with a diagnostic accuracy of 78% compared to 38% and 44% respectively for CT. In this study a lesion as small as 15mm in diameter was diagnosed by PET.

iv) Hepatic metastases

Schiepers' study in 1995 evaluated 76 patients presenting with suspected locally recurrent disease or distant CRC. This confirmed a higher sensitivity and accuracy with FDG-PET (94% and 98% respectively) compared to CT/USS (85% and 93%) for the detection of hepatic metastases (Schiepers et al., 1995a). Delbeke compared FDG-PET with CT and CT portagram in 52 patients treated for CRC and presenting with suspected hepatic recurrence. PET demonstrated an accuracy of 92% compared with CT and CT portagraphy (78% and 80% respectively) for hepatic disease. In this study PET was also more accurate for extrahepatic disease when compared to CT, 92% versus 71% (Delbeke et al., 1997). Ogunbiyi's retrospective review also compared PET and CT in the detection of hepatic metastases and reported a sensitivity of 95% and specificity of 100% for FDG-PET compared to CT (74% and 85% respectively) A higher accuracy for PET compared to CT for delineating multiple liver lesions was also reported (Ogunbiyi et al., 1997a)

More recent studies including that of our own unit have systematically confirmed the benefits of FDG-PET for the detection of both hepatic and extrahepatic metastases from CRC. Zhuang's direct comparison of PET and CT in 80 patients with CLM again highlighted greater sensitivity of PET (100% vs 71.4% for PET and CT respectively) (Zhuang et al., 2000). The clinical value of PET in the assessment of potentially curable liver metastases has been investigated by Topal et al (Topal, 2001). In this prospectively studied group of 91 consecutive patients considered eligible for liver resection after conventional imaging, PET provided additional information regarding distant disease in 11% whilst confirming liver metastases in 99%; although in this study PET also falsely

upstaged 6.6% and understaged 7.7% (all of which had small intra abdominal lesions). In a study by Fong et al PET's greater accuracy in identifying distant disease is again demonstrated (Fong et al., 1999). 40% (16/40) patients had their management influenced by the PET findings with 6 of these patients being spared unecessary laparotomy by virtue of Pet's identification of previously undiagnosed extrahepatic disease. This study again highlighted a problem with PET and the identification of small lesions. Only 25% of hepatic lesions smaller than 1cm were detected by PET, while 85% of lesions larger than 1cm were detected.

Our own prospective study currently in press, evaluated 31 patients initially staged with spiral CT prior to referral for hepatic resection. These patients then underwent FDG PET imaging and the results of the two imaging modalities compared in terms of sensitivity and specificity in addition to the effect that PET had on patient management. PET detected all the lesions (sensitivity 100%, specificity 91%) whilst CT incorrectly diagnosed solitary CLM in 5 patients and failed to detect extrahepatic disease in 4 patients (sensitivity 47%, specificity 91%). This resulted in altered management for 12(39%) of the patients of whom 7 (23%) avoided inappropriate surgery (Arulampalam et al., 2004).

The recently published evidence from Kinkel's meta-analysis of the detection of hepatic metastases from cancers of the gastrointestinal tract using US, CT, MRI and PET, suggests that FDG PET is the most sensitive non invasive imaging modality for the diagnosis of CLM and that the optimal evaluation of patients with CLM should include FDG-PET (Kinkel et al., 2002).

v) Extrahepatic metastases

Lai et al compared FDG-PET with conventional imaging in 34 patients and found unsuspected extrahepatic disease in 11 (32%) patients (Lai et al., 1996). Clinical management was affected in 10 patients directly as a result of PET. Schiepers also reported in his study that a significant number of unexpected extrahepatic metastases could be demonstrated using FDG-PET (Schiepers et al., 1995a).

vi) Impact on patient mangement

The advantage that FDG-PET and PET/CT confer to patient management in the context of recurrent and/or metastatic disease is that they alter clinical management. This may be by avoiding surgery, early commencement of non-surgical treatments or selecting patients suitable for surgical re-intervention. FDG-PET is highly accurate for diagnosing and staging recurrent CRC as demonstrated in a meta analysis by Huebner and colleagues (Huebner et al., 2000). The meta-analysis of eleven studies (349 patients) showed a sensitivity of 97%, specificity of 76% and impact on clinical management ranging between 25% and 34% of cases. Detection of unsuspected metastases by FDG-PET ranges from 13-32% (Schiepers et al., 1995). Large savings could be made if PET was incorporated into the routine management algorithm for recurrent CRC on the basis of a reduction in unnecessary laparotomies (from 10 to 20%) and the increased number of resections with curative intent (Larson, 1994). A recent prospective study where the clinical impact of FDG-PET in patients with suspected or confirmed recurrence was assessed by comparing the treatment plan assigned by the oncologist in 102 consecutive patients. The treatment plan was assigned using conventional staging investigations and

compared to the treatment plan based on the incremental information supplied by PET. The management plan of 54 of the 102 patients was altered as a direct result of unexpected PET findings and in 6 further cases the oncologist would not commit to a plan of management without having access to the PET data. Significantly in this study planned surgery was abandoned in 26 of 43 patients (60%) because of incremental PET findings. Again false negative findings were recorded in 4 patients as a result of the metastases being less than 1cm (Kalff et al., 2002).

Table 1.4 summarises some the studies in which PET has changed patient management.

Author	No patients	Change in management
Beets et al	*35*	*40% (14/35)*
Vitola et al	*24*	*25% (6/24)*
Lai et al	*34*	*29% (10/34)*
Delbeke et al	*52*	*33% (17/52)*
Ogunbiyi et al	*23*	*44% (10/23)*
Valk et al	*78*	*31% (24/78)*
Flamen et al	*103*	*20% (21/103)*
Staib et al	*100*	*61% (61/100)*
Fong et al	*40*	*23% (9/40)*
Arulampalam et al	*42*	*38% (16/42)*
Whiteford et al	*101*	*26% (26/101)*
Meta-analysis		
Huebner	*349*	*25%-34%*

Table 1.4 Summary of the impact PET has made on patient management

1.6.4 Evaluating subclinical treatment response

Accurate information regarding the response to radiotherapy and/or chemotherapy in patients being treated for CRC provides useful guidance in predicting, planning and revising ongoing adjuvant therapy, especially in the context of the

unwanted side effects. Studies assessing the uptake of FDG measured by PET and correlation with the anti-tumour effects of chemotherapy have been reported for certain tumour types including CRC as discussed below (Nakata et al., 1997; Okada et al., 1991).

i) Response to chemotherapy

The available data suggests highest concentration of fluorine-18 fluorouracil ($[^{18}F]FU$) in responsive tumour (Shani et al., 1982). Strauss and Conti demonstrated that lesions with low $[^{18}F]FU$ uptake had a significant increase in volume and no response to treatment (Strauss and Conti, 1991). Findlay et al evaluated the metabolism of CRC liver metastases using FDG-PET before and at intervals after treatment in 18 patients. The findings were compared with tumour outcome conventionally assessed using change in size on CT. The results were expressed as a ratio of FDG uptake in tumour and normal liver (T:L). The T:L ratio 4-5 weeks after treatment was able to discriminate response from non-response both in a lesion-by-lesion and overall patient response (sensitivity 100%, specificity 90% and 75% respectively) (Findlay et al., 1996). There is currently speculation that PET/CT may provide a practical solution for evaluating treatment response due to faster patient throughput and accurate anatomical/metabolic image registration. Debate continues as to whether $[^{18}F]FU$ is superior to FDG in predicting the response to treatment on an individual patient basis (Moehler et al., 1998). There is uncertainty as to how to obtain the most accurate information on tumour response based on morphological imaging (Therasse et al., 2000). There are significant problems applying this methodology (Padhani and Husband, 2000) and in this context the EORTC has already published guidelines suggesting metabolic criteria should be used for this

task (Young et al., 1999). The potential role of PET in this aspect of oncology and particularly in the management of CRC suggests that its uses will increase.

ii) Response to radiotherapy

Similar promise was thought to be present for PET in the evaluation of RT response. There are some problems, most notably demonstrated by Haberkorn (Haberkorn et al., 1991) who evaluated FDG-PET in 21 patients with recurrent CRC undergoing pelvic RT. A correlation was made between the palliative benefit and reduction in FDG uptake in 50% of patients (this was also more accurate than CEA).

More recently, Guillem (Guillem et al., 2000) has demonstrated that FDG-PET augments conventional morphological imaging modalities when used to preoperatively assess response to chemo-radiation for rectal carcinoma. This is primarily because information is available preoperatively that allows sphincter saving surgery to be accurately planned.

In a study of 40 patients who were imaged both pre and post radiotherapy for low rectal cancers, FDG uptake was quantified and found to be a good prognostic indicator in terms of long term prognosis (Oku et al., 2002).

A further application of FDG-PET and more recently PET/CT is the potential ability to reduce RT treatment fields by restricting the target volume to the metabolically active tumour. This is usually smaller than the target volume designated by conventional CT (Kiffer et al., 1998; Rosenman, 2001). Such an assessment could possibly reduce unwanted side-effects of RT.

1.6.5 Biological characterisation using PET

The consideration of the biological characteristics of a tumour allows a more specific formulation of treatment plans and the possibility of better results in cancer therapy (Eary, 1999; Price and Jones, 1995). Currently the analysis of biopsy material is the only way of obtaining patient specific information on tumour biology. Although this technique provides a method of assessing and characterising cancer, it is both invasive and has significant sampling error due to the heterogeneity of tumours and variation between metastatic sites. The unique ability of PET to non-invasively image regional tumour biology in the form of glucose utilisation using FDG has been discussed in this section, in addition to the positive impact that this has had in the management of CRC.

While the success of FDG-PET in CRC has been widely documented, the role of PET in the management of cancer in general is not limited to FDG. Other PET tracers have been developed and are targeted to areas of tumour biology that include protein and membrane biosynthesis, tissue hypoxia and tumour receptor and/or gene product expression. Uncontrolled growth is a characteristic of malignant tumours. Techniques have been known for some time to measure tumour growth rates in tissue specimens but as discussed these have limitations. It has already been demonstrated by Higashi et al that FDG uptake is a measure of cell viability and not proliferation (Higashi et al., 1993). PET has the potential to offer fully quantitative characterisation of tumour growth through the development of these new radiolabelled ligands. A biological process highly relevant to CRC and indeed all cancers is the regulation of the cell cycle and cellular proliferation.

The potential use of PET as a tool for imaging cellular proliferation *in vivo* could open

new avenues in the understanding and treatment of CRC by bridging *in vitro* biological

discovery and clinical medicine.

1.7 The cell cycle

1.7.1 Background

The cell cycle is defined as the fundamental process by which a cell replicates its cellular and genetic material, resulting in the formation of two identical daughter cells. This process is essential to the survival and continuing viability of all cells, and various regulatory mechanisms inherent in the cell cycle ensure that the transmission of genetic material to the resulting daughter cells is performed in an accurate and reliable manner.

i) Early concepts of cell proliferation

As early as 1875, mitotic figures were noted to be present in tissue sections examined under the light microscope. From these findings, it was postulated that a cell could exist in one of two states, either undergoing mitosis or remaining in interphase, which was considered to be an inactive "resting" state. Despite these preliminary observations, however, very little progress was made in the understanding of the underlying biochemical changes induced in mitosis for the next fifty years.

The first major breakthrough, leading to the initial concept of a cell cycle, was based on the work of Alma Howard and Steve Pelc in 1951 (Howard and Pelc, 1951). After labelling the roots of *Vica faba* seedlings with ^{32}P, they performed autoradiography to look for the incorporation of this radioisotope in cells manufacturing new strands of DNA. Their results showed that the process of DNA synthesis was entirely distinct from that of mitosis, and occurred during a discrete period in the middle of the interphase. They thus concluded that the cell cycle was composed of four stages, with the presence of

a long gap phase (G1) between mitosis and DNA synthesis, and a second shorter gap

phase (G2) occurring after DNA synthesis.

ii) Localisation of proliferating cells within a tissue

Using high-resolution autoradiography techniques, Hughes performed a similar

set of experiments aimed at studying the localisation of proliferating cells in different

tissues (Hughes et al., 1958). After injecting tritiated Thymidine (^{3}H-Tdr) into mouse

small intestine, he found that ^{3}H-Tdr incorporation was initially observed only in the

crypt cells of the intestinal epithelium. However, after 24 hours, the presence of ^{3}H-Tdr

was detected in epithelial cells along the entire surface of the villi, and at 48 hours could

even be seen in cells shed into the intestinal lumen. He concluded that cell proliferation

occurred only in a specific population of intestinal epithelial cells, namely the crypt cells,

but the resulting daughter cells migrated up into the intestinal villi and were eventually

shed into the lumen. This led to the suggestion that proliferating cells were restricted to a

specialised compartment of normal epithelial tissues.

1.7.2 Current understanding of the cell cycle

The cell cycle comprises four stages: G1, S, G2 and M. The cycle is governed by

extracellular signals such as the availability of nutrients and growth factors and signals

mediated by cell-cell contact. Transitions from one phase to the next are governed by a

series of cyclin-dependant kinases (CDKs) that bind to positive effectors, the cyclins,

whose levels fluctuate during the cell cycle. These complexes phosphorylate certain

proteins which results in the progression of the cell through the phases. There also exist

inhibitory cyclin dependant kinases which can cause cell cycle arrest by deactivating the complexes and can be triggered by a variety of molecular signals.

i) G1 phase

G1 is the first gap phase of the cell cycle and is defined as the period from the end of mitosis to the start of DNA synthesis. It usually lasts around 5 hours in mammalian cells, but is the most variable stage of the cell cycle and, depending on the physiological condition of the cell, may be prolonged to several days or months.

Cells initially begin cycling in the G1 phase, either from the M phase of the previous round of replication or from a state of quiescence (G0). The G1 phase allows the cell to grow, check the integrity of its DNA and prepare for DNA synthesis, eg, by transcribing for necessary enzymes. In order to proceed to the S phase, the cell needs to pass an important regulatory checkpoint (G1/S) ensuring that it has all the necessary components to successfully initiate DNA synthesis. If the cell is not allowed to progress through the cell cycle it will either enter a state of quiescence (G0) or remain in G1 arrest.

ii) S phase

The S phase lasts around 7 hours in mammalian cells and is the period when the DNA of the parent cell is replicated, resulting in the formation of two identical sets of chromosomes. The cell has mechanisms to ensure that its DNA is duplicated accurately so that the genetic information is transmitted in its entirety between one cell generation and the next. The replicative process must also restrict itself from re-duplicating any portion of nuclear DNA within a single cell cycle. Failure of these regulatory

mechanisms can have serious consequences, resulting in cell death or contributing to cellular neoplastic transformation.

iii) G2 phase

G2 - the second gap phase - is the period from the end of the S phase to the start of the M phase (3 hours). During this stage, the cell ensures that DNA replication has been successfully completed, to form two complete diploid sets of chromosomes. Any errors that may have occurred in the preceeding S phase are corrected at this stage eg, by P53, otherwise the cell will not be allowed to progress past the G2/M check point and may be marked for apoptosis. The cell also undergoes replication of its cytoplasmic organelles and cellular growth in preparation for the final act of cell division.

iv) M phase

During the M (mitotic) phase the cell divides, resulting in the formation of two identical daughter cells. The M phase comprises of four stages: prophase, metaphase, anaphase and telophase (Mazia, 1961).

Prophase is characterised by a series of nuclear changes that are visible under the light microscope. The initial event is the breakdown of the nuclear envelope, which is under the control of specific cyclin/CDK complexes (Gerace and Foisner, 1994). The nucleoli are then dispersed and chromosomal DNA is condensed. Finally, the microtubule spindle apparatus is formed in order to allow the subsequent redistribution of the cell's genetic material.

Metaphase is the stage in which the chromosomes attach themselves to the micro tubules and eventually become aligned on the spindle equator. The whole spindle apparatus then becomes compacted, in readiness for separation of the chromosomal DNA.

Anaphase involves the sister chromatids of each original chromosome beginning to pull apart to form two new, independent chromosomes and move towards opposite spindle poles. This is facilitated by the formation of anaphase promoting complex (APC) proteins which lyse the proteins holding the chromatids together(Glotzer et al., 1991).

In *Telophase* a nuclear envelope forms around each new set of chromosomes and the cell starts to undergo cleavage of its cytoplasmic organelles (cytokinesis). This results in the equal division of cellular and genetic material, and formation of two identical daughter cells.

1.7.3 Cell cycle and cancer

. Several of the molecular mechanisms that regulate the balance between cell proliferation and cell death may be disturbed in tumours. In terms of CRC faults at the check points may remove the regulatory checks of repair. G1/S is governed by the retinoblastoma protein. This is phosphorylated and therefore removed from the inhibitory check point by cyclins/CDKs influenced by growth factors (eg, EGF). Several of the molecular mechanisms that regulate the balance between cell proliferation and cell death, may be disturbed in tumours, often resulting in net cell growth. In CRC, the cell cycle checkpoints can be overcome and the cell driven to proliferate, in a number of ways including:

(a) APC mutations, in both classical adenoma-carcinomas and MSI cancers. When APC is dysfunctional, it cannot contribute to the sequestration and breakdown of β-catenin. Therefore β-catenin accumulates and signals for the overexpression of cyclin D. The latter complexes with CDKs to drive the cell through the G1/S checkpoint, therefore committing the cell to DNA synthesis.

(b) Mutations in the TGFβ pathway molecules, including TGFβRII (in MSI cancers), SMADS 2,4 (in adenocarcinomas). Since the TGFβ pathway increases the expression of inhibitors of cyclins/CDKs, any mutated signalling molecule in this path will result in the decrease of inhibitors. This would allow the cell to transverse the cell cycle checkpoints and continue proliferating.

(c) P53 promotes the expression of inhibitors of cyclins/CDKs. Therefore when dysfunctional, inhibitors are decreased, again allowing the cell to progress throught the cell cycle.

A number of other genes also directly affect the balance of the cell cycle, but are outside the remit of this thesis.

1.8 Cell proliferation

1.8.1 Background

"Unfortunately, long lived organisms such as vertebrates need substantial and continuous cell proliferation through out their extended lives, both for development and long-term maintenance and repair. In teleological terms, the evolutionary imperative of vertebrates has been to find a way to allow cell proliferation when needed, while at the same time efficiently suppressing the genesis of mutated cells leading to deregulated growth. When such measures fail, cancer is the inevitable consequence" (Evan and Vousden, 2001).

Cell proliferation *in vitro* and *vivo* has been studied extensively by using autoradiography to detect uptake of radioactive thymidine into cellular DNA. Autoradiography is a technique used to identify where a radioactive isotope is localised in cells or subcellular components. The process involves covering biological material with photographic film or emulsion. The radioactivity produced by the isotope then causes local exposure of the overlying film or emulsion, which on development can be detected as dark grains close to the location of the isotope. By using this technique the cell nuclei that have incorporated the isotope during the thymidine exposure can then be identified. The proportion of labelled cells at a short interval after administration of tritiated thymidine (the *labelling index or S phase fraction*) is a measure of the proportion of cells that were in S phase. All the basic concepts of cellular proliferation have been derived from experiments using tritiated thymidine and autoradiography. The study of cell proliferation has now largely been superseded by flow cytometry which is an easier method to study cell cycle properties. This technique involves tagging cells with a

fluorescent dye whose binding to the DNA is proportional to the DNA content. The cells are then directed in single file through a laser beam. The intensity of fluorescence induced by the laser light is detected and the number of cells exhibiting different levels of fluorescence is recorded. DNA distributions are then analysed by computer, using mathematical models that allow estimation of the proportion of cells in each phase of the cell cycle.

Thymidine labelling has been used to estimate the cell cycle time T_c and the duration of individual phases of the cell cycle. In many normal tissues of the adult, only a small proportion of the cells are actively proliferating. Of the remaining cells, many are either differentiated or quiescent. Examples of the latter (quiescent) include, bone marrow stem cells, skin cells that participate in wound healing after damage and hepatocytes that proliferate after partial hepatectomy. These non cycling cells that retain their capacity for proliferation are referred to as a G0 population. Most tumours also contain non proliferating cells and in 1962 Mendelsohn introduced the concept of a tissue growth fraction, which is the proportion of cells within a tumour that are actively proliferating (ie progressing through the cell cycle) (Slingerland and Tannock, 1998). He suggested that cells could exist in one of three possible growth states (Mendelsohn, 1962).

i)   actively dividing (cycling cells)

ii)   incapable of further division (terminally differentiated cells)

iii)   presently inactive, but could be stimulated to undergo division (quiescent cells)

Although the growth fraction can be estimated by thymidine labelling and autoradiography, other specific enzymes exist as proliferation dependent markers which can be detected by flow cytometry. The estimate of the growth fraction is useful since most chemotherapeutic agents are more toxic to proliferating cells and the growth fraction would therefore indicate the proportion of tumour cells that might be sensitive to cycle-dependent chemotherapy.

1.8.2 Cell proliferation in normal tissues

The rate of normal cell proliferation varies considerably in different tissues. Table 1.5 below shows examples of normal tissues with differing proliferative properties.

Tissues which are continuously rapidly proliferating	- Bone marrow - Gastrointestinal mucosa - Hair follicles - Testicular germ cells
Tissues which are continuously slowly proliferating	- Tracheobronchial epithelium - Vascular endothelium
Tissues which proliferate in a cyclical fashion	- Glandular female breast cells - Endometrial lining of the uterus
Tissues with the capacity to proliferate after injury	- Liver - Bone
Non-proliferating tissues	- Skeletal muscle - Cardiac muscle - Cartilage - Neurones

Table 1.5 Proliferative properties of normal tissues.

Some tissues virtually cease replication once the body reaches maturity whilst others produce millions of new cells every day up to the time of death. The effects of cytotoxic

drugs will be most obvious in those normal tissues which are dividing most rapidly, and

hence it is risk of toxicity to these tissues which limits the usefulness of the

chemotherapeutic drugs.

1.8.3   Cell proliferation in CRC

In normal colonic mucosa, proliferating cells are predominately located in the

lower two thirds of the crypts one of the first steps in colonic carcinogenesis is increased

cell proliferation and an upward shift of the proliferation zone of colonic crypts. This

expansion of the proliferative compartment has been shown to be a feature at all stages of

malignant progression (Shpitz et al., 1997).

i) Proliferation as a early marker

One of the earliest events in colorectal carcinogenesis is the alteration of the

proliferation of epithelial cells in colonic crypts (Srivastava et al., 2001). Bird et al was

one of the first to describe crypts in mice which were larger, thicker and darker than

normal (Bird, 1987). Further work postulated that these abnormal crypts might be

precursors of cancer and they were described as aberrant crypt foci (ACF) (Tudek et al.,

1989). In the early 1990's ACF were described by Pretlow et al in the human colon

(Pretlow et al., 1991). Cheng et al looked at crypt production in normal and diseased

human colonic epithelium and interpreted the results as that the rate of crypt production

in human colonic epithelium is increased in a number of disease states (Cheng et al.,

1986).

The idea of abnormal proliferation resulting in ACF in humans was furthered by Pretlow when he observed their presence in human colon cancer by staining them with carcinoembryonic antigen (Pretlow et al., 1994).

We now understand that larger ACF with altered morphology, dysplastic histological findings, altered cell kinetics and mutations in some genes involoved in colorectal carcinogenesis, are the most probable candidates for the progression to carcinoma. It is also evident that ACF have most of the requisites necessary for use as practical early biomarkers of cancer risk.

The importance in identifying this alteration in cellular proliferation is critical in the identification of colorectal cancer and seems to be fundamental in the progression of the disease.

ii) Proliferation in colorectal adenomas and polyps

The genetic mutations leading to the transition of normal mucosa through to polyp formation and eventually carcinoma have been discussed in section 1.1.2 and 1.7.3.

Hyperproliferation is believed to develop in pre-neoplastic epithelium implying the involvement of the APC gene. There is currently a lack of understanding into the histogenesis of sporadic human colorectal hyperplastic polyps and colorectal adenomas. It has also been postulated that sporadic adenomas and polyps grow because of elevated rates of crypt fission (Wong et al., 2002). This event involves the basal bifurcation followed by longitudinal division of the crypt secondary to deregulation of the cell cycle.

Studies have shown that a high rectal mucosal proliferation indices is associated with an increase risk of CRC (Deschner et al., 1988; Gerdes et al., 1993; Lipkin et al.,

1987; Paganelli et al., 1990; Risio et al., 1988; Risio and Rossini, 1993; Roncucci et al.,

1988; Rozen et al., 1990). In a study attempting to correlate rectal mucosal proliferation

with the development of adenomas, a cohort of 333 patients who had had at least one

adenomatous polyp removed underwent rectal biopsy from which a labelling index was

calculated. No association was found between rectal mucosal proliferation index and

adenomas (Sandler et al., 2000).

1.8.4 Proliferation as a prognostic marker in colorectal cancer

The role of DNA analysis in the prediction of the outcome of patients with CRC

has been investigated using flow cytometry in a number of studies. Venkatesh et al

performed flow cytometry and DNA analysis on 248 patients with CRC and found that

the combined presence of aneuploidy and an S phase fraction over 20% indicated a

poorer prognosis (Venkatesh et al., 1994). In a study conducted by the North Central

Cancer Treatment Group flow cytometry was again used to assess DNA content and cell

proliferation in 692 patients with stage B2 or C CRC. In this study the proliferation index

was a significantly strong prognostic factor. In addition those patients with diploid

tumours had a higher survival rate than those with nondiploid tumours. When these two

parameters were combined, those patients with both diploid and low proliferative rate

tumours had a five year survival of 74% compared to 54% five year survival for those

patients with high proliferative non diploid tumours (Witzig et al., 1991). A Southwest

Oncology Group study found contradictory evidence in a study using genetic mutational

status and S phase fraction to try and predict the clinical behaviour of CRC. In this

randomised trial of 66 patients with stage II and 163 with stage III disease, where they

received either surgery and observation or surgery and adjuvant levamisole or 5FU +

levamisole, no association was seen between a high proliferative rate in the cancer and a

poor prognosis in either stage of the disease (Ahnen et al., 1998).

The clinical implications that S phase fraction had for the assignment of adjuvant

chemotherapy has been investigated using flow cytometric DNA analysis on resected

specimens from 167 patients with stage I or II CRC. In both stages there were groups of

patients with high and low S phase fractions. Those subgroups with a high S phase

fraction had significantly worse recurrence rates implying that this biological marker

might help in identifying which patients may benefit from chemotherapy (Cascinu et al.,

1998).

1.8.5 Quantifying proliferation using Ki-67

The recent use of immunohistochemistry using the MIB-1 antibody, which

recognises the cell cycle associated Ki-67 protein allows an easier way to assess

proliferation. The human Ki-67 antigen is a huge protein encoded by a single gene on

chromosome 10, whose expression is tightly controlled by the cell cycle. It is expressed

in all proliferating cells during late G1, S, M and G2 phases but not in the G0 phase of the

cycle. It is known that Ki-67 is vital for cell proliferation, since removal of the antigen

results in cessation of the process (Schluter et al., 1993). The application of

immunohistochemical techniques to assess cellular proliferation is preferred as it

preserves the architecture and cytology of histological material without relying on *in vivo*

administration of thymidine analogues (Hall and Levison, 1990; Hall and Woods, 1990)

The antibody which identifies Ki-67 has been shown to be an excellent indicator of proliferation in histological material (Brown and Gatter, 1990; Hall and Woods, 1990), but was limited in surgical pathological practice by only being effective on cryostat sections. The development of the MIB-1 antibody, has allowed the ki-67 antigen to be recognised in formalin fixed and wax embedded material (Cattoretti et al., 1992). It has been shown to be a robust marker of cell proliferation easily applicable to archive material (McCormick et al., 1993).

1.8.6 Ki-67 and CRC

There have been contradictory reports regarding the potential role of Ki-67 as a prognostic indicator in CRC. Ki-67 was selected to assess the proliferation characteristics because of its potential value in predicting both prognosis and those individuals who may or may not benefit from adjuvant chemotherapy. Palmqvist et al showed that those tumours with low Ki-67 expression at the invasive margin had a poor prognosis (Palmqvist et al., 1999), whilst Kimura et al concluded that the tumours with high expression at the site of deepest invasion had a worse prognosis (Kimura et al., 2000). In contrast both Kubota et al who analysed 100 cases of CRC using Ki-67 (Kubota et al., 1992) and Kyzer et al who examined 30 resected specimens of CRC concluded that Ki-67 could not be used as a prognostic determinate in CRC (Kyzer and Gordon, 1997).

The prognostic value of Ki-67 in CRC has recently been revisited by the National Surgical Adjuvant Breast and Bowel Project Collaborative Study Group in a retrospective study of 706 patients with Dukes B and C disease to try and define a marker on which therapeutic decisions could be made with greater precision. Significant prognostic value

was found for patients with Duke's B and C colonic cancer with respect to recurrence free survival as in addition to overall survival. In this study Ki-67 labelling indices were unable to differentiate between groups who might benefit from adjuvant chemotherapy (Allegra et al., 2003).

1.9 Thymidine PET tracers

1.9.1 Background

As previously discussed, the incorporation of thymidine nucleotides into DNA during the S phase, has allowed the study of cellular proliferation in tumour cells.

The thymidine nucleotides arise from two pathways *de novo* and *salvage* (see figure 1.4). The salvage pathway involves exogenous thymidine entering the cell by a process of facilitated diffusion (Vijayalakshmi and Belt, 1988) which then undergoes successive phosphorylations by the enzyme thymidine kinase (section1.10.3) through deoxythymidine monophosphate (dTMP) and deoxythymidine diphosphate (dTDP) to eventually form deoxythymidine triphosphate (dTTP). dTTP is then incorporated into the DNA following polymerisation by DNA polymerase. The *de novo* pathway uses endogenous thymidine by converting deoxyuridine monophosphate (dUMP) to dTMP by the action of the enzyme thymidylate synthase.
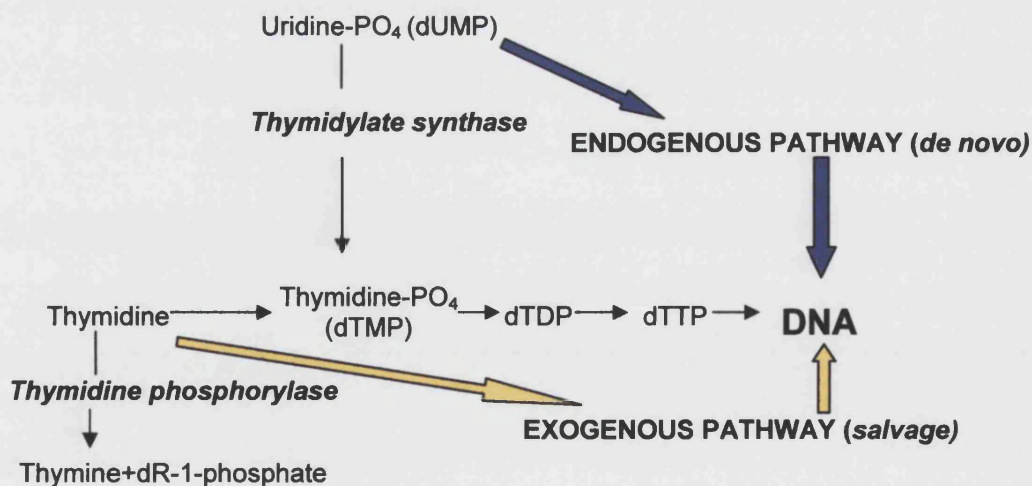
Figure 1.4 *De novo* and *salvage* pathways of DNA synthesis

Thymidine in the precursor pool is derived by both pathways but mainly by local production *(de novo)*, although there is an inverse relationship. The utilisation of the endogenous production can be suppressed by exogenous thymidine is supplied in sufficient amounts and vice versa. Unless there is a shortage of DNA precursor nucleosides the rate of DNA synthesis depends on the "proliferative state" of the tissue and not on the concentration of precursors.

The previous mentioned studies in section 1.10.4 have demonstrated the use of thymidine in the estimation of the tumour growth fraction or labelling index and the relationship that this has with prognosis. The possible implications of how tumours with a higher or lower proliferative rate will respond to both chemo and radiotherapy is a field which has prompted much investigation in the nuclear medicine world through the conduit of thymidine labelled PET tracers.

1.9.2 Thymidine tracers for imaging proliferation

There are three main criteria in choosing a good imaging agent for PET imaging of cell proliferation:

i)   Proliferating cells should take up the tracer and incorporate it into DNA or utilise it in the pathway of DNA synthesis.

ii) Metabolite production which could contribute to images should be kept to minimum.

iii) It must be readily labelled with a positron emitter for imaging.

Radiolabelled thymidine

Since thymidine is not incorporated in the synthesis of RNA, it became the logical choice for measuring cell growth by introduction of the labelled thymidine nucleoside into the pool of exogenous substrate for growing cells. Labelled thymidine nucleotides would not be useful as tracers as they do not cross the cell membrane.

In view of this, the first PET radiotracer developed for the non invasive imaging of cellular proliferation was carbon 11 labelled thymidine. It is a short lived tracer with minimal radiation burden and the potential to be repeated during a course of therapy. [11C]-Thymidine was initially labelled in the methyl position [methyl-11C]thymidine (Christman et al., 1972; Sundoro-Wu et al., 1984) but during the 1990s further progress led to labelling in the ring 2 position, 2-[11C]thymidine. The difference in labelling positions is relevant in terms of metabolite production. Work by Conti and Goethals in the 1990s showed that to [methyl-11C]thymidine principally metabolises to radiolabelled thymine and labelled acidic metabolites (Conti et al., 1994; Goethals et al., 1995). These metabolites have access only into those cells that also accumulate thymidine and may not contribute to the background image in the same manner as more freely distributed metabolites. Shields et al found the main difference in labelling in the ring 2 position is that the principle metabolite is labelled CO_2 ($[11C]CO_2$) which is readily transported into tissues and therefore ubiquitous (Shields et al., 1992; Shields et al., 1996). When compared to the metabolites of the methyl labelled tracer, the likelihood of labelled CO_2 becoming trapped within the cells is much less and hence it is easier to differentiate between the metabolites and the thymidine incorporated into the DNA when one is attempting quantitative models of thymidine kinetics.

Both of these carbon 11 labelled tracers have been used in clinical studies. They have demonstrated uptake in a wide variety of human tumours. Eary et al studied the metabolism of 2-[11C]thymidine using PET in 13 patients with either primary or recurrent brain tumours and showed its potential for imaging brain tumour proliferation (Eary et al., 1999). Van Eijkeren et al looked at [methyl-11C]thymidine and its role in response to therapy in 13 patients with head and neck tumours. High tracer uptake specifically in the outer rim of tumour as compared to the central necrotic area was demonstrated (van Eijkeren et al., 1992). The role of [methyl-11C]thymidine in renal cell carcinoma was investigated in 11 patients by Edgren and colleagues. They looked at pre and post PET scans following treatment with interferon and interleukin-2, and found that the images could correctly identify progressive tumours (Edgren M et al., 1995). The potential of 2-[11C]thymidine being used to detect response to therapy in small cell lung carcinoma and sarcoma was investigated by Shields, who found that tracer uptake decreased after successful chemotherapy but, one week following initiation of therapy tracer uptake remained unchanged in those patients with progressive disease (Shields et al., 1998a). Recently a study by Wells et al assessed proliferation *in vivo* using 2-[11C]thymidine PET in advanced intra-abdominal malignancies. This group found that 2-[11C]thymidine PET derived parameters correlated with Ki-67 immunohistochemistry and that the measurement of 2-[11C]thymidine in tumours using PET can provide a surrogate marker of proliferation and also supports its potential as an early assessor of response to antiproliferative cancer treatment (Wells et al., 2002).

Although both the 2- and methyl labelled [11C]-thymidine show great promise as a PET tracer of cellular proliferation, their widespread use is hampered by the poor image

quality and calculation of proliferation rates due to its rapid in vivo metabolic breakdown and the short half life of C-11.

These impracticalities of its use in routine clinical PET imaging has led to further research in a bid to develop a more stable thymidine analogue which has fewer labelled metabolites using longer lived isotopes. Several groups have looked at alternative tracers labelled with 18F or 124I because of their longer half lives involving the investigation of 18F-labelled 2'-fluoro-5-14C-methyl-1-beta D- arabinofuranosyluracil (FMAU) (Bading et al., 2000; Conti et al., 1995) and 124I-labelled-iododeoxyuridine (Blasberg et al., 2000). This pursuit led to the development of 18F-3'-deoxy-3'-fluorothymidine (FLT).

1.10 Development of FLT

1.10.1 Background

3'-deoxy-3'-fluorothymidine (FLT) was originally investigated as an antiviral chemotherapeutic agent in the treatment of patients with human immunodeficiency virus (HIV) (Flexner et al., 1994). Clinical trials were abandoned secondary to persistent haematological toxicity observed in patients treated with FLT. The first description of Fluorine -18 labelled FLT was by Wilson et al in 1991 (Wilson et al., 1991). Further modifications to the radiosynthesis by Grierson et al (Grierson and Shields, 2000), led to Machulla et al developing a simplified approach for the synthesis of FLT which was easily reproducible for a clinical application (Machulla et al., 2000).

1.10.2 Transport, metabolism and trapping of FLT

FLT enters the cell by the complex method of equilibrative facilitated diffusion. Work by Vijayalaskshmi and Belt found two sodium dependant mechanisms for transport of this thymidine nucleoside in mouse intestinal epithelial cells (Vijayalakshmi and Belt, 1988). Further work involving nucleoside transport in human normal and neoplastic cells demonstrated the presence of two transporters, the nitrobenzylmercaptopurine riboside (NBMPR) *sensitive equilibrative transporter and* NBMPR *insensitive equilibrative transporter* (Belt et al., 1993).

It is difficult to conclude that FLT is a substrate of these sodium dependant transport mechanisms but from cell line experiments it has been shown that initially there is a rapid accumulation of tracer followed by a phase of much slower accumulation (Mier et al., 2002).

1.10.3 Thymidine kinase

The initial rapid accumulation is thought to be associated with the metabolism of FLT. Once within the cell FLT undergoes phosphorylation by the cytostolic enzyme thymidine kinase-1 (TK1). TK1 is the principle enzyme in the DNA – salvage pathway. TK1 catalyzes the one step ATP-dependant phosphorylation of thymidine to thymidine monophosphate which is then incorporated into DNA as decribed in section 1.9.1.

TK1 activity is selectively upregulated in the G1/S transition phase of the cell cycle, reaching its maximum in the late S phase and then declines rapidly in the G2 phase (Sherley and Kelly, 1988). The imbalance in the enzymic characteristics of TK in colon tumours was first demonstrated by Herzfeld et al in 1978 who noticed that the mean activity of TK was several times higher than in non neoplastic colon (Herzfeld et al., 1978). Further work by Weber et al again demonstrated that in rapidly growing human colon carcinoma xenografts the activity of this salvage pathway was again elevated (Weber et al., 1981). Increased activities of TK isoenzymes were also investigated by Sakamoto et al who found a five fold increase in human colon tumour cells when compared to colon polyps (Sakamoto et al., 1985). Following this, he also investigated the effects of carcinogenesis on colonic TK activity in FAP (see section 1.1.2) and highlighted that this enzyme might have potential acting as a biochemical marker in determining the subsequent development of CRC (Sakamoto et al., 1992). In contrast FLT is a poor substrate for thymidine kinase-2 (TK2), one of the other deoxyribonucleoside kinases (Toyohara et al., 2002).

As a salvage pathway enzyme, TK1 fluctuates with DNA synthesis, the activity being high in proliferating and malignant cells and low or absent in quiescent cells (Munch-Petersen et al., 1995). This S phase specific role of the enzyme as a proliferative marker has been investigated in 1,692 primary breast cancer patients with high TK1 values, proving TK1 to be an important risk factor in node negative disease. In addition, TK1 was associated with a beneficial effect in those patients receiving anti-metabolite chemotherapy, leading to the possibility of it having a role in forming the basis for new therapeutic approaches involving DNA salvage pathway inhibition using anti-metabolites (Broet et al., 2001).

The phosphorylation of FLT by TKI, leads to the formation of negatively charged FLT monophosphate (FLTMP) as shown in figure 1.5.
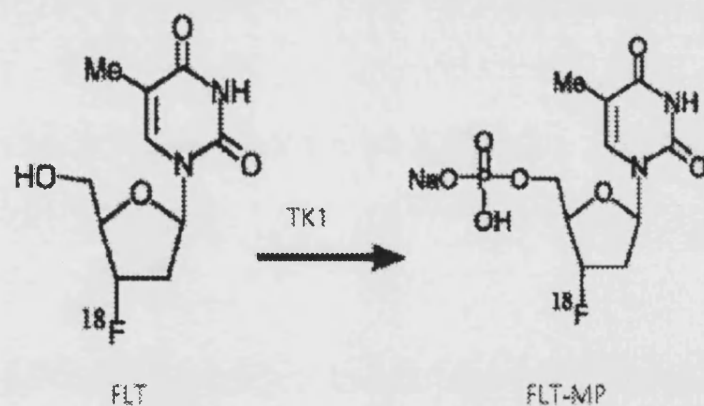
Figure 1.5 Structure of FLT and FLT-MP, following phosphorylation by TK1.

The negative charge is responsible for the intracellular trapping of FLTMP which, in a way analogous to the phosphorylation of FDG to FDG-6-phosphate by hexokinase, leads to the accumulation of radioactivity (see figure 1.6).
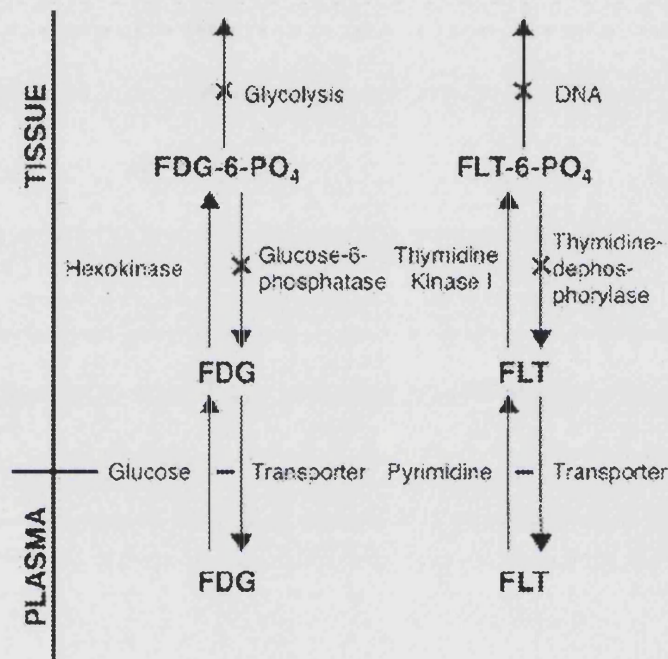
Figure 1.6 Phosphorylation pathways of FDG and FLT (from Positron Emission Tomography scanning: current and future applications; Czernin J and Phelps ME. Annu. Rev. Med. 2002 53:89-112)

Via this metabolic pathway, FLT acts as a surrogate measure of proliferation by reflecting TK1 activity in the cell cycle. Work to validate this has been carried out in cultured human lung carcinoma cells where FLT uptake was positively correlated with cell growth and TK1 activity. When cell cycle progression was inhibited, it prevented an increase in TK1 activity in addition to FLT uptake thus suggesting that FLT images are a reflection of TK1 activity and the percentage of cells in S phase (Rasey et al., 2002). Further work by Toyohara et al, comparing [³H]FLT uptake with [³H]thymidine in 22

asynchronously growing tumour cell lines showed a correlation between [^{3}H]FLT uptake

and both %S phase fraction (R=0.76) and [^{3}H]thymidine uptake (R=0.88) again

demonstrating that FLT uptake reflects tumour cell proliferation. In addition, the authors

found that after 60 minutes incubation, over 90% of the [^{3}H]thymidine was found to be

incorporated into the DNA as compared to negligible (0.2%) amounts of [^{3}H]FLT. The

lack of [^{3}H]FLT incorporation into DNA again highlights that FLT is a marker of cell

proliferation through the enzyme TK1 but is not (as thymidine is) a substrate for DNA

synthesis (Toyohara et al., 2002).

1.11 Aims of thesis

Following the success of FDG PET in the imaging of colorectal cancer I aim to investigate the new tracer of cellular proliferation 3'-[18F]Fluoro-3'-deoxythymidine (FLT) and its potential role in colorectal cancer imaging through conducting both clinical and cellular studies.

In chapter 3, the *in vivo* characteristics of FLT utilisation in colorectal cancer is investigated by comparing different analytical methodologies.

The potential use and impact that FLT could have in imaging CRC is addressed in Chapter 4, by conducting a comparative study with FDG in patients with proven CRC.

Having established that it can be used as an imaging tool in this disease, Chapter 5 attempts to assess if it can be used to quantify cellular proliferation *in vivo*, by correlating quantification of *in vivo* uptake of FLT in CRC with quantification of proliferation using immunohistochemistry.

Finally in Chapter 6 the potential role of FLT in assessing response to therapy is attempted by conducting *in vitro* experiments with CRC cell lines and the chemotherapeutic agent 5 Fluorouracil.

The conclusions from this work are discussed in chapter 7.

CHAPTER 2

Materials and Methods

2.1 Patients

The protocols for specific laboratory studies are described within the relevant chapters. To avoid repetition, this chapter covers the methodology which is common to all the clinical studies.

2.1.1 Patient recruitment

The patients who took part in the following studies were all prospectively recruited from surgical and oncology outpatient clinics. Inclusion criteria were simply the presence of primary or metastatic CRC or a combination of the two. The diagnosis of CRC was made on either histology or clinical and radiological follow up. Radiological follow up consisted of computerised tomographic colonography (CTC) or virtual colonoscopy (VC), see section 2.5 for details. In order for the studies to be conducted, approval was obtained from the Ethics Committees of University College London (UCL) and University College London Hospital NHS Trust (UCLH) (appendix B). Additionally the relevant approval from the Administration of Radioactive Substances Advisory Committee (ARSAC) was also obtained (appendix C).

The patient data set were stored within a Dell™ personal computer using Microsoft Excell™ software. The data were handled in accordance with the Data Protection Act and comprised the patient's:

i)   Name

ii)   Age

iii)   Date of birth

iv)   Disease information

v)   Results of imaging

At no time did investigations relevant to this thesis hinder the routine process of

clinical investigation and treatment of these patients.

2.2   Whole body FDG-PET scan

2.2.1   FDG

The FDG used for the studies within this thesis was obtained from 4 centres:

i)   Addenbrookes Hospital, Cambridge (Wolfson Brain Imaging Centre)

ii)   Hammersmith Hospital (IRSL Cyclotron Unit)

iii)   St Thomas' Hospital (PET Centre)

iv)   PET Net Pharmaceuticals (Mount Vernon Hospital)

Arrival of the tracer would be between 9.00 and 9.30am and, prior to injection into a patient, notification that it had passed its quality control would be confirmed by fax from the producing cyclotron. The dose calibrator in figure 2.1 was used to assay the FDG which underwent daily quality control testing before the tracer consignment was assayed (see appendix D). The delivery details documented the volume of liquid dispensed into the FDG vial, the time at which the FDG was measured prior to dispatch, in addition to the assayed activity. This information was recorded on a radiopharmaceutical holding patients record sheet (appendix E).

Figure 2.1 Dose calibrator

FDG is drawn out of the dispensing station using a 23 gauge needle and a 5ml syringe in a lead syringe holder. Using the dose calibrator and the decay chart (appendix F) a dose of up to 400MBq (although a higher dose can be administered in heavier patients) was prepared for patient injection. The guidance for the clinical administration of radiopharmaceuticals is in appendix G.

2.2.2 Patient preparation

To achieve normoglycaemia, patients were asked to starve for six hours prior to the scan but were allowed to drink water. For tracer quantification purposes a patient information sheet was used to record a brief history, the patient's height (cm), weight (Kg) and blood glucose level (mmol/l) (checked on a commercial glucometer (Glucometer Elite, Bayer Pharmaceuticals, Newbury, Berkshire, UK). A glucose level below 8.5mmol/l was accepted as a cut off for the studies in this thesis, in line with the protocol for clinical imaging in the Institute of Nuclear Medicine. The injected dose of tracer and the residual left in the syringe post injection were also recorded so an accurate administered dose could be calculated.

Prior to injection, the patient was cannulated using a 16 gauge cannula inserted into a forearm vein. To aid relaxation and help prevent the uptake of FDG in skeletal muscles 5mg of oral diazepam was also administered. Following injection the patient was left alone for 45 – 60 mins and asked to lie still before scanning.

To achieve standardisation of the methodology patients were not routinely catheterised or given a diuretic to reduce renal tract accumulation of FDG, but were asked to empty their bladder immediately prior to scanning.

The patient was positioned on the scanning bed with feet facing away from the gantry with a pillow placed under the knees for comfort and arms placed on either side. Strapping was placed around the arms for support and to help keep them still.

Data sets from the base of the skull to the upper third of the lower limb were obtained for all whole body scans.

2.2.3 Acquisition of whole body FDG scan

In all patients except for two patients in chapter 3, Whole body FDG-PET imaging was performed in 2D mode using the Discovery LS^{TM} (GE medical systems, Milwaukee, USA) which is the hybrid PET/CT scanner shown in figure 2.2. These two were imaged using the GE Advance^{TM} (GE medical systems, Milwaukee, USA). In chapters 4 and 5 the PET emission datasets were attenuation corrected utilising the CT capability of the Discovery LS^{TM} (Visvikis et al., 2003). Spiral CT scans were acquired using a speed of rotation and couch movement of 0.8s and 22.5mm per rotation, respectively, with a slice thickness of 5mm. The CT images were subsequently converted to maps of PET attenuation coefficients using a bilinear transformation (Visvikis et al., 2003). Transaxial emission images of 4.3×4.3×4.25mm^3 (matrix size 128×128×35) were reconstructed using ordered subsets expectation maximisation (OSEM) with two iterations and 28 subsets. These slices were re-orientated to produce whole body coronal and sagittal images.

96
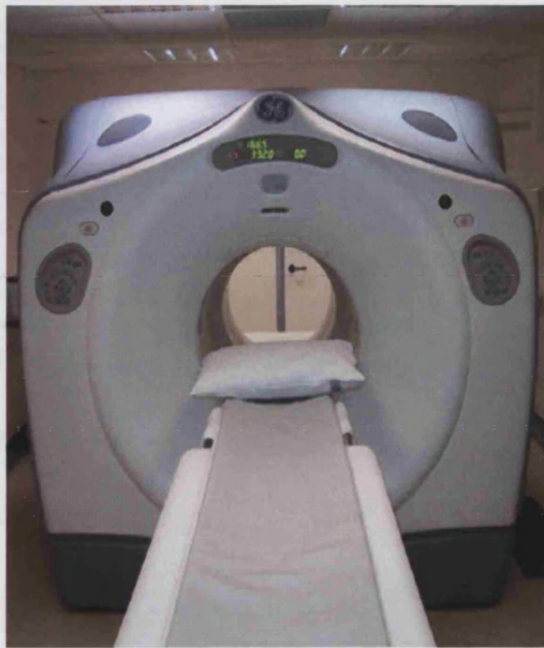
Figure 2.2 Discovery LS™ hybrid PET/CT scanner (GE medical systems, Milwaukee, USA)

In order to minimise any potential bias introduced by using different attenuation correction techniques within the patient group considered in chapter 3, all of the patients included in that group had their PET images corrected for attenuation effects using the two rotating ^{68}Ga/^{68}GE rod sources.

2.3   Whole body FLT- PET scan

2.3.1 Radiosynthesis of FLT

The FLT used for the studies within this thesis was produced by the IRSL

Cyclotron Unit (Hammersmith Hospital). This was developed by Cleij et al at the IRSL

(Cleij MC et al., 2001), using an automated synthesis system, a photograph of the system

with a corresponding schematic diagram below is shown in figure 2.3 .The complex

radiochemistry leading up to this method of FLT synthesis is outside the scope of this

thesis but below is a simplified, brief description of the final production method for

human use with references to the components seen in figure 2.3.

Enriched $H_2{}^{18}O$ was irradiated and transferred into a glassy carbon vessel (figure

2.3). Kryptofix 2.2.2 (15mg, 40μmol) and K_2CO_3 (30 μmol) in acetonitrile (1ml) was

added to the [^{18}F]fluoride and the vessel heated to 140°C for 6min under helium. From

reservoir 2 a second addition of acetonitrile (0.2ml) was made and the vessel heated to

170°C for 3min. Dimethyl Sulfoxide (DMSO) (1.0ml) was then added from loop 1 over

30 seconds and the mixture stirred for 10min at 170°C. A solution of the [^{18}F]FLT

precursor (20mg) in DMSO (0.2ml) was added from loop 2 over 10s. The vessel was

sealed and the reaction mixture heated for 10min at 170 °C. The vessel was then cooled to

100 °C over 5min. Aqueous 1M Hydrochloric acid (HCL) was added from loop 3 and the

reaction mixture stirred for 1min. An aqueous solution of (NaOAc) (0.5M, 1.5ml) from

reservoir 3 was then added and the reaction mixture passed through a neutral alumina

Sep-pak. From reservoir 4, 2ml of water was transferred via the reaction vessel through

the Sep-pak. The combined aqueous eluate was loaded onto a semi-prep C_{18} column
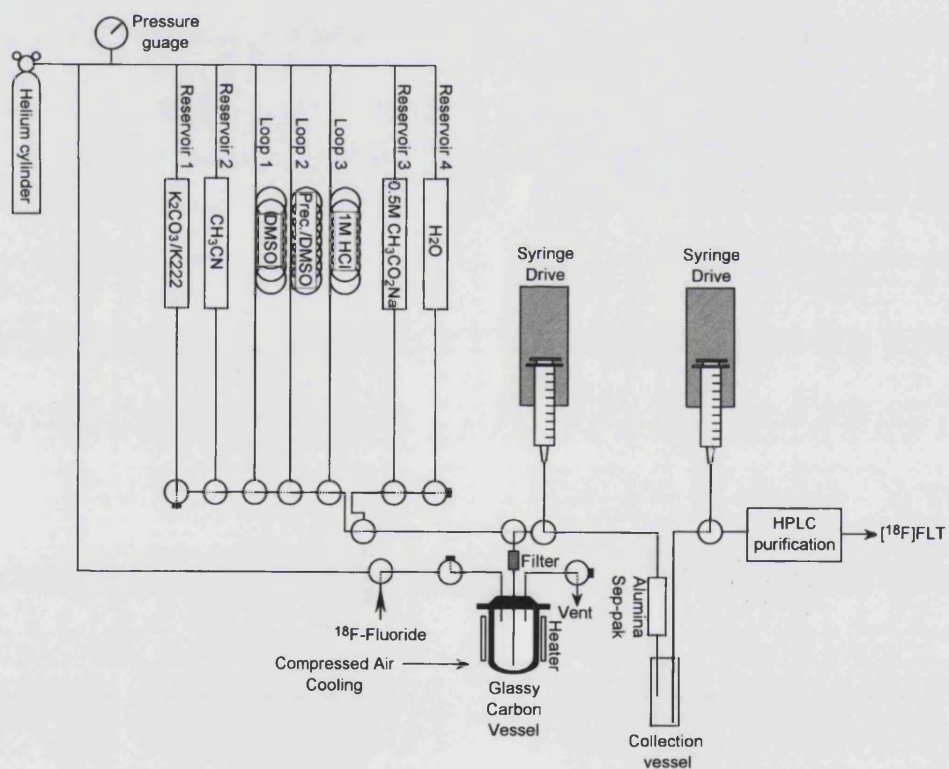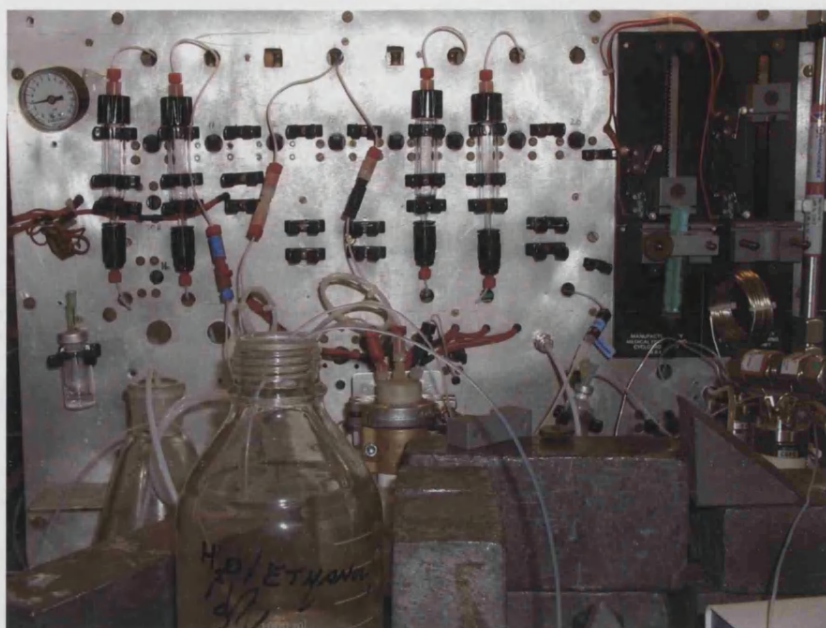
Figure 2.3 Automated FLT synthesis system (top) with schematic diagram of apparatus (bottom).

(Phenomenex Luna, 250mm, 5μ) and eluted with 10% ethanol at a flow rate of 7.0ml/min. The eluate was monitored for radioactivity and absorbance at 254nm. [^{18}F]FLT was eluted between 10-12min. The radiosynthesis produced between 1.85 − 3.70 GBq of tracer in 60min using this automated synthesis system.

Prior to dispatch from the IRSL, the FLT would undergo quality control testing; received doses were >95% pure.

2.3.2 Dose calibration

On arrival, the FLT was assayed using the dose calibrator in an identical manner as previously described for FDG. The same information recording drawing up process was also employed (see section 2.2.1).

2.3.3 Patient preparation

For FLT scanning patients were not asked to starve, as glycaemic state has no influence on cell proliferation. The rest of the patient preparation was as described for FDG in (section 2.2.2).

2.3.4 Acquisition of whole body FLT- scan

The same hardware was utilised to acquire whole body FLT images as has been previously described (section 2.2.3). The datasets were also attenuated corrected in the same manner.

2.4 Evaluation of tracer uptake

A number of strategies exist for quantifying tracer uptake. For this thesis the following methods in increasing order of complexity were employed:

2.4.1 Visual analysis

Visual qualitative inspection of static images are made after tracer accumulation reaches its plateau concentration. This technique is useful for the identification of focal areas of high tracer accumulation within metabolically active areas. The advantage of visual analysis is that it is simple but the interpretation of subtle changes is difficult.

Whole body data was analysed in terms of the pattern of distribution of labelled FDG and also with respect to the measurement of tracer uptake at a specific site. The quality of the data obtained depends significantly on the figures of merit of the instrument used, software available and amount of tracer administered. Normal and significant FDG uptake is always seen in the brain, frequently, but variably, in the myocardium, stomach, liver, spleen, muscle and the lumen of the gastrointestinal tract. The bone marrow is seen, with variable intensity, often reflecting response to chemotherapy. The FDG tracer is eliminated by the kidneys, which are depicted along with the urinary bladder. Since the data is recorded in 3D, data sets formatted into any plane (transaxial, coronal, and sagittal) can be displayed and inspected.

Consensus reporting was used to analyse and issue a clinical report on each FDG-PET scan. This procedure involved visual inspection of coronal, sagittal and transaxial images for each patient in addition to the CT data in those scans acquired using the GE Discovery LS™. Those present at each reporting session would include at least one

Nuclear Medicine physician of consultant grade and the physicist and radiographer who carried out the injection and imaging.

Direct comparisons were made between the FDG PET scan and the corresponding FLT PET scan by a consensus opinion using visual inspection on a lesion by lesion basis.

2.4.2 Regions of interest

With the exception of chapter 6, a region of interest (ROI) approach was used to semiquantitate tracer uptake within both normal and malignant tissue.

In the case of the tumours, ROIs were drawn over all identified lesions in the images. Since the use of ROIs that encompass the lesions in their entirety, or the use of the slice with the maximum count density, may not provide an accurate activity concentration in the tumour active region, the method validated by both Lodge et al and Eary et al was employed (Eary and Mankoff, 1998; Lodge et al., 1999). Lodge's study used ROIs to look at FDG uptake in soft tissue masses and Eary investigated FDG metabolic rates in sarcoma. For each of the ROIs, five consecutive slices were used. The slices selected were comprised from the one with the maximum count density over each volume of interest and the four immediately adjacent slices.

2.4.3 Semi-quantitative analysis of tracer uptake (Standardised uptake values)

In order to obtain more than just qualitative findings in cancer studies semi-quantitative evaluations have been adopted. One such evaluation is the standardised uptake value (SUV) which is synonymous with the differential uptake ration (DUR) or

differential absorption ratio (DAR) .These parameters relate to the value of activity concentration found in a certain tissue volume of interest to the injected activity per the patient's body weight. This allows inter individual differences and varying amounts of administered activity to be taken into account. It must be remembered with this technique that the amount of activity found in a region is not always static and may change after tracer injection by increased uptake of the PET tracer or by washout of the tracer from the tissue; this is considered in more fully quantitative methods which are discussed below. SUVs are commonly used in PET oncology studies allowing an index of tracer uptake in a tumour which may permit differentiation between benign and malignant lesions.

For the studies in this thesis, SUV was defined as:

$$SUV = \frac{A \times W}{A_{inj}}$$

Where (A) is the average tumour activity concentration in kBq/ml, (W) the patient's body weight in kg and (A$_{inj}$) the injected activity in kBq (Graham et al., 2000; Takeuchi et al., 1999)

The calculated value relates to the activity concentration found in a certain tissue region of interest (ROI) to the activity per the patient's body weight. In this way inter individual differences and varying amounts of administered activity are taken into account. The amount of activity found in a region is, however, not always static and may change after tracer injection by increased uptake of the tracer or by washout of the tracer from the tissue.

2.4.4 Quantitative analysis of tracer uptake

A quantitative measurement of local tracer utilisation can be obtained using a kinetic model that closely resembles the movement of the tracer *in vivo*.

These types of kinetic studies were used in chapter 3 to provide a means of obtaining values for physiological parameters for FDG and FLT in absolute units. For example using FDG, glucose metabolic rate can be determined in mol/min/g. The metabolic rate of a tracer is quantified by using the time course of radioactivity in tissue and in blood. This provides a more detailed description of the uptake characteristics and the possibility to determine individual rate constants. The explanation of this follows and is in terms of rate of glucose metabolism (MR_{gluc}) using FDG and is given by:

$$MR_{gluc} = (CP/LC) \cdot \{K_1 \cdot K_3/(K_2+K_3)\} = (CP/LC)K_i$$

CP is the plasma concentration of glucose.

K_1 and K_2 are rate constants for forward and reverse capillary transport of FDG.

K_3 refers to the rate of phosphorylation of FDG.

LC is the lumped constant relating FDG kinetics to that of glucose. Although this constant has been evaluated for brain (Lodge et al., 1999), it is not clear what value this should take in tumours. For the studies of this thesis the accepted value of 1 was used.

K_i is the net rate of influx of FDG.

For the calculation of this measurement, a dynamic imaging sequence (section 1.5.2) with simultaneous arterial blood sampling (section 3.3.3) is used and the model rate constants are estimated by fitting the tissue and plasma tracer concentrations data to the compartmentalised model which is shown schematically below. A fourth parameter can be introduced (K_4), this represents the rate of dephosporylation of the tracer. The

104

three-compartment model of FDG kinetics with the respective rate constants is demonstrated in figure 2.4. The same model is shown in relation to FLT metabolism in figure 2.5.
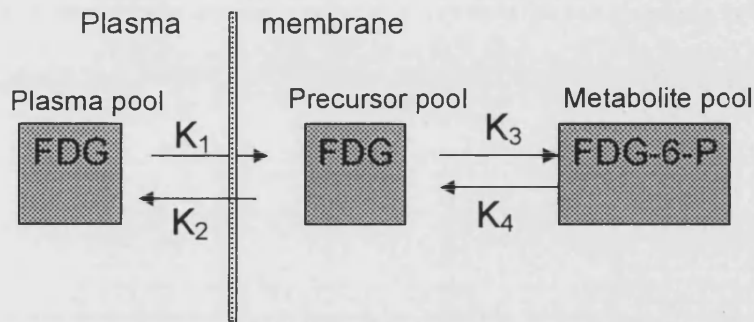
Figure 2.4 Three compartment model of FDG kinetics
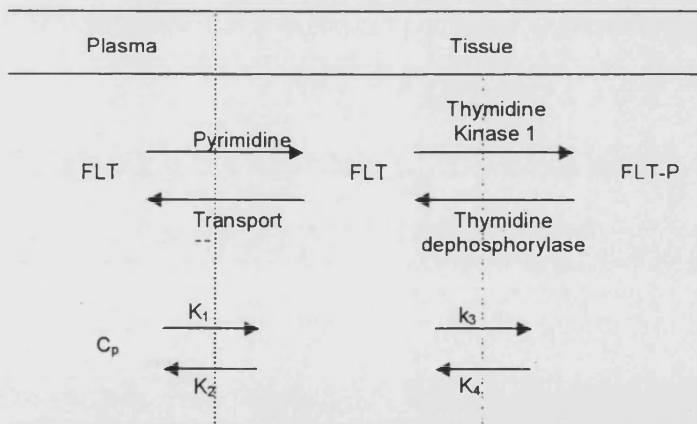
Figure 2.5 Metabolic pathway of FLT within three compartment kinetic model.

The two methods used in chapter 3 to fully quantify uptake of FLT were Patlak graphical analysis and Non linear regression.

i)   Patlak graphical analysis

Patlak et al developed a model which can be used for any tracer where uptake in the final compartment is irreversible and assumes no dephosphorylation and therefore K_4 to be zero. Although it must be realised that if K_4 is not zero then there will be an underestimation of the metabolic rate of the tracer. This method does not allow for the calculation of the individual rate constants K_1 and K_3 (Patlak et al., 1983).

This is based on the assumption that the ratio of the tracer concentration in tissue to that in plasma is linearly increasing when plotted as a function of normalised time, and is given by the following expression:

$$\frac{C_i(t)}{C_p(t)} = K_i \frac{\int_0^t C_p(t')dt'}{C_p(t)} + V$$

where, $C_i(t)$ and $C_p(t)$ is the tracer concentration in tissue and plasma at a particular time point t respectively, K_i is the tracer blood-tissue transfer constant or influx rate constant, V is a constant related to the blood volume.

For chapter 3, visual inspection was used to determine from the Patlak plots the time point where the linear behaviour commenced. K_i as the net influx constant was subsequently obtained from the slope of this linear part of the plot in units of ml/g/min.

ii) Non linear regression

The most straight forward method used to estimate the metabolic rate of a tracer is by fitting tissue time activity curves to a two-tissue compartment model using an arterial input function and non-linear regression routines by means of a mathematical model (Huang et al., 1980). This method has the advantage of not only obtaining the K_i but also the enzyme (K_3) activities.

There is debate regarding whether the hydrolysis of FDG-6-PO$_4$ to FDG (K_4) by phosphatase should be taken into account when estimating the metabolic rate of glucose. Original work by Sokoloff et al and furthered by Reivich et al (Reivich et al., 1979; Sokoloff et al., 1977) demonstrated negligible hydrolysis in the brain and therefore did not take K_4 into account. The opposite was found by Okazumi et al in hepatocellular carcinoma, where K_4 values were found to be similar or greater than K_3 this can be partly explained by the high level of glucose-6-phosphatase activity.

It is now accepted that for each tumour the presence and possible effect of K_4 should be investigated in order to establish its inclusion.

Dynamic imaging sequences as discussed in section 1.5.2 are required in order to establish time-activity curves. In addition arterial sampling as described in chapter 3 is also needed for the determination of an input function as well as blood time activity curves.

A three compartment (4K) model was used in conjunction with non-linear regression analysis. The kinetic constants describing the tracer pharmacokinetics for the three compartment model used were: K_1 and K_2 as the influx and efflux constants

respectively between the plasma to the free tracer compartment, while K_3 and K_4 are the

rates of phosphorylation and dephosphorylation respectively.

2.5 Computerised Tomography

2.5.1 Patient preparation

i) CT abdomen, pelvis, liver and chest

Patients are asked to not eat anything for four hours prior to the scan and can drink non-fizzy drinks upto one hour before the scan. No other special preparation is required. Oral contrast may be given just prior to CT of the abdomen and pelvis.

ii) CTC (CT pneumocolon)

Bowel preparation in order to clean the colon was required and this took place the day before the examination. Preparation involved ingestion of one sachet of oral picolax the day before the CTC (between 7.30 and 9 am for a morning appointment and before 7pm for an afternoon appointment). Patients were encouraged to drink clear fluids (approximately 500ml per hour) continuously and a low residue diet was allowed until approximately 18 hours prior to the scan. Immediately before the scan, patients were required to drink two glasses of water.

2.5.2 Image acquisition

i) Abdomen, pelvis and liver

CT scans of the abdomen and pelvis were contrast enhanced and performed in either a Somatom Plus 4 or a Somatom Plus 4 Volume Zoom (both Siemens AG Medical Engineering Group, Forchheim, Germany). The contrast used was Omnipaque 350 (Nycomed Amersham plc, Amersham Place, Little Chalfont, Bucks, UK.). Scanning protocol with the Somatom Plus 4 for the abdomen and pelvis involved 5mm contiguous

slices after giving 100ml intravenous contrast at 4ml per second with a 45-second delay.

For bi- or triphasic liver imaging patients were scanned at 20s, 50s, 180s with slices being 5mm thick at 2.5mm intervals. For the Plus 4 Volume Zoom CT scanner, abdomen and pelvis imaging involved dynamic multislice imaging with 3mm contiguous reconstructions after giving 100ml intravenous contrast at 4ml/s with a 45 second delay. For bi- or triphasic liver imaging patients were scanned at 35s, 50s, 180s with slices being 3mm thick at 1.5mm intervals.

ii) Chest

Standard, non-contrast enhanced scans were performed as detailed above.

iii) CTC (CT pneumocolon)

Patients were given 120ml of Omnipaque 350 intravenously at a rate of 5ml/s and scanned after a 25s delay. Scanning took place in the prone and supine positions (in order to reduce faecal artefact that may obscure mucosal lesions) after an initial scanogram was taken.

2.5.3 Image reconstruction and analysis

All data was processed on the CT scanner Siemens workstation where images were reconstructed accordingly. Images were usually formatted into the transaxial plane, but when necessary coronal and sagittal prints were produced on a SUN microsystems workstation.

A Radiologist of specialist registrar or consultant grade evaluated all images. In addition, all CT scans were presented at a weekly CRC MDT meeting where they were re-evaluated by a Radiologist of consultant grade. All films were visually analysed.

2.6 Confirmation of diagnosis and follow up

In line with guidelines issued by the government on optimal individualised care for patients with a confirmed diagnosis of CRC, a multi disciplinary team (MDT) managed all those patients presented in this thesis. This group consisted of both medical and allied healthcare professionals. Included in the group were radiologists, nuclear medicine physicians, surgeons, medical and clinical oncologists as well as nursing staff. The objective of the MDT is to offer the CRC patient the optimal care by harnessing the expertise of a variety of medical specialities, rapid referral between the specialists and maintenance of high standards through audit.

This group made consensus decisions regarding the clinical management of complex cases and therefore formed an ideal forum to present both PET and CT data in order to decide management based on this and relevant clinical information.

All diagnoses in the studies related to this thesis were confirmed either on histological evidence following biopsy or surgery or by careful clinical and radiological follow-up within the CRC MDT.

CHAPTER 3

Characterisation of *in vivo* FLT uptake in colorectal cancer

3.1 Background

PET allows the quantitative measurement of the concentration of positron-emitting tracers within a three-dimensional object *in vivo*. By using different radioligands, specific types of regional tumour metabolism can be measured. In the case of FDG the final aim has been the quantitative determination of glucose uptake. Since tumours exhibit a variety of different histological characteristics, the measurement of the rate constants within a "compartmentalised system" discussed in section 2.4.4 has to be independent, in order that values for physiological parameters in absolute units can be obtained. This will lead to a quantitative measurement of local tumour utilisation with regard to that tracer.

In this situation individual rate constants may be determined with the help of a dynamic PET measurement. This requires arterial blood sampling simultaneously with the PET image measurement. The resulting time activity curves can be evaluated by fitting the measured data to the dynamics of the tracer model so that the rate constants may be obtained.

The dynamic approach to determine individual rate constants is not readily compatible with the whole body PET protocols described in section 2.2.3. Dynamic rate constant measurements require additional imaging time, therefore this is not practical for routine clinical use and for the most part is limited to scientific investigations into new tracers. The acquisition of this dynamic data is described in the methodology of this chapter.

3.2 Aims

The aim of this chapter is to study the *in vivo* metabolism and pharmacokinetics of FLT in patients with primary and metastatic CRC. The objectives are to

i) compare uptake patterns of FDG and FLT.

ii) investigate potential methods for the quantitative assessment of in-vivo FLT utilisation.

iii) compare semi-quantitative with fully quantitative measures of FLT uptake.

3.3 Methods

3.3.1 Patient recruitment

All patients recruited for this study presented with either primary of metastatic CRC. This cohort was made up of patients referred internally to the UCLH NHS trust multidisciplinary team in addition to those referred from peripheral district general hospitals.

All patients were asked to give written consent following a full explanation of the procedure (appendix H).

Pre-scanning preparation details for both FDG and FLT imaging can be found in chapter 2.

3.3.2 Dynamic data acquisition

A total of eleven patients with a total of 20 malignant lesions (4 primary, 6 liver metastases, 5 lung metastases, and 5 extrahepatic metastases) were included in this investigation. All patients underwent FDG scanning followed by an FLT investigation with a median intervening period of 4 days (range 1-7). Imaging comprised of a 60min dynamic acquisition which commenced immediately following bolus tracer administration. The location for the dynamic acquisition was such that wherever available, multiple lesions were included in the field of view. That location was determined in conjunction with the CT scans available.

All data was acquired in 2D mode using the GE Advance in the case of 2 patients and the GE Discovery LS in the remaining 9. For the latter cases the CT facility was used to aid in the exact localisation of lesions. In order to keep all parameters during data

acquisition consistent within the group of patients included in this study, the CT attenuation correction capability of the GE Discovery LS was not employed. All emission datasets were corrected for attenuation using data acquired with two rotating ^{68}Ga/^{68}Ge rod sources.

The dynamic acquisition comprised of the following frame durations: 15 x 5 seconds, 3 x 15s, 6 x 20s, 11 x 60s, 9 x 300s. The time of transmission acquisition was 3 mins per axial field of view, which has been shown in the past by Visvikis et al to be reliable in reducing the overall data aquistion time without compromising the accuracy of SUV measurements (Visvikis et al., 2001). Transmission data was corrected for post-injection emission contamination and processed using an unsupervised segmentation algorithm prior to its utilisation for the attenuation correction of the emission data as described by Bettinardi et al (Bettinardi et al., 1999).

Transaxial emission images of 4.3 x 4.3 x 4.25mm^3 (matrix size 128 x 128 x 35 slices per axial field of view) were reconstructed using Ordered Subsets Expectation Maximisation (OSEM) with 2 iterations and 28 subsets. All images were decay corrected to the time of the first frame of the dynamic series and both scatter and random corrections were applied.

Following the end of the dynamic acquisition a whole body scan was performed with emission frames of 5min per bed position as described in section 2.2.3.

3.3.3 Acquisition of blood sampling data

Both arterial and venous blood was analysed in each FLT study. No blood sampling was undertaken during the FDG scans. Arterial blood was drawn from an

117

arterial line inserted into the patient's radial artery. Prior to this, bilateral arterial supply to the hand was confirmed and documented with hand held Doppler (Huntleigh Healthcare). Any doubt in the detectable presence of both a patent radial and ulnar artery excluded the patient from the study. The local anaesthetic lignocaine (2%, 0.5-1ml) was infiltrated subcutaneously followed by insertion of a 20 gauge cannula into the radial artery. The cannula was connected to a 3-way tap to aid rapid blood letting. Intermittent flushing of the line with heparinised saline prevented the arterial line from clotting off.

Venous sampling was carried out through a designated line, on the opposite side to the arterial line. This was via a 16 – 18gauge cannula which was inserted into a large forearm vein or into a vein in the ante-cubital fossa. Again a 3-way tap was attached and the line was regularly flushed.

In order to allow access to both the arterial and venous lines during the dynamic acquisition phase of the scan, the patient was positioned with arms above the head, supported by both arm and head rests. Figure 3.1 demonstrates the patient position used including the sites of both sampling cannulas. In addition, the venous line used for tracer injection is also shown.

A series of manual blood samples were taken from the arterial and venous lines during acquisition of the dynamic scan. A stop watch was started which coincided with the start of the scan enabling sampling at specific time points. A sample was taken every 7s for the first 2min post injection, followed by 30s intervals for the next 2min. Between 5-10min, a sample was drawn every minute, followed by 5min sampling up to 30 minutes. Thereafter blood samples were taken in 10min intervals until the end of the scan.

Figure 3.1 Patient positioning for arterial and venous blood sampling. The arterial and venous sampling cannulas are shown (a) and (v) in addition to the injection cannula (i).

The blood samples were collected in labelled 2ml syringes and a portion of each sample was centrifuged in the Eppendorf Minispin (Eppendorf AG, Hamburg, Germany) to obtain plasma information (figure 3.2). Activity concentration in both the blood from the original sample and plasma from the centrifuged sample for both the arterial and venous blood was measured using a Gamma counter (1282 Compugamma, Universal Gamma Counter, Wallac, Crownhill, Milton Keynes, UK.) shown in figure 3.3. The counter had previously been cross calibrated with the scanner.
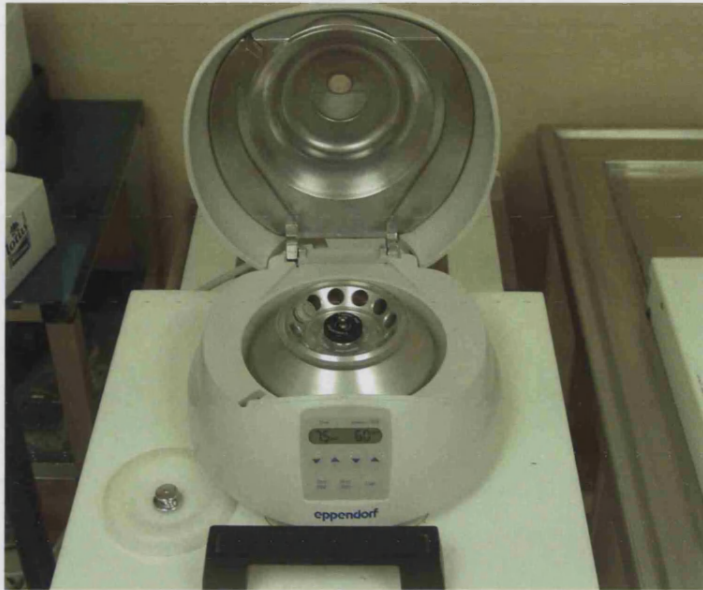
Figure 3.2 Eppendorf minispin centrifuge (Eppendorf AG, Hamburg, Germany)

Figure 3.3 Gamma counter (1282 Compugamma, Universal Gamma counter, Wallac, Crownhill, Milton Keynes, UK.)

3.3.4 FLT metabolite analysis

At certain time points 10ml volumes of blood were withdrawn for FLT metabolite analysis. These time points were at 5min, 15min, 30min, 60min and 90min post injection. After the blood was centrifuged, cell – free plasma was prepared by mixing plasma (1ml) with methanol (9ml). Following centrifugation (3000rpm, 10minutes) the supernatant was concentrated *in vacuo* and the residue reconstituted in mobile phase [MeCN – 0.1M KH_2PO_4 (15 : 85 v/v)]; 1.5ml. The reconstituted sample was filtered (Millipore MV Syringe filter, 0.4μm, Waters, Elstree, Herts, UK.) before injection on a Waters μ-Bondapak C18 column (300 X 7.8mm; Waters, Elstree, Herts, UK.) and eluted with 0.1M potassium dihydrogen phosphate-acetonitrile (85: 15v/v) at 3ml/min. The HPLC eluate was monitored sequentially for absorbance at 286nm and radioactivity. The fraction of unchanged FLT was determined by integrating the areas under the radioactive curve for each sample. FLT eluted on this system had a retention time of 9min.

3.3.5 Data analysis

i) Regions of interest and time activity curves

Regions of interest approach as described in section 2.4.2 was used to analyse the reconstructed FDG and FLT images in order to obtain time activity curves (TACs) for malignant lesions in addition to the normal liver. Since bone marrow has been another organ identified as having high physiological uptake of FLT (Shields et al., 1998b), TACs were also obtained for normal bone marrow.

To construct a TAC, ROIs were identified in an image created from the sum of the last three frames of the dynamic acquisition series and then placed over the complete

series. In the normal liver, ten 20mm diameter regions were drawn in the late summed image and projected to the whole of the dynamic series. The mean of these ten average activity concentrations was subsequently calculated for each image in order to yield the normal liver TAC. For the normal bone marrow, three ROIs were placed in consecutive slices over the same vertebra.

ii) Image derived input function

The image derived, input function utilises the measured activity in the abdominal aorta of human subjects to non-invasively estimate blood-pool input function in abdominal PET scans.

To calculate the image derived input function ROIs were placed over the abdominal or thoracic aorta (AA and TA), depending on the body location where the dynamic images had been acquired. These ROIs were drawn over six consecutive transaxial slices on the summed image of the frames acquired between 30s and 60s post injection. These same ROIs were then projected onto the complete dynamic datasets and TACs were subsequently derived.

iii) Standardised uptake value

Standardised uptake values were calculated using the method described in section 2.4.3.

iv) Patlak analysis

The linearised model for irreversible tracer uptake developed by Patlak was used (Patlak et al., 1983) and has been described in detail in section 2.4.4(i).

iv) Non linear regression and three compartment model

A weighted non-linear regression algorithm was used to fit the plasma or image derived input function and the tissue TACs to this model. All the plasma and image derived input functions were corrected for the presence of metabolites prior to their use in the model fitting. In both models all kinetic constants were estimated by minimising the sum of square differences between the tissue TACs and the model output values. The data was also fitted with a K_4 set equal to zero and described forthwith as the three compartment model (3K). This 3K model was derived in order to further determine the effect of dephosphorylation in the first 60 minute dataset used in this analysis as previously explained in section 2.4.4 .

A combination of the individual kinetic parameters was determined from both the 4K and 3K model. The K_i by non linear regression analysis was calculated using the following expression in order to provide a direct comparison to the K_i (patlak) determined using Patlak analysis.

$$K_i(NLR) = \frac{K_1 * k_3}{k_2 + k_3}$$

The kinetic modelling described in this section was performed using JAVA based software called PMOD (Biomedical Image Quantification & Kinetic Modelling Software, www.PMOD.com) (Burger and Buck, 1997).

3.3.6 Statistical analysis.

A paired two-sided t test and correlation analysis was used (Microsoft Excell™

software) in order to assess the significance of any differences in the kinetic constants

obtained using the quantitative methods (Patlak, NLR(4K) and NLR(3K)) for deriving *in*

vivo measures of FLT utilization evaluated in this study. The correlation between the

SUVs and these quantitative indices was also assessed. In addition, the statistical

significance of any differences in the K_i values obtained as a result of using image

derived compared to measured plasma input functions was evaluated. All statistically

significant levels were set at 5% ($p < 0.05$).

3.4   Results

3.4.1 Time activity curves

The time course of SUVs for both FDG and FLT is shown in figures 3.4 and 3.5 respectively.

These figures demonstrate TACs for two liver metastases and two lung metastases present in one of the eleven patients who underwent dynamic scanning using both tracers. In the case of the FLT there is rapid accumulation up to 10min post injection, which is subsequently followed by a much slower rate of SUV increase when compared to the TAC seen with FDG.
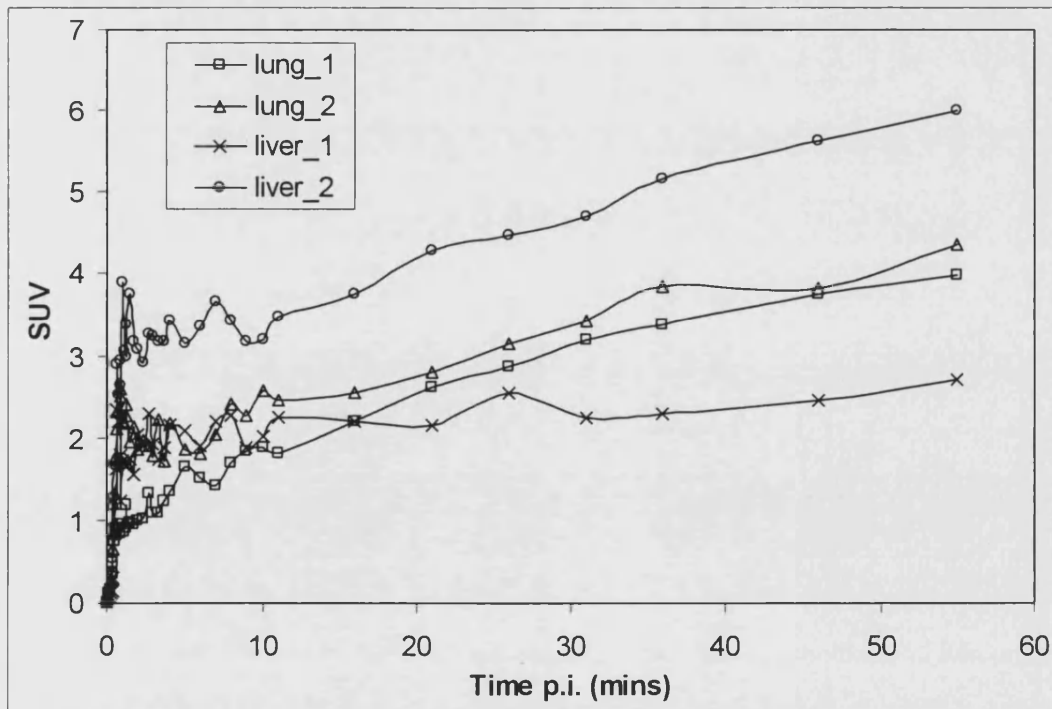
Figure 3.4 FDG time activity curve for two liver and two lung metastases from the same patient.
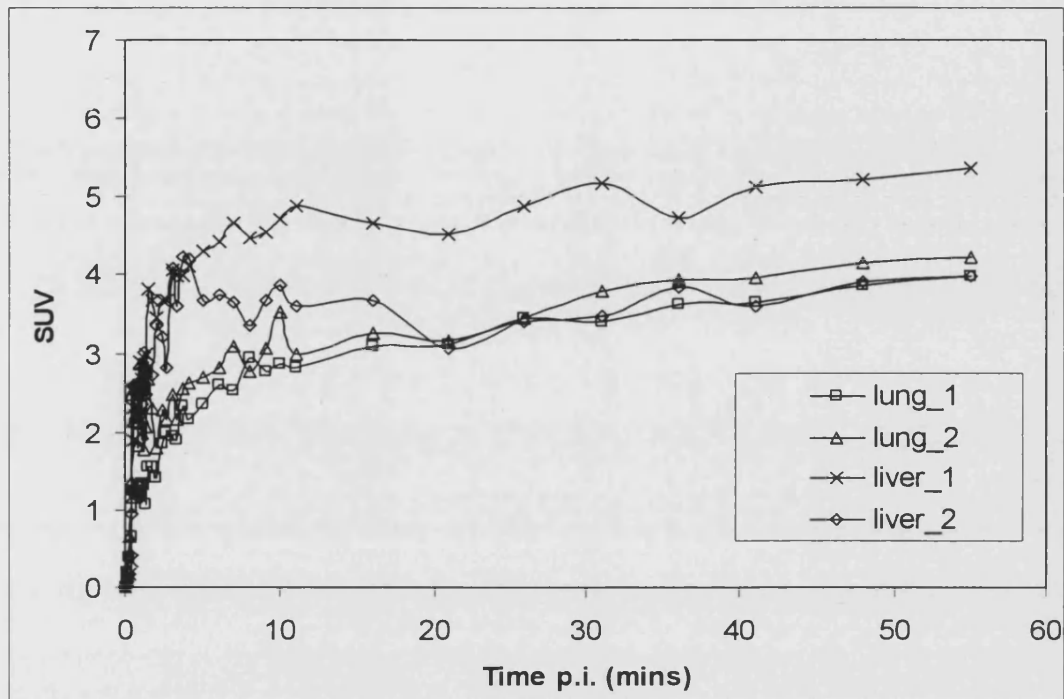
Figure 3.5 FLT time activity curve for two liver and two lung metastases from the same patient.

The temporal response of the uptake of FDG and FLT in normal liver and a solitary liver metastasis from the same patient is shown in figures 3.6 and 3.7 respectively. In addition figure 3.7 demonstrates the high physiological uptake of FLT which is expected to be seen in the rapidly proliferating bone marrow.

The areas of high physiological uptake seen graphically in these figures are demonstrated in figure 3.8, which displays the normal uptake pattern of FLT.
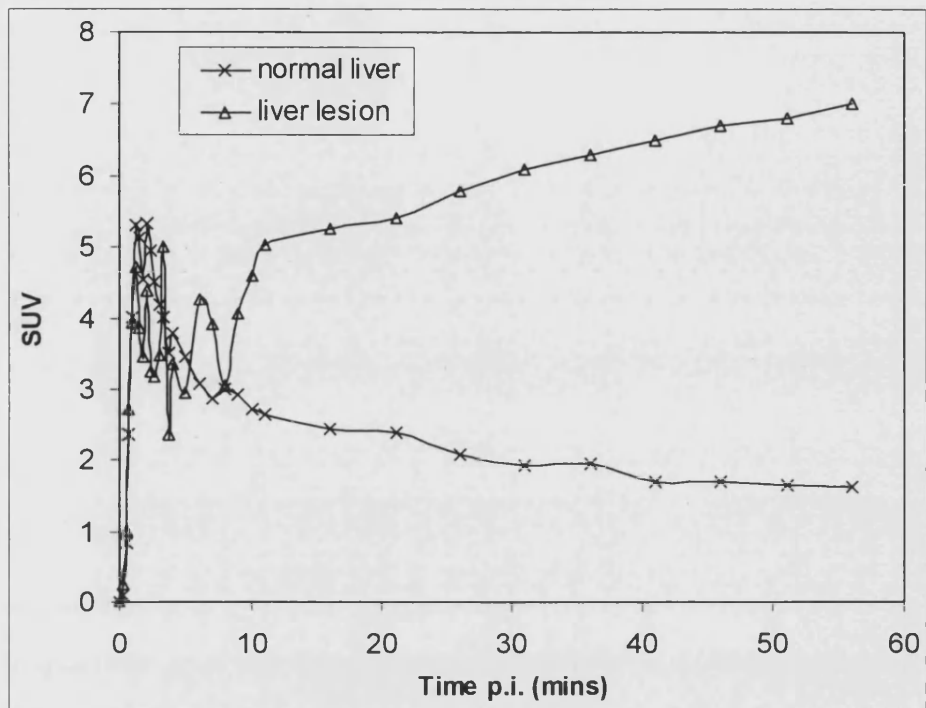
Figure 3.6 FDG time activity curve comparing uptake in normal liver and a liver metastasis.
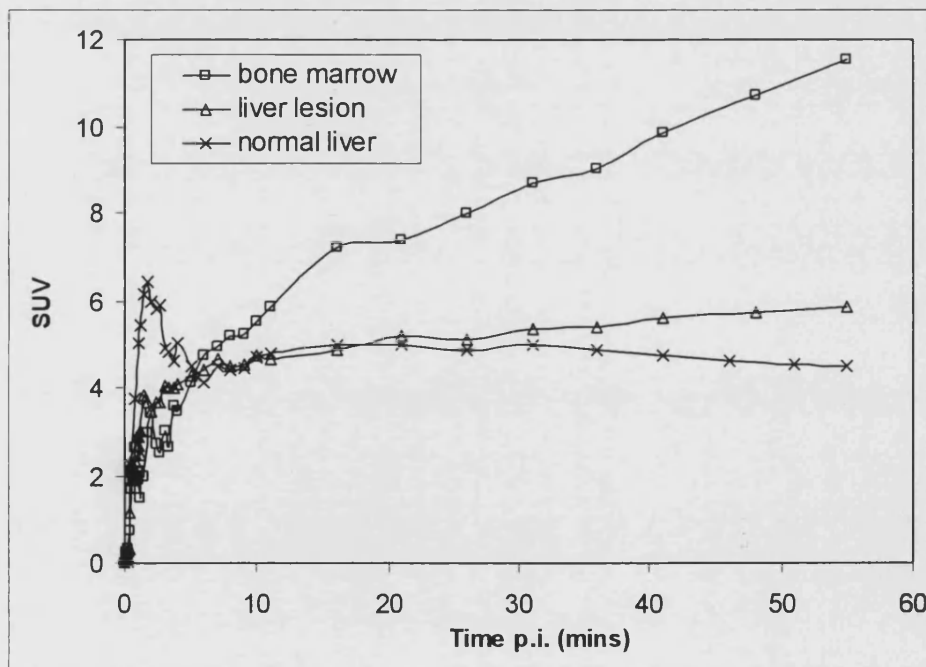
Figure 3.7 FLT time activity curve comparing uptake in normal liver and bone marrow with that of a liver metastasis.
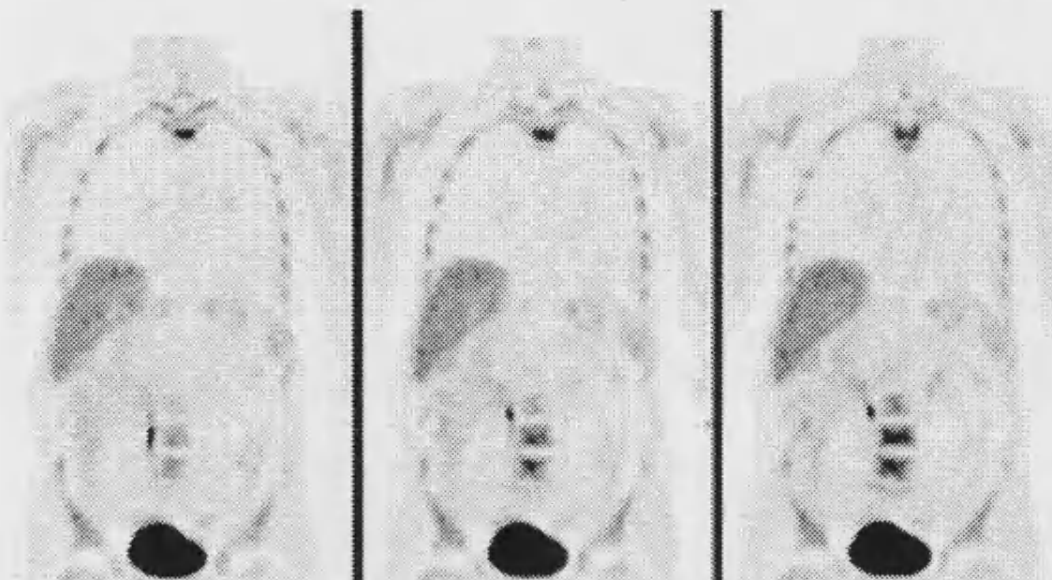
Figure 3.8 Normal FLT uptake demonstrated in coronal whole body images. Increased physiological activity is seen in the liver, bone marrow, right ureter and bladder.

3.4.2 Metabolite analysis

Deproteinisation of plasma with 9 equivalents of acetonitrile before HPLC analysis consistently recovered greater than 85% of the total ^{18}FLT radioactivity in plasma. The percentage of radioactivity that precipitated with proteins showed no relationship with sampling time.

Metabolite analysis on HPLC of samples, revealed that 2 radioactive metabolites of FLT were eluted off of the column before the unchanged parent with retention times of 4.2 and 5.5 min (figure 3.9) The parent compound eluted 11min after the sample was placed on the HPLC column. By this time 90-100% of the injected radioactivity was

recovered.
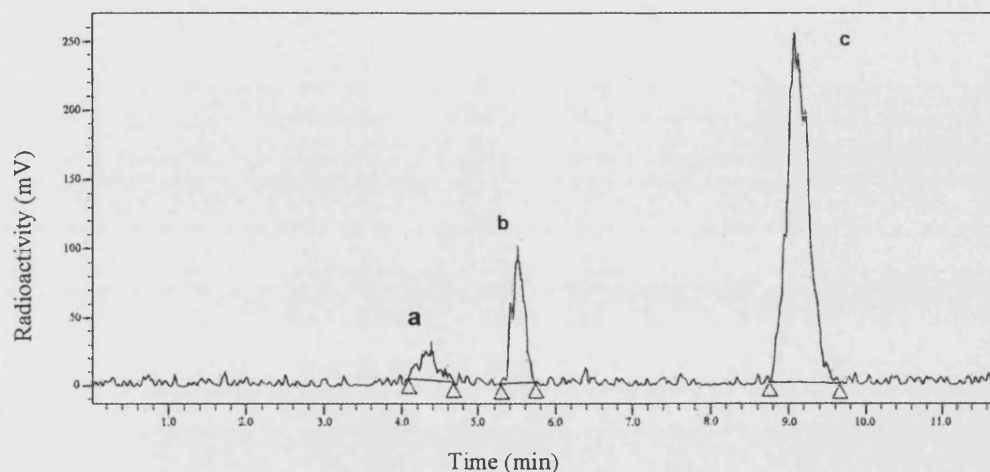
Figure 3.9 Chromatogram demonstrating the temporal relationship of the different radioactive components in arterial plasma. The chromatogram shown is of a plasma sample taken at 60mins post FLT injection. The two polar metabolites are shown by peak (a) and peak (b). The parent compound is seen in the third peak (c).

The time course (15min - 90min) of the parent compound and the metabolites is shown as a percentage fraction of the total plasma activity in figure 3.10. The fraction of radioactivity in the plasma attributed to unchanged [18]FLT, 60min after injection ranged from 55–80% (mean 68.9%, SD 7.8%). Although the amount of metabolites in the plasma increased steadily from <4% at 5 min p.i,. to <30% at 60 min p.i., the rate of increase after 60min was greatly reduced.

For the arterial input function, the ratio of tracer concentration between blood and plasma was ~1.05-1.15, while in the case of the venous blood this difference was <10%. Although on the fraction of unchanged parent obtained from venous and arterial plasma, there was a tendency for venous plasma to slightly overestimate the fraction of plasma radioactivity attributed to FLT.

129
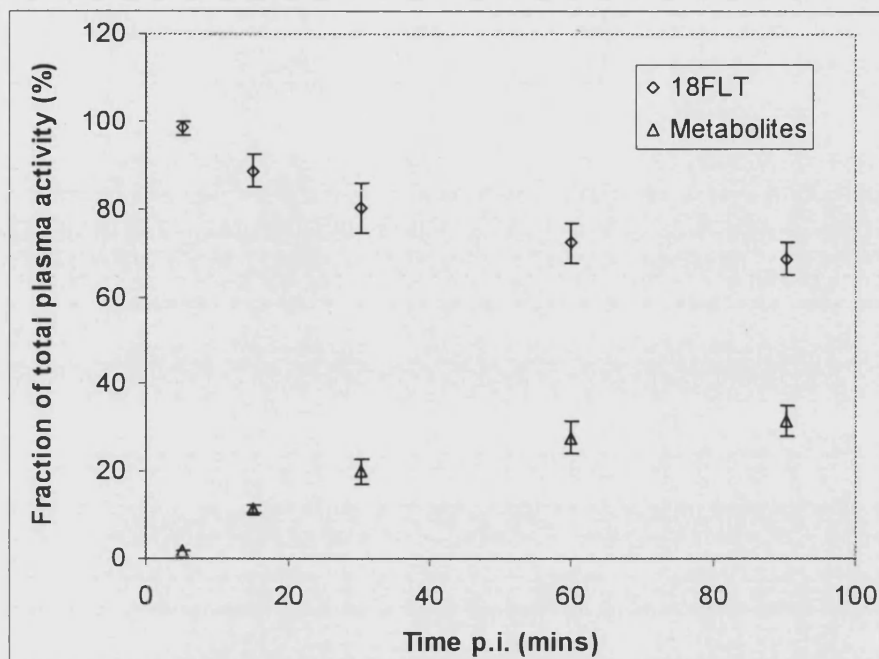
Figure 3.10 Plot demonstrating the average time course of the parent compound and the metabolites as a percentage fraction of the total plasma activity (error bars demonstrate the range of values obtained for the 11 patients).

3.4.3 Patlak analysis

The input function obtained using the abdominal or the thoracic aorta was in excellent agreement with the plasma input function as shown in figure 3.11. There is an inevitable slight time delay demonstrated between the input function derived from the arterial sampling and the one derived from images of the abdominal aorta.
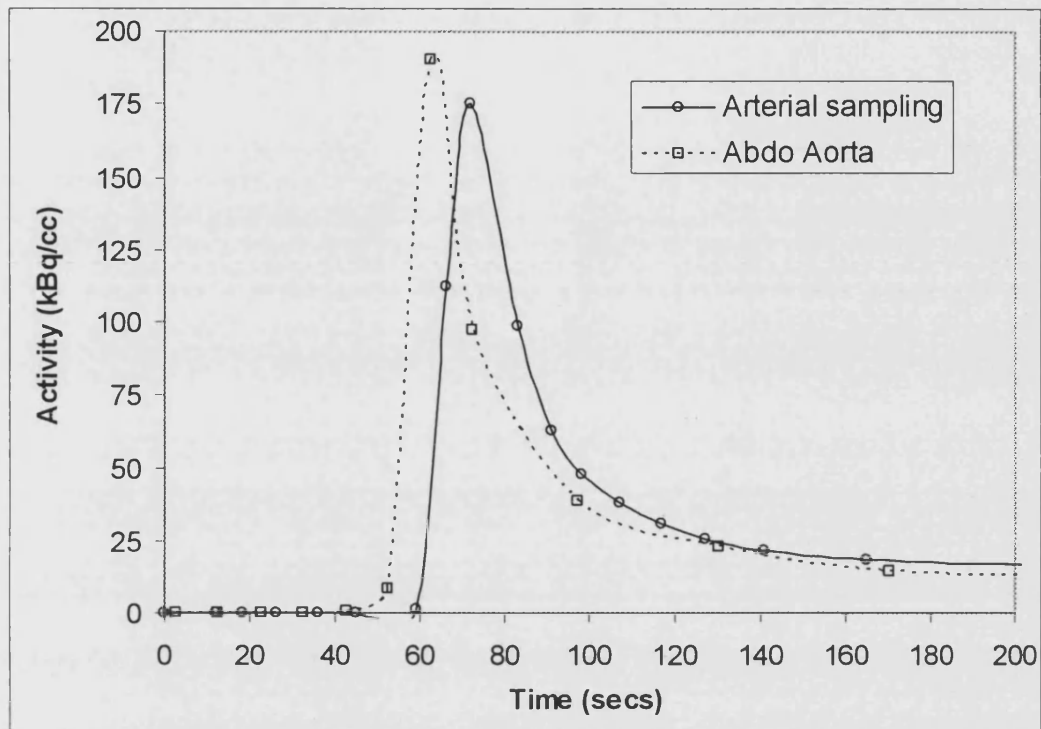
Figure 3.11 Plot demonstrating for the same patient the relationship between a blood input function derived using arterial blood samples and that derived using ROI analysis over the arterial aorta in a series of dynamic FLT images.

The mean time between injection and the start of the linear phase in the Patlak plot was found to be 250sec ranging between of 3-7 minutes. Using the data from the start of the linear phase an accurate fit was observed up to the 60min data used in the analysis. An example of a Patlak plot for one of the liver lesions is shown in figure 3.12. The mean K_i values obtained for the bone marrow and the lesions, using the plasma input function in the fitting of the model are shown in table 3.1.

$$\frac{C_i(t)}{C_p(t)}$$

$$\frac{\int_0^t C_p(t')dt'}{C_p(t)}$$
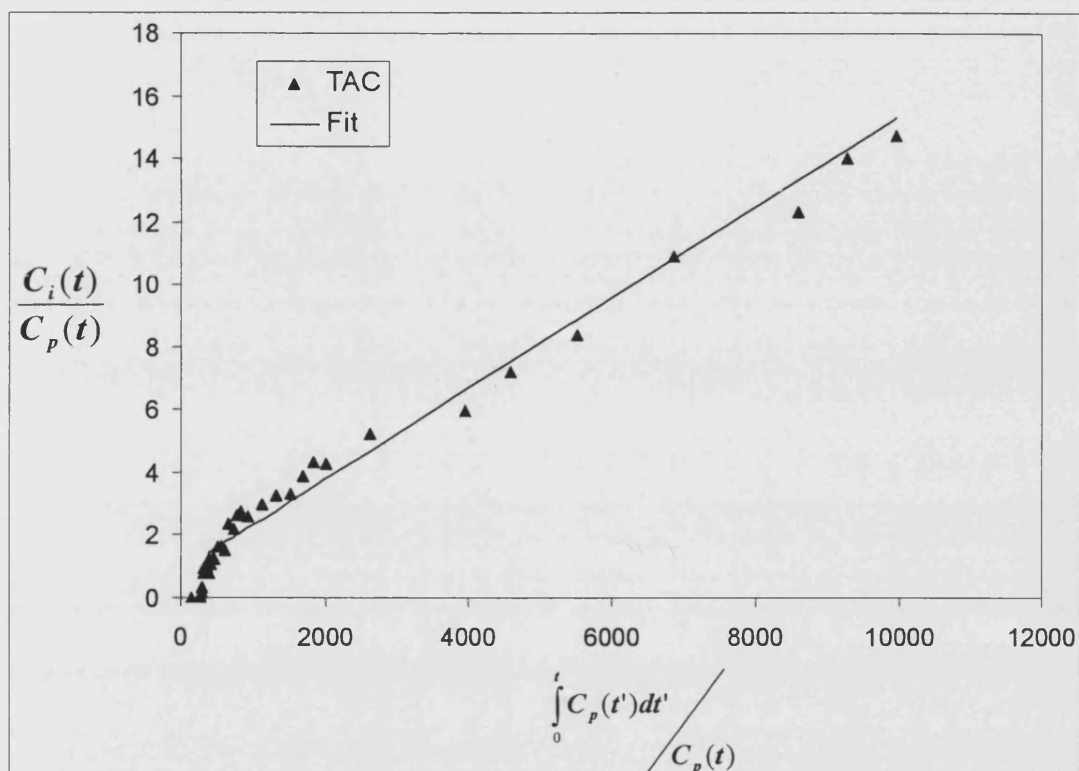
Figure 3.12 Example of a Patlak plot for a liver metastasis.

Patlak	Mean K_i (ml/gr/min)	Standard Deviation	Range (ml/gr/min)
BONE MARROW	0.125	0.064	0.095 – 0.219
LESIONS	0.092	0.036	0.035 – 0.143

Table 3.1 Mean K_i values for normal bone marrow and lesions (primary / liver / lung / extrahepatic) using Patlak analysis with arterial blood derived input function.

132

In comparison, the use of the image derived input function, including both the abdominal and thoracic aorta resulted in a mean difference of <4.5% in the estimation of K_i.

No statistically significant differences were obtained between the two methodologies.

The correction for the presence of metabolites in the plasma input function again did not result in a statistically significant difference in the K_i values (p>0.01).

Very good correlation ($R^2 = 0.8551$) between the proliferation rate expressed by the influx rate constant K_i values and the corresponding SUVs measured from the same lesions using the last frame of the dynamic dataset acquired is shown in figure 3.13.
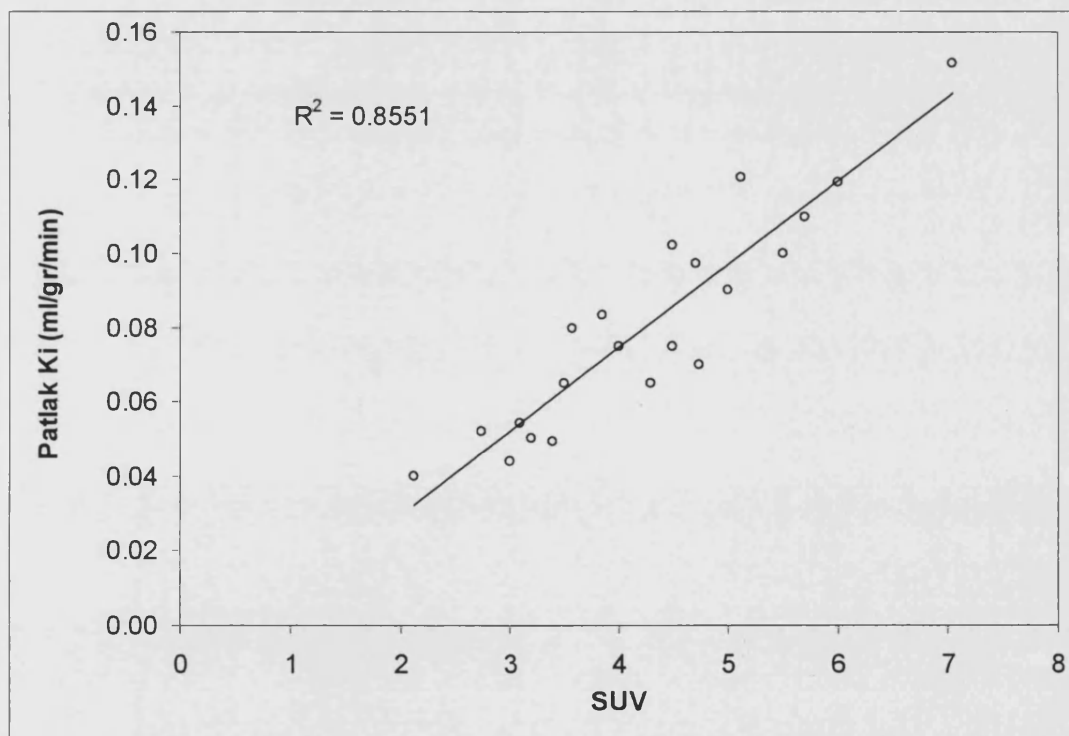
Figure 3.13 Plot of proliferation rate (K_i) using Patlak analysis and the SUVs measured from the same lesions.

3.4.4 Non-linear regression

Mean K_i for both 3K and 4K values for the malignant lesions (primary, liver, lung and extrahepatic) and the bone marrow are shown in the tables 3.2 and 3.3 below.

3K	Mean K_i (ml/gr/min)	Standard Deviation	Range (ml/gr/min)
BONE MARROW	0.102	0.054	0.068 – 0.179
LESIONS	0.079	0.029	0.031 – 0.135

Table 3.2 Mean K_i values using NLR analysis and 3K model.

4K	Mean K_i (ml/gr/min)	Standard Deviation	Range (ml/gr/min)
BONE MARROW	0.092	0.058	0.052 – 0.144
LESIONS	0.085	0.0	0.039 – 0.141

Table 3.3 Mean K_i values using NLR analysis and 4K model.

Again no statistically significant differences were found between the utilisation of the plasma or the image derived input functions.

The average value of K_4 was not significantly different than zero in both lesions and bone marrow, although it was slightly higher in the case of the lesions as shown in table 3.4.

K_4	Mean K_4 (ml/gr/min)	Standard Deviation	Range (ml/gr/min)
BONE MARROW	0.001	-	-
LESIONS	0.004	0.002	0.0015 – 0.009

Figure 3.4 Average value of K_4 in lesions (primary, liver, lung and extrahepatic) and bone marrow.

Additionally a worse correlation was demonstrated between the SUVs and the corresponding K_i (4K) (R^2=0.49) in comparison to K_i (3K) (R^2=0.85).
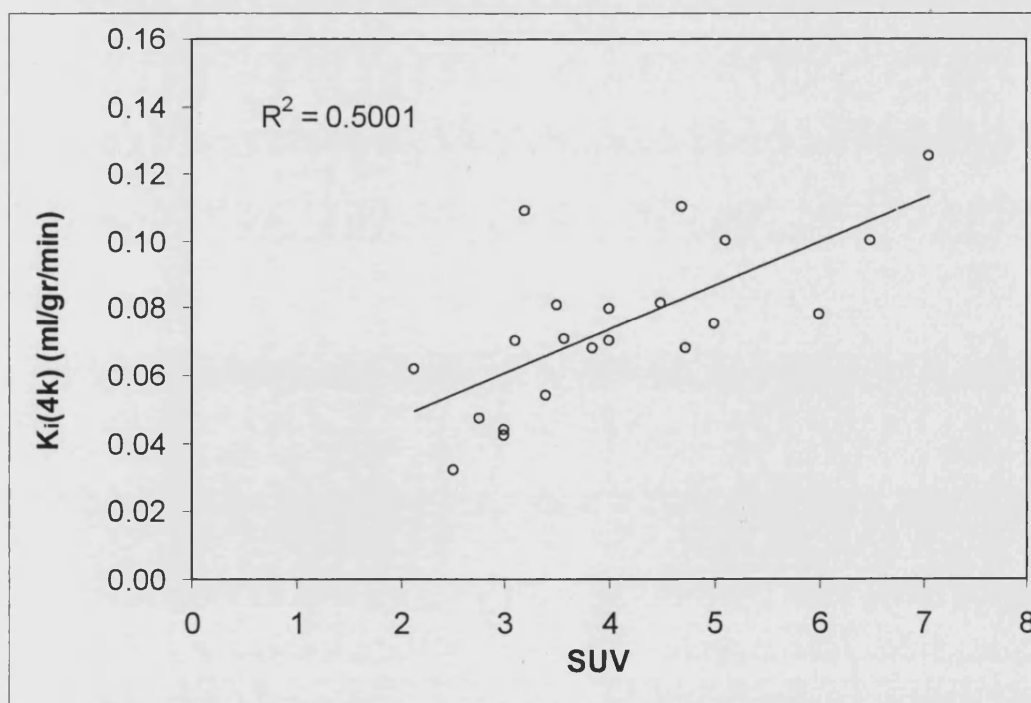
Figure 3.14 Correlation between K_i determined using (4K) model and the corresponding SUVs.
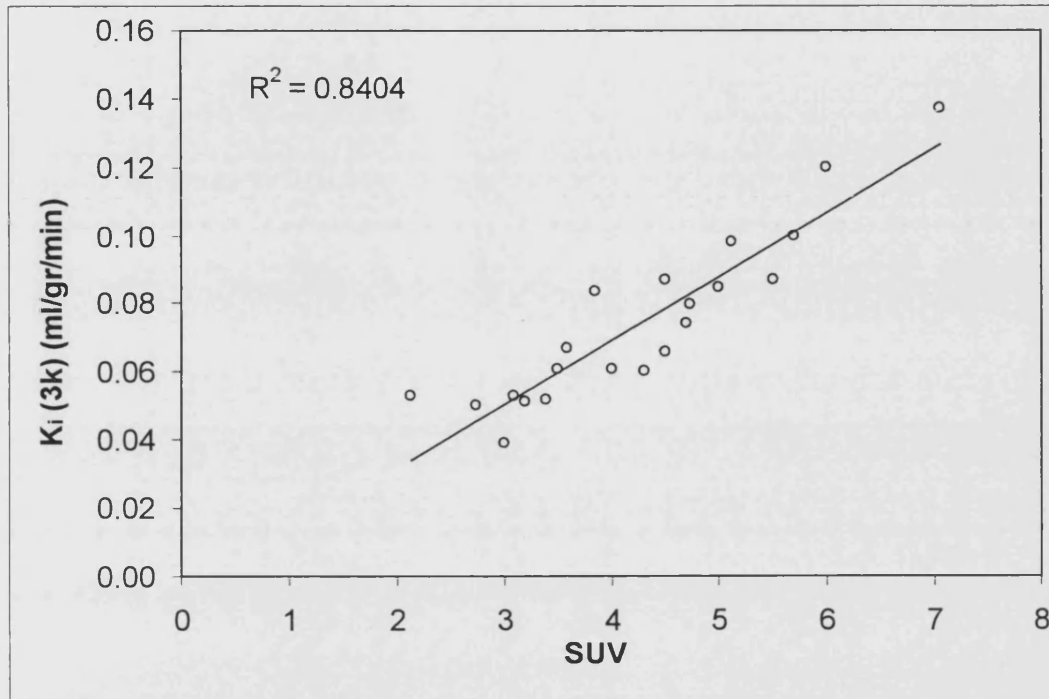
Figure 3.15 Correlation between K_i determined using (3K) model and the corresponding SUVs.

Finally figure 3.16 shows that the K_i derived from the linear part of the Patlak analysis correlated highly ($R^2 = 0.9362$) with the equivalent parameter derived from $K_i(3K)$.
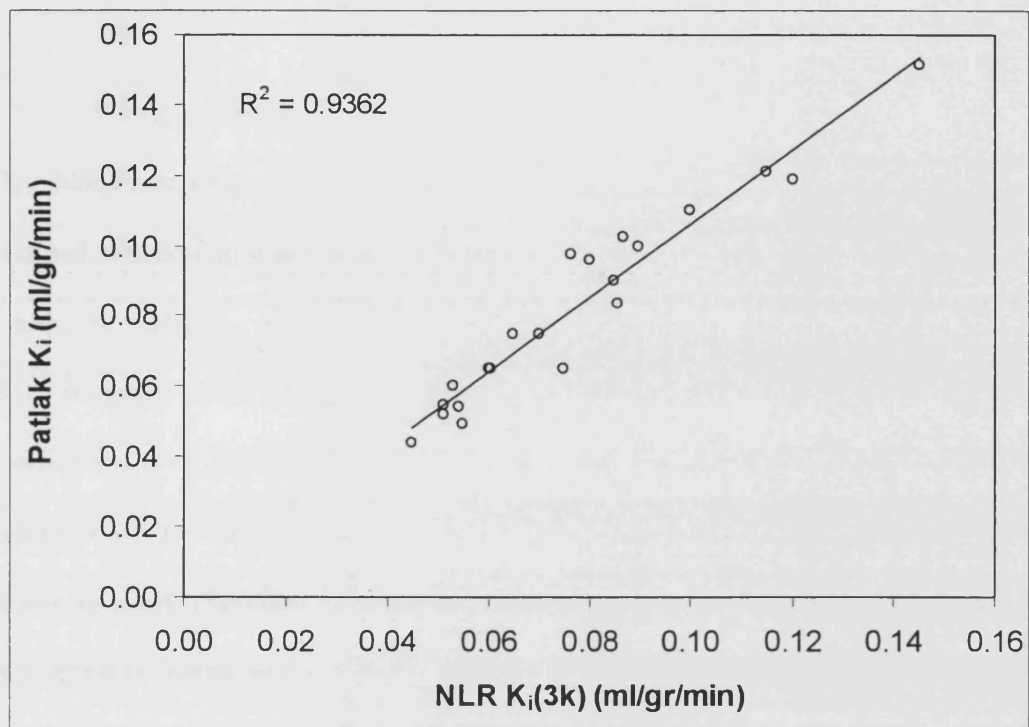
Figure 3.16 Correlation between K_i derived from Patlak analysis and that derived using NLR (3K) model.

3.5 Discussion

Previous metabolite analysis carried out in dogs has shown 90–97% of activity in late blood sample as unmetabolised ^{18}FLT (Shields et al., 2002). In the same animals, this limited metabolism was also associated with low liver uptake. However, the results of our study in relation to FLT metabolism in humans demonstrate the presence of approximately 70% of the activity as unmetabolised tracer at 60min p.i. This is in addition to the presence of significant uptake and retention in the liver. The slower rate of increase of the metabolites in plasma observed after 60min p.i is in agreement with previous work (Shields et al., 2000) that has suggested a preferential clearance of the glucuronide compared to the parent compound in urine after 60min p.i.

The methodology employed for the metabolite analysis in our study was chosen for its high level of reliability and it can be used in a routine clinical setup. In this study two metabolites have been observed, which is in contrast with the work carried out previously by Shields et al (Shields et al., 2002) where only the presence of glucuronide was reported. In view of these findings and the fact that further characterisation of the two metabolites was not carried out due to unavailability of technical resources, I have hypothesised that these metabolites are free F18 in addition to glucuronide. One possible reason behind this could be that the method of analysis used in this work, with the use of online detection of the radioactivity and deproteinisation of a large volume of plasma (1 ml) followed by concentration prior to HPLC analysis, is more sensitive.

The time activity curves demonstrate a rapid tracer accumulation followed by a slow increase in the rate of uptake. At the same time there is persistent activity in the normal liver (see figure 6) even at 60min p.i. On the other hand, the corresponding FDG

investigations demonstrate a higher increase in the rate of uptake following the initial tracer accumulation. These observations may have significant impact in optimizing the time of acquisition for FLT scans in CRC, suggesting that there may be no significant improvement in lesion detectability by delaying imaging protocols.

The Patlak model is based on the assumption that although there may be number of tissue compartments which reversibly communicate with the plasma, there must be at least one tissue compartment in which the trace is irreversibly trapped. An additional requirement for the linear behaviour to be observed is that there must be sufficient time passed such that the arterial plasma and the free tissue compartment have reached an equilibrium state. This is the reason for an initial period of curvature expected in the Patlak plots which corresponds to the period prior to the equilibrium being achieved between the plasma and free tissue compartments. The excellent linear fit observed following the initial period of equilibrium in the tracer concentration between the plasma and the free tissue compartment, suggests that no significant dephosphorylation takes place within the first 60min p.i. In addition, this hypothesis is further supported by the better NLR fits obtained with the 3K model in comparison to including a non-zero K_4. A high correlation was also observed between the net influx constants obtained using the Patlak analysis and the NLR 3K model.

This work has not targeted the quantitative modelling of FLT in normal liver as the study was not designed to measure a double input function which would take into account the dual blood supply of the liver. However this does not prevent quantitative evaluation of the lesions since malignant lesions of the liver are supplied by the hepatic artery only (Kemeny and Ron, 1999).

Shields et al were the first to explore the kinetics of FLT clearance from the blood and uptake into tissues by again studying normal and tumour bearing dogs, additionally bone marrow biopsies were obtained to validate the *in vivo* results. In this study a three compartment model was used to investigate the retention of FLT by intracellular phosphorylation. The dephosphorylation rate (K4) was found to be approximately zero and was not significant during a 60min study. There was reasonable agreement between the phosphorylated FLT fraction and the unmetabolised FLT fraction using this theoretical dog model and the experimental data obtained from the DNA extraction (Shields et al., 2002).

The potential of non-invasive methodology for the quantitative assessment of [18]FLT *in vivo* has been also assessed in this chapter. Firstly, the results show that the use of venous plasma samples in monitoring the presence of metabolites as a function of time leads to no significant differences compared to the use of arterial plasma. Secondly, the use of an image derived input function, using either the abdominal or the thoracic aorta, does not introduce statistically significant differences in the calculation of the influx rate constant. Ohtake et al, Germano et al and van der Weerdt et al, have all previously investigated the validity of using an image derived input function for FDG quantitation and demonstrated that non-invasive, accurate measurements of the arterial input function by dynamic PET imaging are possible and represent a clinically viable alternative to arterial blood sampling (Germano et al., 1992; Ohtake et al., 1991; van der Weerdt et al., 2001). Similar such work has never been carried out in the case of FLT.

Both these results support the use of non-invasive methodology for the quantitative assessment of FLT uptake *in vivo* using Patlak analysis. Finally in this

tumour population a good correlation was found between the SUVs and the influx rate

constant obtained using either the Patlak analysis or the NLR(3K).

3.6   Conclusion

In conclusion, various techniques for the characterization of FLT uptake in vivo in patients with primary and metastatic colorectal cancer were investigated. When TACs were compared to FDG TACs, there was lower uptake as a function of time. In terms of quantitative analysis our study has demonstrated that the behaviour of FLT in-vivo utilization can be well characterized by a 3k model for data up to 60min p.i. In addition, a high correlation was demonstrated between the NLR(3K) and the simplified Patlak analysis with either measured or image derived input functions. The good correlation seen between SUVs and the quantitative measures of FLT utilization in terms of the net influx constant K_i suggests that non-invasive methodology may be used to assess the proliferation rates of CRC tumours with FLT.

In view of these findings, in the subsequent chapters of this thesis SUVs have been used to quantify the uptake of FLT.

CHAPTER 4

Potential clinical role of FLT in imaging colorectal cancer.

4.1 Background

FDG has without doubt gained a clinical role in the diagnosis and staging of patients with CRC. On the cellular level, FDG, which is a glucose analogue, measures the metabolic activity, hence reflects cell viability within a given tumour. Whether cells are actively dividing or are quiescent is not distinguishable. Therefore it is recognised that FDG is not, and cannot be, a specific tumour marker, hence the efforts to develop new ^{18}F-labelled tracers which may become clinically useful in the molecular characterisation of disease.

The production of the thymidine analogue FLT has provided us with the opportunity to study cancer cell proliferation in a routine clinical environment. Although the potential role of FLT PET is to image cellular proliferation, it is as yet unknown whether it is sensitive enough to be used to image CRC.

There are no studies in the published literature investigating the role that this new tracer could have in CRC. Therefore in this chapter a comparison is made, in the same patients on a lesion by lesion basis, between glucose utilisation/cell viability using FDG and cellular proliferation using FLT, in primary and metastatic CRC. The aim of this work is to investigate the potential role of FLT PET as an imaging modality in CRC by comparing its accumulation with that of FDG in malignant and normal tissue.

4.2 Aims

i) Establish if FLT PET can be used to image CRC in a clinical setting.

ii) Directly compare uptake of FDG and FLT on a lesion by lesion basis using SUVs.

iii) Directly compare uptake of FDG and FLT in normal liver and bone marrow using SUVs.

4.3 Methods

4.3.1 Patient selection

All patients were prospectively recruited from among routine surgical and oncology outpatients. Inclusion criteria were the presence of primary CRC, metastatic CRC or a combination of the two. Lesions were identified by conventional imaging modalities including the use of multi-phase enhancement patterns with multi-slice computed tomography (CT), as described in section 2.5. All patients gave written informed consent, and the study was approved by the Hospital Ethics Committee (appendix B) and the Administration of Radioactive Substances Advisory Committee (ARSAC) (appendix C).

A total of 23 patients with 61 malignant lesions were recruited. These comprised 15 males and 8 females with a median age of 69 years (range 50-87years). Four patients had solitary primary lesions, six had both primary tumours and liver metastases, six presented with just liver metastases and three had malignant lung lesions in addition to liver metastases. The remaining four patients had peritoneal lesions (table 4.1) Malignancy was confirmed histologically in 18 lesions, by laparotomy findings in 14 and by clinical and radiological follow-up using conventional techniques in the remaining 29 lesions.

	Distribution of lesions			
Patient	Primary tumour	Liver metastases	Lung metastases	Peritoneal metastases
1	1	3	-	-
2	-	3	1	-
3	1	4	-	-
4	1	-	-	-
5	-	2	3	-
6	-	1	2	-
7	-	1	-	2
8	-	2	-	-
9	1	-	-	-
10	-	3	-	-
11	-	-	-	3
12	1	1	-	-
13	-	2	-	-
14	-	5	-	-
15	-	4	-	-
16	-	-	-	1
17	1	1	-	-
18	1	-	-	-
19	1	1	-	-
20	1	-	-	-
21	-	1	-	-
22	1	4	-	-
23	-	-	-	1
Total number of lesions	10	38	6	7

Table 4.1 Distribution of lesions (n=61) within the patients in the study.

4.3.2 Imaging

Patients underwent whole body FDG and FLT PET scans as per the protocols in chapter 2 within a median period of 6 days (range 1-22 days). FDG and FLT tracers were prepared as described in chapter 2 with a mean administered dose of 377MBq (SD 21) and 360MBq (SD 53) respectively. All patients underwent whole body scanning at mean

of 59min p.i (SD 8) for FDG and a mean of 63min p.i (SD 6) for FLT. This timing of the data acquisition for FLT was determined from the TACs studied in chapter 3.

Standardised uptake values (SUVs) were obtained for each lesion. For each patient, regions of interest (ROI) were drawn over the tumour and normal tissue images (normal bone marrow and normal liver). As described in section 2.4.1, five consecutive slices were used and consisted of the slice with the maximum count density and the four immediately adjacent slices. In the case of the normal bone marrow and liver, the ROI was placed over the same vertebra and the same area of normal liver for both the FDG and FLT scans. SUVs were subsequently calculated using the methodology described in sections 2.4.2 and 2.4.3.

4.3.3 Statistical analysis

A two sided paired t test and correlation analysis was used to assess the significance of differences between the uptake of the two tracers on a lesion by lesion basis (Microsoft Excell™ software).

4.4 Results

The whole-body study in figure 4.1 shows a comparison between the normal physiological uptake of FDG and FLT. There is prominent uptake by bone marrow, a highly proliferating tissue, in addition to significant accumulation within normal liver. As with FDG, excretion is via the kidneys and urinary bladder. In contrast to FDG, FLT does not cross the intact blood-brain barrier and hence exhibits no cerebral uptake.
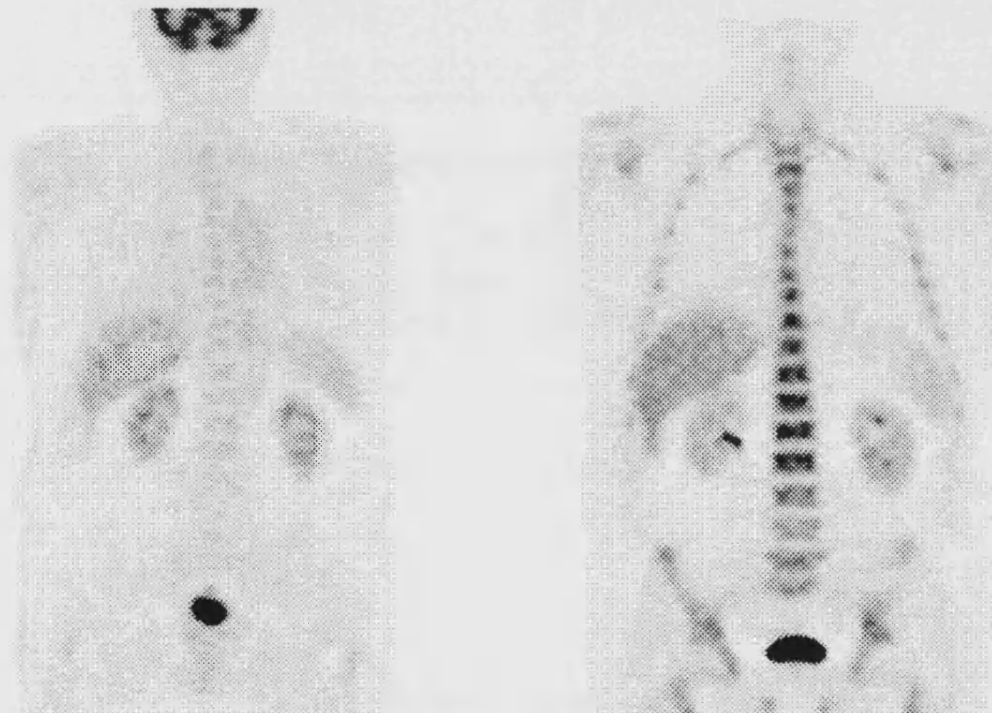
Figure 4.1 Comparison of normal physiological uptake of FDG and FLT. There is increased accumulation of FLT within the normal liver and bone marrow. Excretion via the urinary bladder is noted with both tracers, whilst only FDG is seen to cross the blood brain barrier.

Of the 61 malignant lesions, 60 (99%) were imaged with FDG-PET. Lesions were grouped together as primary tumours and liver metastases, while extrahepatic metastases

were subdivided into lung and peritoneal lesions. Findings are described below for the different groups.

All ten (100%) of the primary tumours (six rectal and one each in the sigmoid colon, transverse colon, ascending colon and caecum) were successfully imaged using both FDG and FLT. Although on visual inspection all of these primary lesions showed increased uptake as compared to their surrounding structures, the avidity of these tumours for FDG was far greater than that of FLT. When this difference was semi-qauntitated using SUVs, FDG showed an approximate two fold increase in uptake when compared to FLT. Figure 4.2 shows this difference in a primary adenocarcinoma of the rectum which demonstrates how primary CRC is seen as avid for FLT but to a lesser extent than with FDG.

FDG   **FLT**
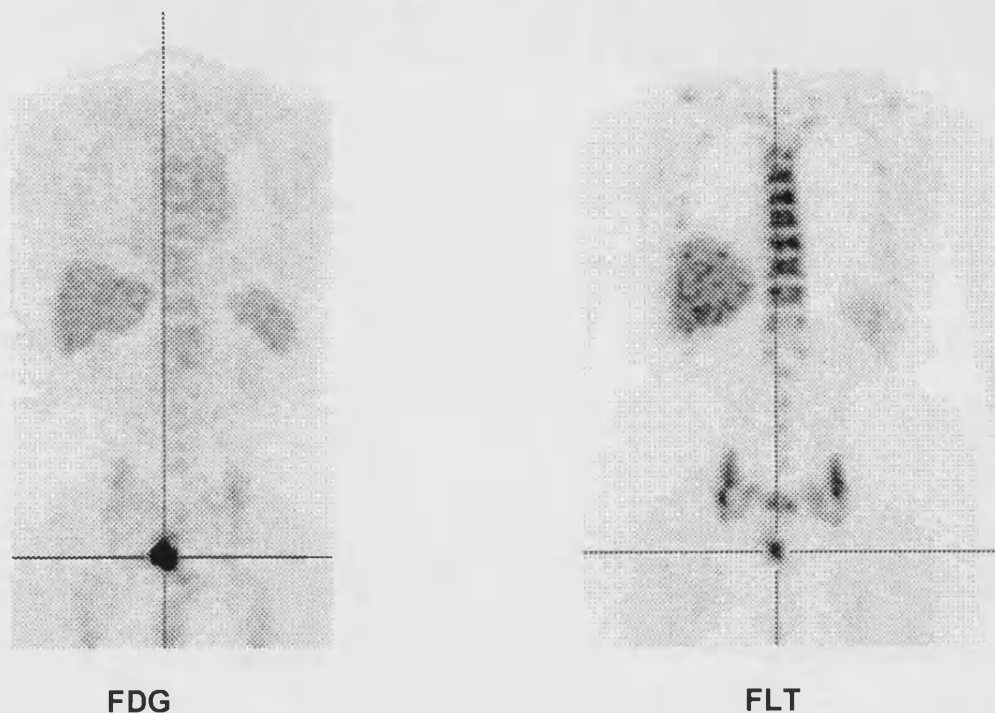
Figure 4.2 Primary carcinoma of the rectum showing avidity for both FDG and FLT.

FLT showed avidity for five of the six (83%) lung lesions which were imaged successfully with FDG. The thorax showed very little uptake of either tracer. Those lesions visualised using FLT demonstrated similar SUVs when compared to FDG (mean 4.5 and 5.5 respectively). One of the patients with a primary rectal tumour, who was originally included in the primary group, underwent a staging scan and appeared to have diffuse bilateral areas of avid FDG uptake within the lung fields. The symmetry of these lesions raised the suspicion of sarcoidosis and this was confirmed on biopsy. Interestingly these lesions were not seen as avid for FLT.

All six (100%) peritoneal tumour deposits showed increased uptake of both tracers. Once again there was an obvious increase in the intensity of FDG as that of FLT which was also reflected in the SUVs. In one case, FDG exhibited significantly increased uptake in a peritoneal lesion, which was also thought to be malignant in nature during resection. Subsequent full histological examination found this lesion to be made up of inflammatory cells secondary to fat necrosis. This same lesion had displayed no avidity for FLT during pre operative scanning. This case is shown in figure 4.3 and at 14 month post operative follow up there is still no evidence for malignant disease at that site using both metabolic and cross sectional imaging methods.

Image 1

Image 2

A

B
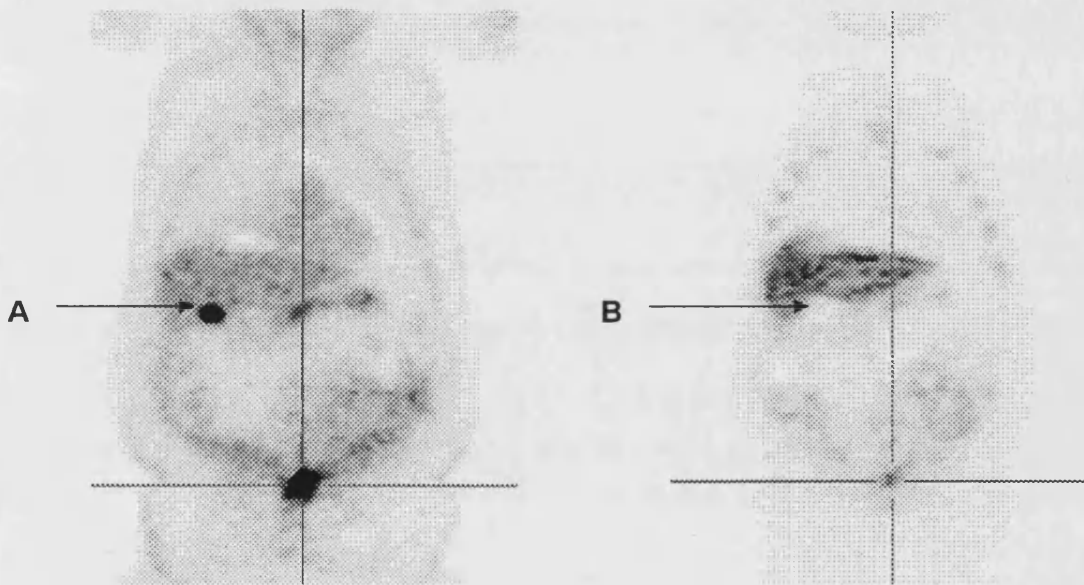
Figure 4.3 Image 1 shows increased uptake of FDG by peritoneal tumour recurrence marked by the cross in addition to abnormal uptake by an inflammatory lesion (A). Image 2 again shows increased activity from the peritoneal tumour recurrence using FLT but no abnormal focus in the area of inflammatory activity.

Of the 38 liver metastases, 37 (97%) showed accumulation of FDG. The false negative liver lesion was a 1cm metastasis lying inferior to a larger lesion. This smaller metastasis was not visualised using either tracer but became evident during liver resection. In contrast only 12 of the 38 liver lesions (32%) were visualised using [18]FLT. An example of multiple liver metastases seen with FLT is demonstrated in figure 4.4; it is

152

interesting to note that the pattern of FLT distribution within the lesions differs from the pattern seen with FDG. More of a doughnut appearance is seen with FLT indicating that perhaps there is less true tumour in the outer rim and more central necrotic tissue than is demonstrated by the FDG uptake.

FDG   **FLT**
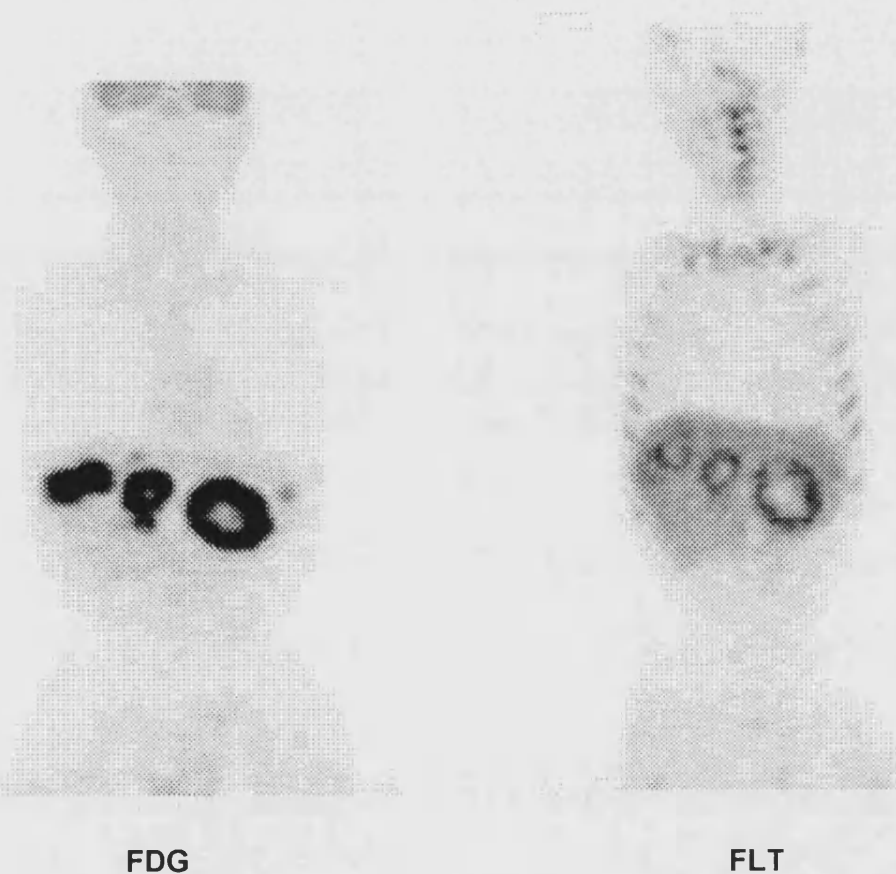
Figure 4.4 Multiple liver metastases seen with both FDG and FLT.

The lack of visualisation of the majority of liver lesions (n=26, 68%) using FLT is highlighted in a case of a patient with a solitary liver metastasis shown in figure 4.5. The intense uptake of FDG can be seen against the relatively low liver background uptake. In

comparison, the corresponding area in the FLT image in fact displays lower uptake as compared to the high FLT liver background.
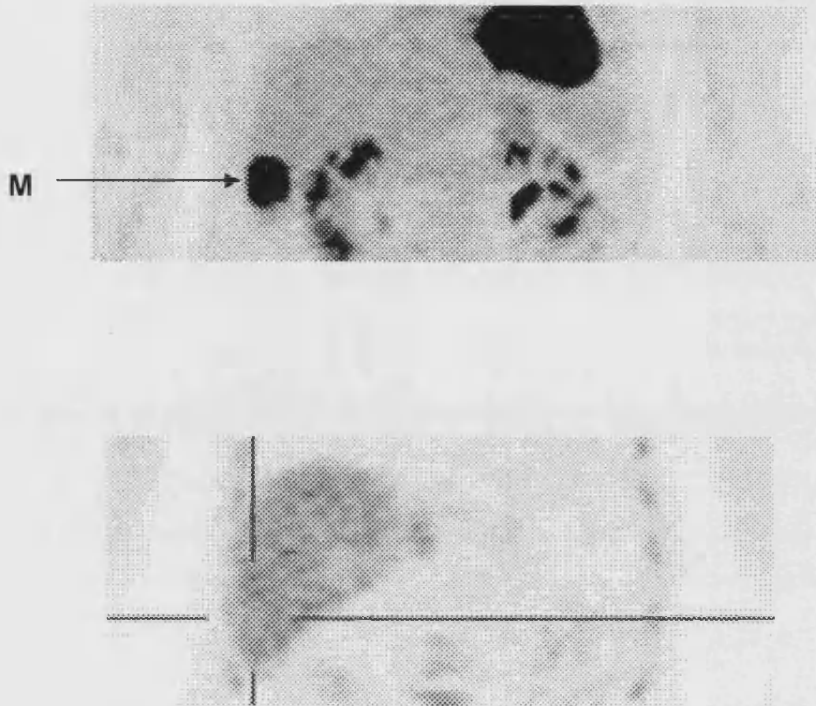
Figure 4.5 Liver metastasis (M) displaying high uptake of FDG. The corresponding area in the FLT image displays lower activity in comparison to the background normal liver.

All means, standard deviations and ranges of SUVs are shown for each tissue type in table 4.2. In summary, in primary CRC, the almost two fold increase in SUVs is evident. The mean uptake values for the tracers in colorectal lung metastases were similar for the 2 tracers, whereas uptake of FDG in malignant peritoneal disease was on average 1.7 times higher than that of FLT. The 32% of liver metastases visualised with FLT demonstrated comparable SUVs to FDG (mean SUV 6.3 vs 6.5 respectively).

154

	Tissue	SUVs			
		^{18}FDG		^{18}FLT	
Malignant		Mean (SD)	Range	Mean (SD)	Range
	Primary	7.6 (2)	3.9 – 13.4	3.9 (1.7)	2.1 – 7.3
	Liver	6.3 (2.6)	2.9 – 11.7	6.5 (1.6)	4.2 – 9.1
	Lung	5.5 (1.3)	3.5 – 7.0	4.5 (1.5)	2.5 – 6.8
	Peritoneal	6.5 (2.4)	4.4 – 10.2	3.9 (1.3)	2.8 – 6.1
Non malignant					
	Liver	2.1 (0.4)	0.8 – 2.7	4.5 (1.2)	2.7 – 7.9
	Bone marrow	1.5 (0.4)	0.8 – 2.4	7.2 (1.3)	4.5 – 9.7

Table 4.2 Summary of SUVs for malignant and non malignant tissue

For those lesions visualised with both tracers (n=34), there is no correlation (R^2=0.03) of SUVs (figure 4.6). A lesion by lesion avidity of the respective is shown in table 4.3
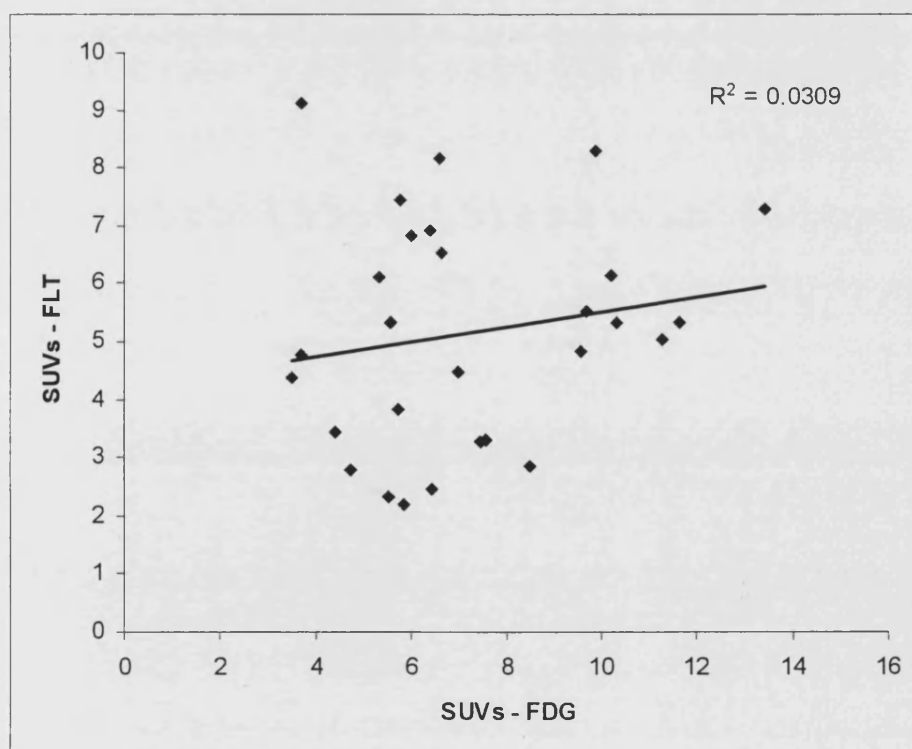
Figure 4.6 In the lesions visualised by both tracers (n=28) no correlation was seen as measured by SUVs.

155

| Patient | Lesions | Avidity | |
		^{18}FDG	^{18}FLT
1	Primary (sigmoid colon)	√	√
	Liver metastases 1	√	√
	2	√	√
	3	√	√
2	Lung metastases	√	√
	Liver metastases 1	√	X
	2	√	X
	3	√	X
3	Primary (transverse colon)	√	√
	Liver metastases 1	√	√
	2	√	√
	3	√	√
	4	√	√
4	Primary (caecum)	√	√
5	Lung metastases 1	√	√
	2	√	√
	3	√	√
	Liver metastases 1	√	√
	2	√	X
6	Liver metastases	√	X
	Lung metastases 1	√	X
	2	√	√
7	Peritoneal metastases 1	√	√
	2	√	√
	Liver metastases	√	X
8	Liver metastases 1	√	√
	2	X	X
9	Primary (ascending colon)	√	√
10	Liver metastases 1	√	X
	2	√	X
	3	√	X
11	Peritoneal 1	√	√
	2	√	√
	3	√	√
12	Primary (rectal)	√	√
	Liver metastases	√	√
13	Liver metastases 1	√	X
	2	√	X
14	Liver metastases 1	√	X
	2	√	X
	3	√	X
	4	√	X
	5	√	X
15	Liver metastases 1	√	X
	2	√	X
	3	√	X
	4	√	X
16	Peritoneal metastases 1	√	√
	2*	√	X
17	Primary (sigmoid)	√	√
	Liver metastases	√	√
18	Primary (rectal)	√	√
19	Primary (rectal)	√	√
	Liver metastases	√	X
20	Primary (rectal)	√	√
	Lung (lesions)†	√	X
21	Liver metastases	√	√
22	Primary (rectal)	√	√
	Liver metastases 1	√	X
	Liver metastases 2	√	X
	Liver metastases 3	√	X
	Liver metastases 4	√	X
23	Peritoneal metastases	√	√

Table 4.3 Avidity of the respective tracers for tumour tissue on a lesion by lesion basis. Peritoneal lesion avid for FDG but found to be inflammatory on histology (see fig4.3). † lung lesion avid for FDG but sarcoidosis on histology.

4.5 Discussion

This is the first study to compare and contrast uptake of the two tracers FDG and FLT in CRC. Results from this work have found no significant correlation between the uptake of FDG and FLT in malignant CRC lesions (R^2=0.03). This lack of correlation provides further evidence that FDG uptake, which depends on glucose metabolism and reflects cell viability (Higashi et al., 1993) does not correlate with cellular proliferation as depicted by FLT.

Both tracers displayed 100% sensitivity when imaging primary CRC. For visualisation of extrahepatic lesions, FDG and FLT demonstrated sensitivities of 100% and 92%, respectively, however false positives and false negatives were encountered.

The specific cases of the inflammatory peritoneal lesion thought to be malignant owing to the increased uptake of FDG and the sarcoid lung lesions showing intense uptake of FDG, highlight the potential pitfall of false positives secondary to increased tracer uptake by macrophages. It is interesting to note that none of these lesions showed avidity for FLT. This demonstrates a specificity which may be useful for further characterisation of equivocal lesions.

One false negative lung lesion was encountered when using FLT. This type of false negative lung metastasis secondary to CRC has previously been reported when imaging with FLT (Buck et al., 2002). The reasons for such findings are unclear and need to be elucidated by further work. Histological analysis, in addition to a quantitative assessment of the proliferative activity of these lesions, is imperative to ascertain why the tumour is not visualised against such a low background as that seen in the thorax with FLT.

False negative liver lesions pose a significant problem in the field of CRC as 30% of patients ultimately develop liver metastases (section 1.3.4). A wide range of treatment options are now available, but selection of the most appropriate depends on accurate staging. Of the 38 liver lesions presented, only 12 were visualised with FLT unlike FDG which correctly identified 37 of the 38 lesions. A possible explanation for this is the high background activity due to the metabolism of FLT.

High hepatic uptake of FLT was first described by Shields et al in 1998 (Shields et al., 1998b). This work was conducted using canine subjects and a pilot study involving one human with non-small cell carcinoma of the lung was included. Using the canine model quantitative analysis of intravenous blood sampling and dynamic PET imaging was performed (as has been carried out in human subjects in chapter 3 of this thesis). Selective uptake in the bone marrow was demonstrated with a mean SUV of 4.6 and low uptake in the brain was observed. FLT was excreted by the kidneys and HPLC analysis of the dog urine revealed over 95% of the activity was present as unchanged parent compound with late blood sampling also showing 90-97% remaining unchanged. In the human subject similar uptake patterns as those found in this study were demonstrated in the bone marrow and kidneys. The most interesting finding was the unexpectedly high uptake which was observed in the liver (SUV 7.6 at 64min) compared to the low uptake in canine hepatocytes. This high SUV value for liver uptake in the one human study compares well to what was found in the cohort of patients studied in this chapter.

The divergent liver uptake finding is explained by the difference between dogs and humans in the hepatic glucuronidation of 3'-azido-3'-deoxythymidine (AZT) related compounds, where the biotransformation rate was shown to be much lower in dog

hepatocytes than human ones (Nicolas et al., 1995). The process of FLT glucuronidation within the liver leading to this high background uptake is best explained by examining the hepatic metabolism of the drug from which it was developed AZT. Prior to exerting its antiviral effect AZT undergoes sequential intracellular phosphorylation in a way analogous to FLT. In addition to this phosphorylation pathway, the alternative pathway of AZT metabolism is the formation of AZT glucuronide within the liver (Good et al., 1990; Moore et al., 1995). This reaction is catalysed by the enzyme UDP-glucuronosyltrtansferase resulting in compounds which are more water soluble, less toxic, and easier to excrete in the bile and the urine (Barbier et al., 2000; Veal and Back, 1995). This theory is supported by the significantly higher normal liver SUV (mean 4.5) in FLT scans as compared with FDG (mean 2.1). Accordingly, the detected hepatic lesions were those with SUVs higher (mean 6.5) than those recorded for the normal liver. This suggests the existence of a minimum 'uptake threshold' which has to be exceeded to allow the detection of hepatic lesions with FLT. On the other hand, the lack of FLT uptake in colorectal liver metastases may be a good prognostic sign. The lack of visualisation of lesions may reflect the less aggressive nature of these tumours by virtue of them having a lower proliferative rate (Slingerland and Tannock, 1998). This is investigated in the following chapter.

4.6 Conclusion

FLT generally demonstrates lower cellular trapping and hence lower SUVs in comparison with FDG. The demonstration of no correlation between the retention of the two tracers further confirms that there is no direct relationship between glucose utilisation and the uptake of FLT in tumour cells. The poor sensitivity which FLT displays in the detection of colorectal liver metastases makes it a poor candidate as a staging tool for CRC. Although lacking in sensitivity, FLT does have the potential to improve the specificity for the detection of CRC. The prognostic implications of the uptake of this novel tracer need to be assessed in terms of response to chemoradiotherapy and ultimately survival.

CHAPTER 5

Quantifying cellular proliferation in colorectal cancer: a comparison of FDG and FLT PET with immunohistochemistry

5.1 Background

The only reliable methods dictating what, if any, adjuvant therapy patients with CRC will receive, are the Duke's grading system(Dukes., 1932), and the TNM staging system introduced by the American Joint Committee on Cancer (Compton et al., 2000). These in addition to the histological grade of the tumour are reviewed in section 1.2.3. Seventy years since the introduction of Duke's staging coupled with the more recent TNM system and the histological grade of the tumour remain the only reliable methods dictating what, if any adjuvant therapy patients with CRC will receive.

Unfortunately under current guidelines, which have been set up in light of the above prognostic indicators, there is still a cohort of patients who unnecessarily receive toxic chemotherapy whilst others who could potentially benefit from it are not recommended to receive it.

This has led to the attempt to try and define a marker on which therapeutic decisions could be made with greater precision. The potential value of quantifying cellular proliferation using the Ki-67 antigen present in the cycling cell, has led to an effort to predict populations of individuals with CRC who may or may not benefit from adjuvant chemotherapy. This has been highlighted in section 1.10.6.

However present methods to assess tumour proliferation require a tissue sample and are therefore limited by potential morbidity and sampling problems. A non invasive method to assess proliferation might avoid unnecessary biopsies and permit serial assessments during cancer therapy. Having established that FLT-PET can be used for the imaging of CRC *in vivo*, I now move on to ascertain whether the images produced are indeed those of cellular proliferation and their potential value.

5.2   Aims

The aims of this chapter are to

i)   Compare the uptake of FDG with cellular proliferation as quantified using

MIB-1 (anti-Ki67 antibody) immunohistochemistry.

ii)   Compare the uptake of FLT with cellular proliferation as quantified using

MIB-1 (anti-Ki67 antibody) immunohistochemistry.

iii)   Evaluate the role of PET in quantifying *in vivo* cellular proliferation in CRC.

5.3 Methods

5.3.1 Patient selection

Ten patients (5 male, 5 female), median age 68 years (range 54-87), with 13 resectable primary or recurrent CRC were recruited at diagnosis from local surgical clinics. Patient demographics can be seen in table 5.1. Written informed consent was obtained following approval from the Local Ethical Committee and the ARSAC committee (appendix B and C). All patients underwent whole body FDG scanning followed by an FLT scan with a median intervening period of 5 days (range 1-19).

Following surgical resection, the lesions were sent for routine histopathological assessment in addition to immunohistochemical analysis.

5.3.2 Imaging

Acquisition of the whole body scans in addition to tracer and patient preparation is covered in the general materials and methods in Chapter 2.

Scanning data was acquired at a mean time of 57mins (SD 10) p.i and 62mins (SD 12) p.i for FDG and FLT respectively. Post injection image acquisition time for FLT was determined through the work carried out in chapter 3 with respect to the time activity curves. Specifically the images were acquired at a significant time after the initial 10min rapid accumulation phase, thus allowing for the tracer uptake to plateau. Mean injected activity was 371MBq (SD 24) for FDG and 351MBq (SD 52) for FLT.

A ROI approach as described in Chapter 2, was used to obtain SUVs in order that the uptake of the respective tracers could be quantified and compared.

5.3.3 Immunohistochemistry

Routine histological examination was performed on 4µm thick haematoxylin and eosin (H&E) stained sections. Immunohistochemistry was performed by using 3µm thick sections cut from paraffin blocks and dried overnight at 60°C. Sections were taken from xylene (2 changes), through graded alcohols (100% and 70%) to water. Antigen retrieval was performed by pressure cooking for 2 minutes in a conventional 15lb pressure cooker. The slides were cooked for 2mins, then flushed with running tap water.

The slides were then rinsed in 0.05% Tween 20 in Tris buffered saline (TBS/Tween) in an incubation tray. Endogenous peroxidase activity was blocked for 10 minutes using a commercially available peroxidase blocking solution (DAKO, Ely, Cambridgeshire, UK.). The sections were rinsed in TBS/Tween and then primary mouse monoclonal antibody (MIB-1 (DAKO, Ely, Cambridgeshire, UK.) diluted 1/50 in TBS pH7.4) was applied for 60 minutes at room temperature.

The sections were rinsed in TBS/Tween and secondary antibody (goat anti-rabbit/mouse), (DAKO, Ely, Camdridgeshire, UK.) was applied for 30 minutes. The sections were again rinsed in TBS/Tween and streptavidin-horseradish peroxidase was applied for 30 minutes. After rinsing in TBS/Tween, diaminobenzidene, used as a chromogen, was applied for 7mins. A haematoxylin counter stain was applied for 2mins.

Sections were dehydrated through graded alcohols (70% and 100%), cleared in xylene (2 changes) and mounted with DPX.

5.3.4 Examination of sections

Sections of tumour were identified on the H&E slides and the corresponding MIB-1 sections were examined independently by 2 experienced observers A and B, blinded to the results of the scans.

Three MIB-1 stained sections of tumour were used for each lesion in order to account for tumour heterogeneity. Thirty high power fields (x40 objectile lens) were examined and 50 tumour cells were assessed per field using a graticule, making a total of 1500 cells per case. A labelling index (LI) was calculated as the percentage of positive staining nuclei out of all nuclei examined. 'Positive' nuclear staining was regarded as staining of the entire nucleus. Nuclei with no staining or nucleolar staining only were regarded as negative.

5.3.5 Statistical analysis

Inter-observer reliability was assessed using Pearsons correlation coefficient, linear Regression analysis using the SPSS 10.0.7 statistical software package (SPSS, Inc.,Chicago, IL, USA) was employed to correlate uptake of both FLT and FDG with MIB-1.

5.4   Results

Histopathology of the lesions (n=13; 5 primary cancers, 5 liver metastases and 3 peritoneal deposits) confirmed adenocarcinoma in 12 of the 13 cases. The remaining case was thought to be a malignant peritoneal recurrence by pre-operative CT, [18]FDG PET imaging and at intraoperative evaluation, but on microscopic histological examination it was found to be an inflammatory lesion secondary to fat necrosis.

There was excellent inter-rater reliability between the two observers responsible for quantifying proliferation using MIB-1 immunohistochemistry, with a Pearson's correlation coefficient of 0.9 (figure 5.1).
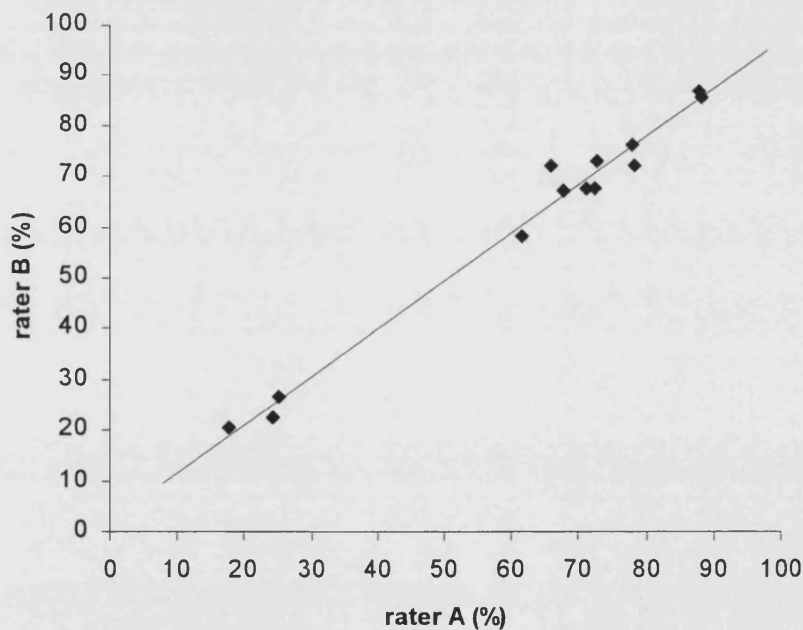
Figure 5.1 Inter rater correlation between observer A and B (Pearsons correlation coefficient of 0.9)

Patient demographics in addition to quantification of tracer uptake and the corresponding LI's can be seen in table 5.1. All five primary tumours and both malignant peritoneal lesions were visualised with increased focal uptake as compared to the surrounding tissue using both FLT and FDG. The SUVs of these primary lesions ranged between 5.9 and 5.7 for FDG and 1.4 and 5.5 for FLT. The corresponding LIs of these lesions ranged between 67% and 77%.

Patient	Gender	Age (yrs)	Weight (Kg)	Resected lesions	FDG (SUV)	FLT (SUV)	Labelling Index (% MIB-1)
1	M	87	72	Primary (asc colon)	9.2	3.5	69
2	M	66	82	Peritoneal recurrence	7.6	3.3	60
				Peritoneal lesion†	7.8	-	23
3	F	78	54	Liver metastases 1*	5.5	-	19
				Liver metastases 2*	11	-	26
4	F	75	63	Primary (rectal)	9.6	4.8	70
				Liver metastases	3.7	9.1	87
5	M	62	85	Primary (caecal)	9.7	5.5	77
6	F	60	58	Liver metastases	3.7	4.8	73
7	M	59	70	Primary (trans colon)	8.5	2.9	67
8	F	54	55	Primary (rectal)	5.9	1.4	69
9	F	67	95	Peritoneal recurrence	4.5	2.6	75
10	M	71	65	Liver metastases	4.7	6.1	87

Table 5.1 Summary of patient dermographics, SUVs and labelling indices.

All of the five liver metastases were shown to be avid for FDG but only three of these lesions were clearly seen to be avid for FLT. All three FLT avid metastases showed a corresponding high proliferation labelling index (73%, 87% and 87%).

The three lesions (peritoneal inflammatory lesion and 2 liver metastases) which did not show increased uptake of FLT and were therefore not visualised using this tracer had corresponding low proliferation rates as determined by the LIs, ranging from 19 – 26.

The SUVs for all thirteen lesions seen with FDG ranged between 3.7 and 11 compared to a range of 1.4 – 9.1 for the 10 lesions visualised using FLT .

There was statistically significant correlation (R=0.8, p<0.01) between the SUVs of the 10 tumours visualised with FLT and the corresponding LIs (figure 5.2).
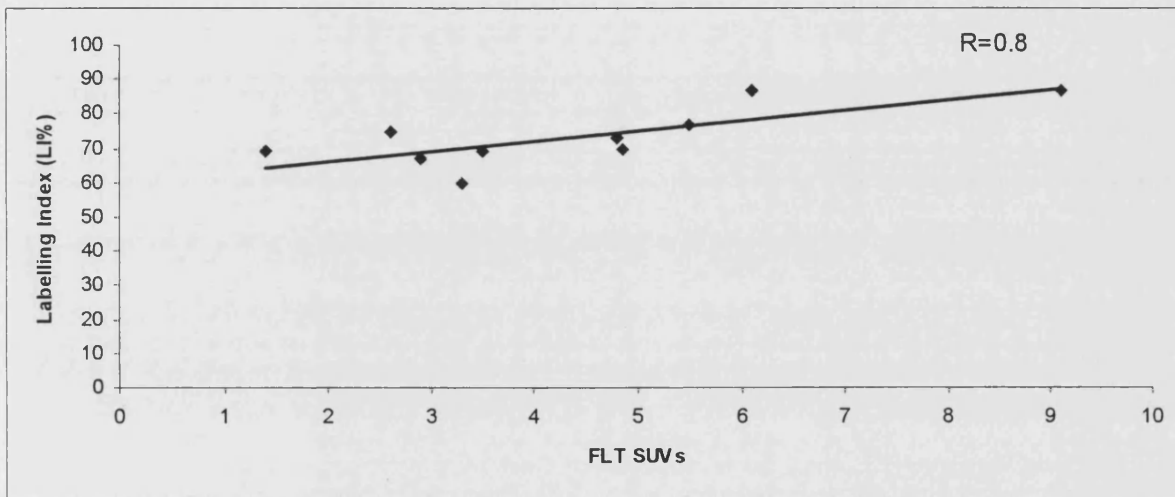
Figure 5.2 Correlation between SUVs of the 10 tumours visualised with FLT and the corresponding LIs. (R=0.8).

No such correlation (R=0.4) was demonstrated in the case of the FDG avid lesions and LIs (figure 5.3).
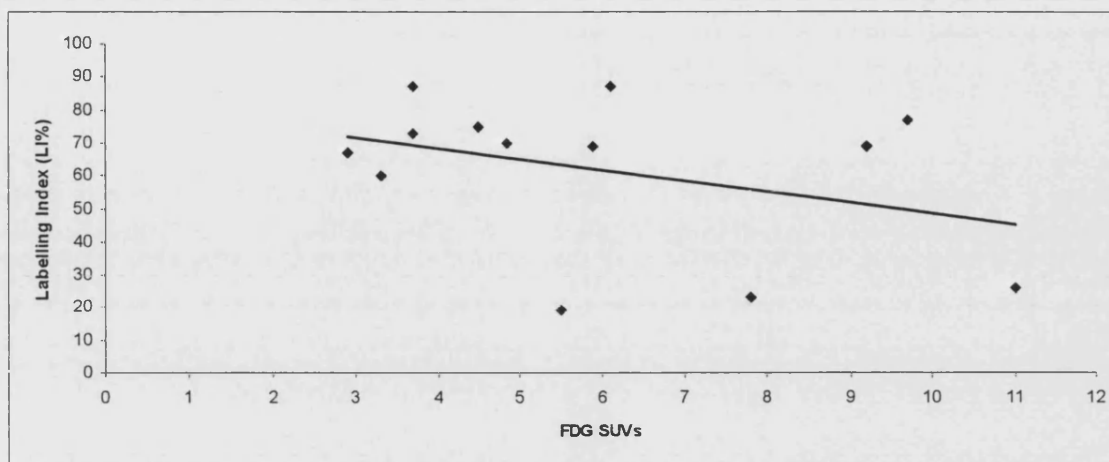
Figure 5.3 Correlation between SUVs and those lesions seen avid for FDG (R=0.4).

Three specific cases demonstrating the differences between uptake of both tracers and the corresponding LIs are shown in figure 5.4. The resected tumour specimens represented are a primary caecal carcinoma (a) and two colorectal liver metastases from separate patients (b) and (c). The macroscopic histology is compared to how the distribution of the tracer is seen in the PET images using both FDG and FLT. The lower cellular trapping of FLT as compared to FDG is clearly seen. In addition the high liver background secondary to the glucuronidation of the FLT within human hepatocytes is demonstrated. The liver metastases shown in (b) which can be seen against the high background also shows a very high LI of 87% as demonstrated in the MIB-1 microscopic slide section shown. The LI of the liver metastases from the second patient (c) is significantly lower and therefore is not seen against the background liver in the FLT PET image.

170

MACRO	FDG	FLT	MIB-1

a

b

c

LI 77%

LI 87%

LI 19%
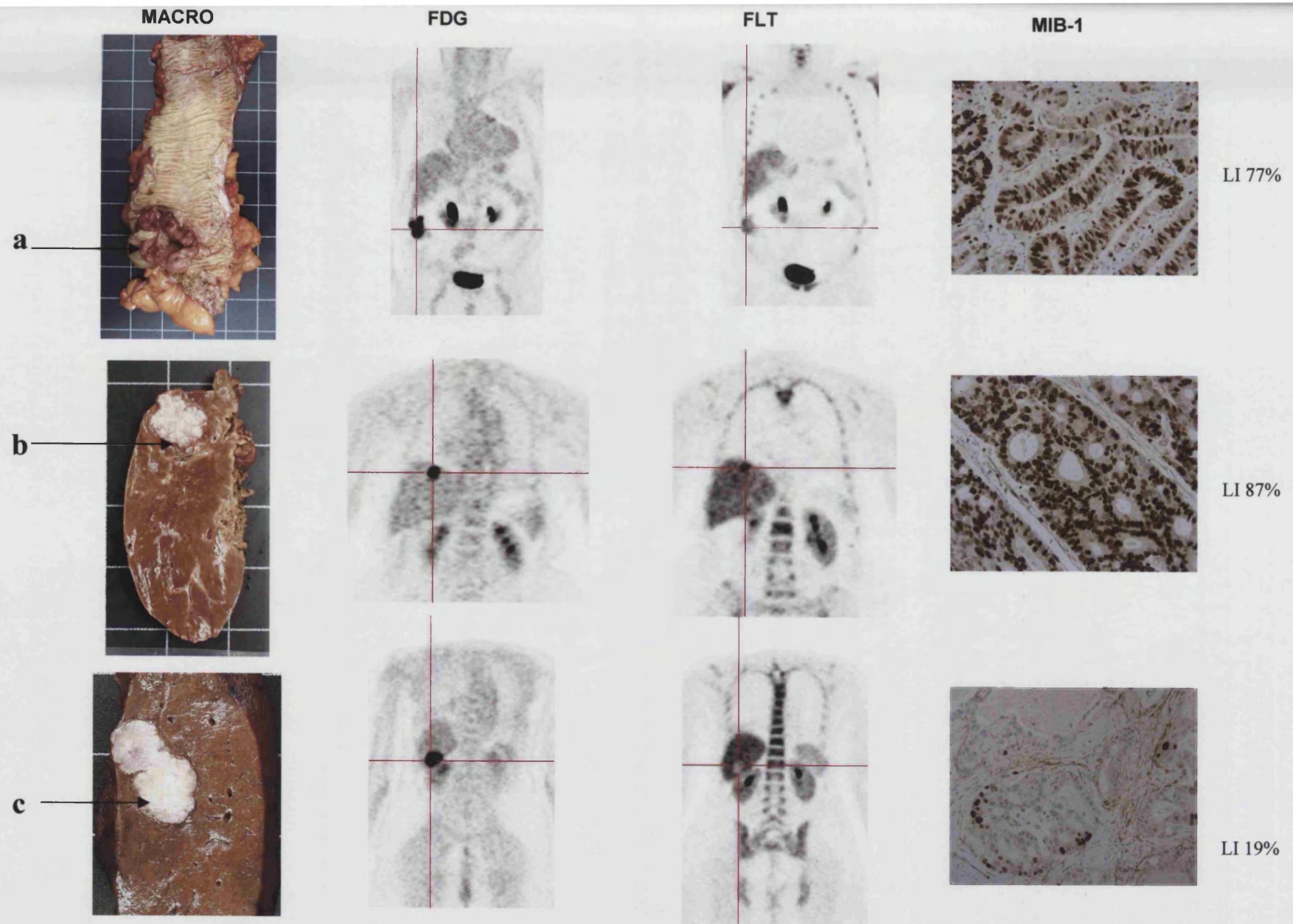
Figure 5.4 Specific cases demonstrating differences between FDG, FLT and corresponding labelling indices.

5.5 Discussion

There is no previously published data comparing FLT-PET and immunohistochemistry in the quantification of proliferation in CRC. The results from this chapter suggest that FLT reflects proliferative activity in CRC as determined by MIB-1 staining, with a strong correlation (R=0.8). Therefore, it is possible to non-invasively acquire an *in vivo* measurement of proliferation equivalent to an immunohistochemical marker. The lesions successfully imaged with FLT demonstrated higher SUVs in addition to higher LIs when compared to those lesions not visualised by FLT which were shown to have correspondingly lower SUVs and LIs.

The lack of correlation between the LIs and FDG in this study supports previous *in vivo* and *in vitro* evidence that FDG is not a specific marker of proliferation. Higashi et al has demonstrated in ovarian cell lines that the utilisation of glucose by tumour cells represented by FDG uptake is not a reflection of cell proliferation as measured by DNA flow cytometry and 3H-Thymidine incorporation, but is strongly related to the number of viable tumour cells (Higashi et al., 1993). Buck et al attempted to use FDG-PET *in vivo* in order to estimate proliferative activity as a means of differentiating pancreatic cancer from chronic active pancreatitis. In this study, again no correlation was found between FDG uptake and cellular proliferation using MIB-1 immunostaining (Buck et al., 2001). Although it is generally accepted that a highly proliferating cell would need proportional amounts of energy, supplied by glucose metabolism, metabolic activity is also needed for other cell functions, therefore the two processes of glucose metabolism and proliferation would not necessarily correlate.

172

It is known that the glucuronidation of FLT within the liver leads to high hepatic background activity which may inhibit its diagnostic utility as demonstrated in Chapter 4. This was again exemplified by the failure of FLT-PET to identify 2 of the 5 liver metastases against this high liver background. However, both these lesions displayed low proliferation LIs (19% and 26%) suggesting relatively slow growth compared to the remaining 3 liver metastases (LIs of 87%, 87% and 73%). The fact that certain liver lesions are not seen with FLT may have prognostic implications in terms of aggressiveness of these tumours.

Unfortunately it was not possible to carry out surgical resection and subsequent histology on the "metabolically silent" lung metastasis described in chapter 4. Such an investigation might have yielded valuable information which would have contributed to our understanding as to why certain colorectal lung metastases do not show avid for FLT despite the very low thoracic background. Proliferation indices tend to correlate well with aggressiveness of some tumour types, eg, lymphoma and breast adenocarcinomas. In terms of colorectal carcinomas, clear evidence does not as yet exist, with conflicting results from different trials detailed in section 1.10.6. The most recent report, a retrospective analysis of 706 patients by the National Surgical Adjuvant Breast and Bowel Project Collaborative Study Group, does suggest that proliferation has prognostic implications (Allegra et al., 2003). The relationship between proliferation and tumour behaviour for liver metastases is as yet unknown.

The only published work to date using FLT-PET to quantify proliferation in humans *in vivo*, has been in studies investigating lung lesions. In a prospective study of thirty patients with solitary pulmonary nodules in which all the cases had histological

assessment, FLT uptake using SUVs was compared to proliferative activity as quantified with Ki-67 immunohistochemistry. This showed that FLT PET had a sensitivity of detecting malignant lesions of 86% on qualitative review and agreed with the results of this chapter in that uptake correlated significantly with proliferation rate (correlation coefficient 0.87) (Buck et al., 2002b). Further work, investigated ten patients with either histologically proven or clinically suspected non-small cell lung cancer. In this study, as in chapter 3 of this thesis, arterial and venous blood sampling with dynamic PET imaging was carried out in order that both the SUVs and the FLT flux determined by Patlak analysis could be utilised. These were compared to determine any correlation with Ki-67 proliferation indices. Excellent correlations were found between $SUV_{average}$ measures of FLT uptake (R=0.84) and Ki-67 scores with even stronger correlations using Patlak derived FLT influx (R=0.94) (Vesselle et al., 2002). These two studies have shown that FLT uptake can be used to image lung tumours and can be used to asses proliferation rates. Both authors of these respective studies felt that it might have a role to play in the further characterisation of lung lesions as well as the determination of prognosis and therapy.

In addition to malignant lung lesions, the role of FLT as an imaging agent of proliferation has been investigated *in vitro*, in a murine model using SCID mice and in human disease in B-cell lymphoma (Wagner et al., 2003). The findings of this work again found good correlation between SUVs and the Ki-67 labelling index of the tissue biopsies in the human cohort (R=0.95). The mouse lymphoma model showed that the injected dose per gram of FLT correlated with the *in vivo* Bromodeoxyuridine (a uracil analogue) labelling index. Following a 240min incubation period the *in vitro* studies revealed that

12.5% of the total FLT applied was trapped within the cell and approximately 1% was recovered from the DNA. The incorporation of FLT into DNA has also been investigated using a rat model and asynchronously growing tumour cell lines. In the former samples of rat spleen and intestine were removed for DNA analysis and separation following administration of FLT, where DNA incorporation was found to be only 2% (Lu et al., 2002). A second study used asynchronous human cell lines to which [^{3}H]FLT was added and following incubation both cell cycle measurements and DNA extraction was performed (Toyohara et al., 2002). FLT uptake correlated well with %S-phase fraction (R=0.76) in addition to [^{3}H] thymidine uptake (R=0.88). Although [^{3}H]FLT incorporation into the DNA fraction was again negligible (0.2%). The results from these studies show FLT correlates with proliferation markers, in fact it is an extremely accurate surrogate measure of cellular proliferation although its lack of incorporation into DNA does not, at present allow it to be a direct marker.

The very nature of PET allows the metabolic assessment of the whole tumour in its heterogeneic entirety overcoming inherent problems with tissue sampling. The excellent correlation in terms of CRC, shown by the work in this chapter coupled with the lung tumour studies (Buck et al., 2002; Vesselle et al., 2002), have demonstrated that PET's unique ability to quantitate the uptake of the tracers used, non-invasively and *in vivo*, can open new avenues in the assessment of malignancy by functional imaging.

This has the potential to offer the clinician a further prognostic marker with which to assess the aggressiveness of the disease and perhaps allow a more precise method for therapeutic decisions to be made. In real terms, a decision regarding response to chemotherapy in CRC is usually judged 6 weeks into a 12 week treatment cycle. The

potential of avoiding 6 weeks of unnecessary toxic chemotherapy by establishing the non-responders from the responders at a pre-treatment stage is a prospect which cannot be ignored.

Future work will help in validating FLT-PET as a potential tool for the non-invasive *in vivo* assessment of CRC and may enable more accurate evaluation of the antitumoural effects of new as well as established anticancer drug treatments aimed at competing with DNA synthesis.

5.6 Conclusion

This chapter has demonstrated that FLT PET may be used as a non-invasive method of quantitating cellular proliferation in CRC. The tracer FDG, on the other hand, does not offer this. This might allow CRC to be imaged at a pre-treatment stage and define the population of patients who might benefit from neo-adjuvant therapy. In addition, it may also help in identifying a group of patients with recurrent disease who would not benefit from first line chemotherapy as a result of the low proliferation rate of the tumour as demonstrated by the low SUV on FLT-PET imaging.

CHAPTER 6

Monitoring 5-Fluorouracil chemotherapy response in colorectal cancer using FLT *in vitro.*

6.1 Background

5-Fluorouracil (5FU) has been the mainstay of chemotherapy for CRC. The metabolic pathways and current evidence supporting its clinical role are covered in detail in section 1.4.2.

Briefly, the rapid metabolism of 5FU produces by one pathway, 5-fluorouridine triphosphate (5FUTP) which is incorporated directly into RNA. A second deoxynucleotide synthesis pathway enables 5FU to exert two independent effects. The metabolism of 5FU to 5FUTP allows incorporation directly into genomic DNA with potentially cytotoxic results. Alternatively the production of 5-fluorodeoxyuridine monophosphate (5-dFUMP) inhibits thymidylate synthase thus depleting the production of thymidine monophosphate, which is an indispensable precursor of *de novo* DNA synthesis. When this occurs, the thymidine necessary for DNA synthesis has to be acquired through the salvage pathway.

FLT is phosphorylated to FLTMP by the S phase specific enzyme TK (section 1.12.3). This leads to the intracellular trapping of the tracer via the salvage pathway of DNA synthesis. The cytotoxic effect of 5FU chemotherapy necessitates that cells employ this pathway in order to obtain thymidine for DNA synthesis.

Current knowledge of tumour biology has allowed greater opportunities for cancer treatment. Much interest has been shown in the development of molecules which have the potential to interfere with cell cycle control. As for all clinical trials pharmacodynamic endpoints need to be defined for anti-cancer agents. Non-invasive imaging using PET is a particularly attractive option to assess these end points in terms of

tumour response to therapy. Its proven value using FDG has already been discussed in section 1.6.4.

In this chapter the impact on FLT uptake that the administration of 5FU has on CRC cells *in vitro* is assesssed. CRC cell lines are employed to create a model to look at the potential role of FLT PET in monitoring response to therapy in 5FU treated CRC.

6.2   Aims

The aims of this chapter are to:

i)   Optimise growth over time for two CRC cell lines to mimic actively growing *in vivo* CRC tumours.

ii)   Quantify the dose response cytotoxicity of 5FU in the two CRC cell lines.

iii)   Establish the uptake of FLT over time in the CRC cell lines.

iv)   Investigate the impact that 5FU has on the uptake of FLT in CRC cell lines to establish its role in monitoring treatment response *in vitro*.

6.3 Methods

6.3.1 Materials and cell lines

i) **Materials:** Plastic consumable items were bought from Nunc (VWR, Poole, Dorset, UK), while chemicals were obtained from Cambrex Biowhittaker (Woking, Berks, UK), unless otherwise stated.

ii) **Cell lines:** The human colorectal cancer cell lines used were: HT29, derived from a primary colorectal cancer and SW620, derived from a colorectal lymph node metastasis (both from the European Collection of Animal Cell Cultures, Porton Down, Wilts, UK).

6.3.2 Routine maintenance

HT29 and SW620 cells were routinely grown in $75cm^2$ flasks in Dulbecco's Modified Eagle's Medium (DMEM) containing 2mM glutamine, supplemented with foetal calf serum (FCS, 10% v/v) and penicillin & streptomycin antibiotic mixture (100 IU/ml and 100 µg/ml respectively), at 37°C. All work described below was carried out within 15 cell passage numbers for each cell line to avoid differences due to phenotypic drift.

To propagate the rolling stock of cells and also obtain cells for carrying out the proposed experiments, cells were allowed to grow to near confluence levels (approximately 90%), washed in phosphate buffered saline (PBS) followed by washing in 0.02% Ethylenediamine tetracetate (EDTA) in PBS and enzymatically disaggregated using trypsin (1mg/ml in EDTA/PBS). PBS removes any serum (FCS) while EDTA chelates (and therefore "removes") calcium; the latter, like FCS, is inhibitory for trypsin action. Disaggregated cells were harvested in medium supplemented with FCS to partially

neutralise trypsin, centrifuged (400g, 5min) to separate cells from trypsin-containing supernatant and again resuspended in fully supplemented medium. Cells were either (i) passaged into flasks (at between 1:3 to 1:8 ratios), gassed using 10% CO_2 and grown at 37°C, in a dry incubator for stock, or (ii) counted using a haemocytometer and resuspended at appropriated dilutions for further experiments as described below.

6.3.3 Basic experimental protocol

To determine the pattern of uptake of radioactive tracer early after chemotherapy, experiments were designed as follows: Cells were seeded and allowed to settle and grow for 48 hours (2 days). At this time point, 5FU was added for 2 hours and then removed from the cells. Radiotracer uptake was investigated immediately after 5FU removal (day 0 of 5FU treatment), and 1 and 2 days later, ie, day 1 and day 2 post 5FU treatment. The total time cells were in culture was 4 days; 2 for cells to settle down and grow and 2 for experiments. From this point onwards in the text, days 0, 1 and 2 refer to time post 5FU treatment. Specific experimental conditions were defined from pilot studies described below.

6.3.4 Optimisation of seeding densities

Six-well plates (growth area of 9.5cm^2 per well) were chosen to carry out investigations in 5FU cytotoxicity and subsequent radiotracer uptake, so that end-of-experiment harvesting would result in cell numbers sufficient for counting under a light microscope (5FU effects) and volumes large enough (2ml) for scintigraphy (radiotracer uptake).

The purpose of this pilot study was to determine appropriate seeding densities - for 6-well plates - for the two cell lines which would result in actively growing cell populations (mimicking actively growing in vivo tumours) without reaching confluence. Cell concentrations from 100,000 cells per well to 500,000 cells per well (volume of 2ml) were seeded and left to adhere and grow for 48, 72 or 96 hours, ie times which correspond to days 0, 1 and 2 post 5FU treatment. Cells were washed and disaggregated with trypsin/EDTA (200μl) as described previously, centrifuged and resuspended in fully supplemented medium, before counting cell numbers using a heamocytometer.

The seeding densities which gave appropriate growth without reaching confluence for all time points was 200,000 cells per well for HT29 and 200,000 cells per well for SW620. These plating concentrations were used for all experiments described below.

6.3.5 Dose response cytotoxicity of 5FU

HT29 and SW620 cells were seeded in 6-well plates and allowed to grow for 48 hours. 5FU (2μg/ml to 150μg/ml) was placed in the wells (2 ml per well) and cells were incubated (37°C, CO_2 incubator) in the dark for 2 hours (because 5FU is photosensitive). Drug containing medium was removed from the wells, cells were washed twice in PBS and fully supplemented medium was replaced. Parallel experiments were stopped at day 0, immediately after 5FU removal, or days 1 or 2. Cells were trypsinized and then counted on a haemocytometre as described. Tryphan blue dye (Sigma, Poole, Dorset, UK.) was added to the cell mixture before counting to identify dead cells – which take up the dye (Tryphan Blue exclusion method). Every 6-well plate had at least one untreated well as internal control. This study determined the dose for treating cells as 50μg/ml,

which resulted in non-significant killing on day 0 (up to 10%), with killing on days 1 and 2 significant at 50% and 75% respectively.

6.3.6 Uptake over time of radiotracers

HT29 and SW620 cells were seeded in 6-well plates and allowed to grow for 48 hours, as described previously. FLT (100KBeq per well) was placed on the cells for 5 to 180 minutes. The experiment was stopped at the different time points using ice-cold PBS (3x 2ml washes) and the cells were rapidly trypsinised. All washes and final cell aliquots were placed in the gamma counter (figure 3.3) to obtain a measure of the activity present in each cell sample.

6.3.7 Radioactive tracer uptake in 5FU treated cells

SW620 cells (200,000 per well) were seeded in 6-well plates and allowed to grow for 48 hours, as described previously. Cells received 5FU (2 ml of 50μg/ml per well) and were incubated in the dark for 2 hours (37°C, CO_2 incubator). At that time, 5FU was removed, cells were washed twice with PBS and given fully supplemented medium. Cultures were given FLT (100KBeq per well, 90 min) on days 0, 1 or 2 post 5FU treatment. The experiment was stopped with ice-cold PBS (3 washes) and cells were trypsinised and counted on the gamma counter. Wells on each plate were given no radiotracer but were used for counting cell numbers from both 5FU treated and untreated cultures. Results are expressed as radioactivity present per viable cells. Only SW620 cells were used for this experiment, since a persistent infection at that point, made HT29 cell growth and FLT uptake suspect.

6.3.8 Statistical analysis

To establish the significance of the effect of 5FU on cell growth, the Mann Whitney test was used with a $p < 0.05$ as significant (SPSS 10.0.7 statistical software package, Inc, Chicago, IL).

To correlate change in FLT uptake with cell killing, non linear regression analysis was used.

6.4   Results

6.4.1 Optimisation of seeding densities

Cells were seeded at different concentrations in 6-well plates and allowed to grow for 48, 72 or 96 hours. Results are shown for concentrations between 100,000 and 300,000 (figure 6.1).

(a)

(b)
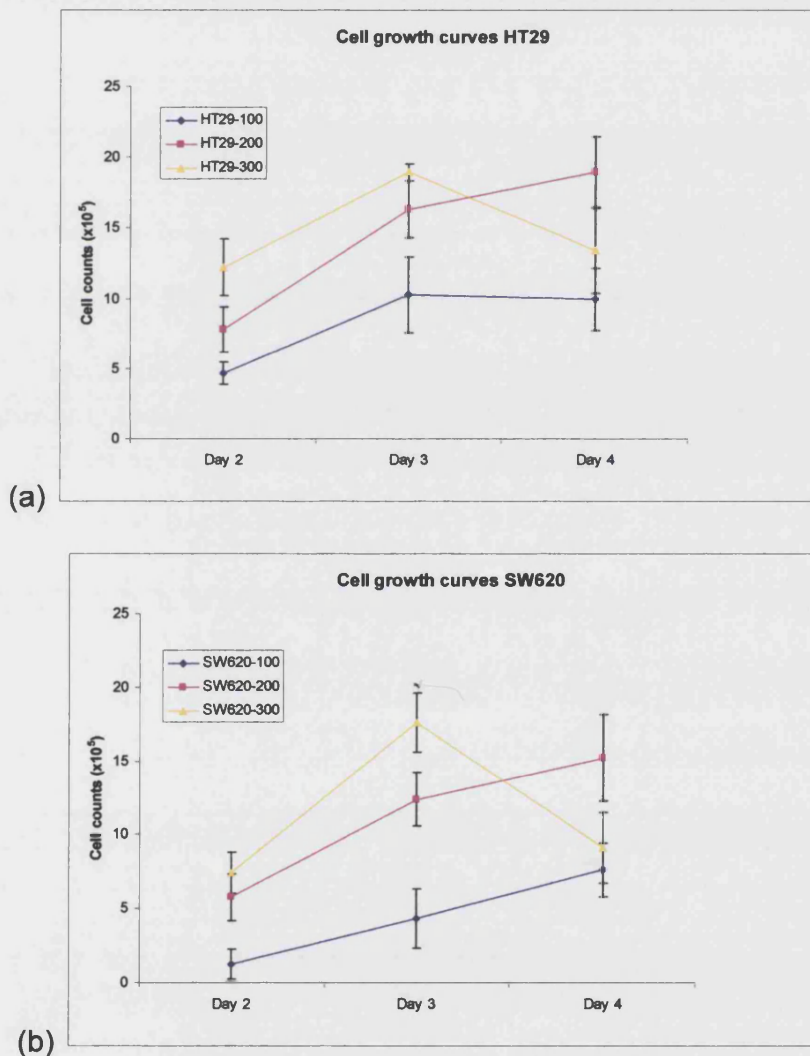
Figure 6.1 Cell growth curves at seeding densities between 100, 000 and 300,000 for HT29 (a) and SW620 (b). In the colour key, 100, 200 and 300 refers to 100,000, 200,000 and 300,000 cells respectively. Results are shown as mean and standard deviation of 4 experiments.

The highest seeding concentration for both cell lines (300,000 cells per well) usually resulted in maximum growth by 72 hours. Visual inspection under the light microscope confirmed confluence in these wells, at this time point. Thereafter, the number of cells in the well either stayed stationary or started decreasing, due to contact inhibition. A confluent state for the cells would not mimic an actively growing *in vivo* tumour. The smaller concentrations of 100,000 gave a small number of cells at 48 hours which rarely exceeded 40% confluence by eye. Therefore, 200,000 was considered more appropriate for the experiments. Furthermore, this level of growth would allow for a enough cells to survive and counted after 5FU exposure.

6.4.2 5FU cytotoxicity

Cells were exposed to various concentrations of 5FU and resultant cytotoxicity was quantified immediately after 5FU removal (day 0), or at days 1 and 2 post 5FU treatment. Growth of cells (expressed as percent of control) immediately after exposure to the drug (day 0) was not significantly different from control untreated cells, for any of the concentrations tested. This was evident for both cell lines as is demonstrated in figure 6.2. On day 1 post treatment, a dose-dependent decrease in %cell number was noted. This was maximal at doses equal or greater than 25μg/ml and produced approximately 50-55% drop in cell number compared to controls, for both cell lines. A further decrease in cell numbers (70-83% of controls) was seen on day 2 with all concentrations tested, with significant killing shown for 50 and 75μg/ml 5FU.

Effect of 5-Fluorouracil on HT29 Colorectal Cancer Cell Number

(a)
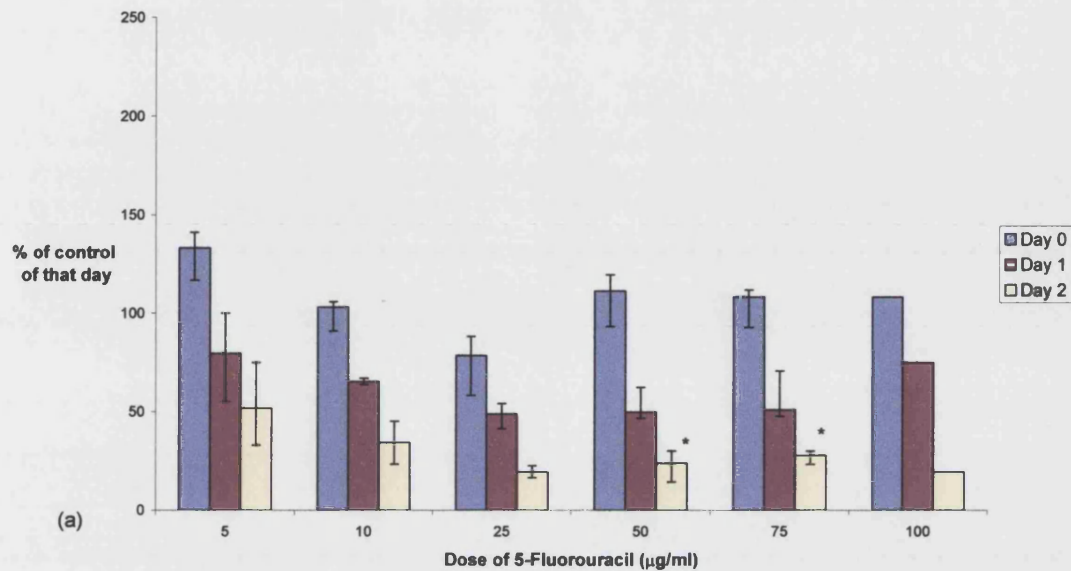
Effect of 5-Fluorouracil on SW620 Colorectal Cancer Cell Number

(b)
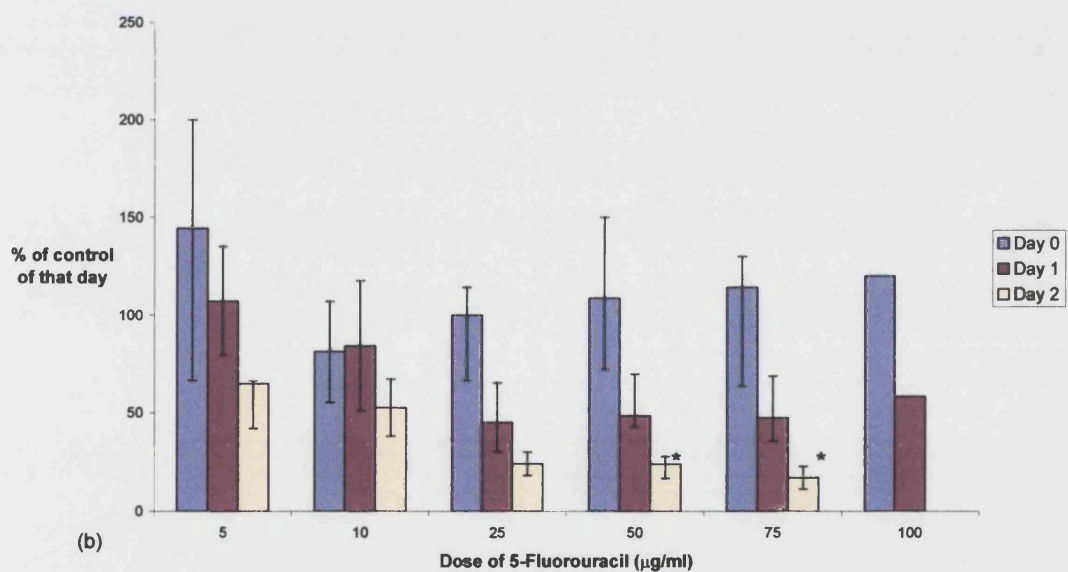
Figure 6.2 Effect of 5FU on cell number for both cell lines, HT29 (a) and SW620 (b). Results are shown as medians and ranges of 4 experiments; apart from the dose 100µg/ml.

* significantly less growth than control was observed by 2 days post treatment at 50 & 75 µg/ml ($p < 0.05$, Mann Whitney)

188

Figure 6.4 shows absolute cell numbers over the time period of the experiment. HT29 cells (figure 6.4(a)) which received no 5FU always grew well. However, the effect of even the smallest dose of 5FU on the absolute cell number was quite profound, with cells hardly growing after 5FU administration on day 0. Similarly to HT29 cells, SW620 cells which were not treated with 5FU grew well over the course of the experiment (figure 6.4(b)). Unlike HT29, SW620 cells still grew after 5 and 10μg/ml 5FU administration, but to a lesser extend than control untreated cells. However, at concentrations greater than 25μg/ml, growth was stunted. The 5FU concentration chosen for contacting further experiments was 50 μg/ml.
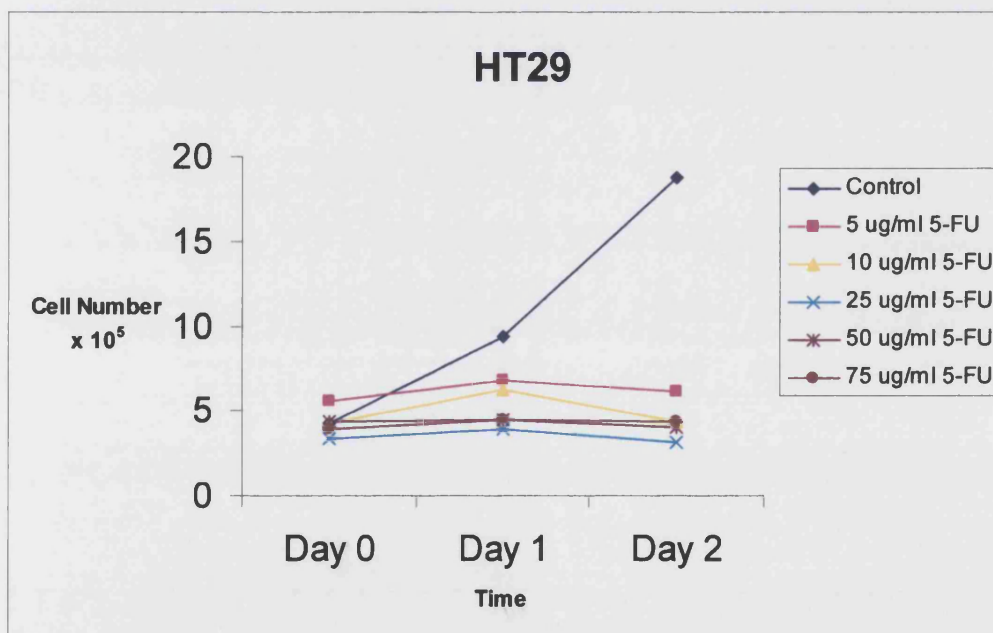
(a)
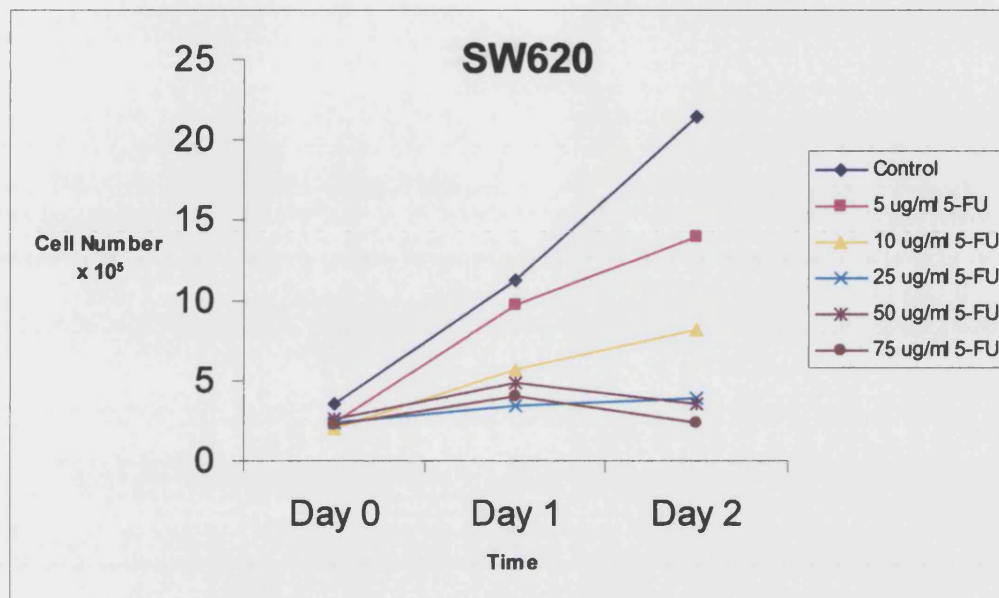
(b)

Figure 6.3 Absolute cell numbers over time following exposure to 5FU (5 - 75µg/ml) at days 0,1,2 post - treatment for HT29 (a) and SW620 (b). Examples of one experiment per cell line shown.

6.4.3 FLT uptake over time

To determine a time when the uptake of FLT by cells would reach saturation, the radiotracer was administered from 5 to 180 minutes. A steadily increasing uptake of cellular FLT was seen over the first 45–60min of exposure, with saturation observed by 90 minutes, for both cells lines (figure 6.4) Therefore, 90 minutes was chosen as exposure time to FLT for subsequent experiments.
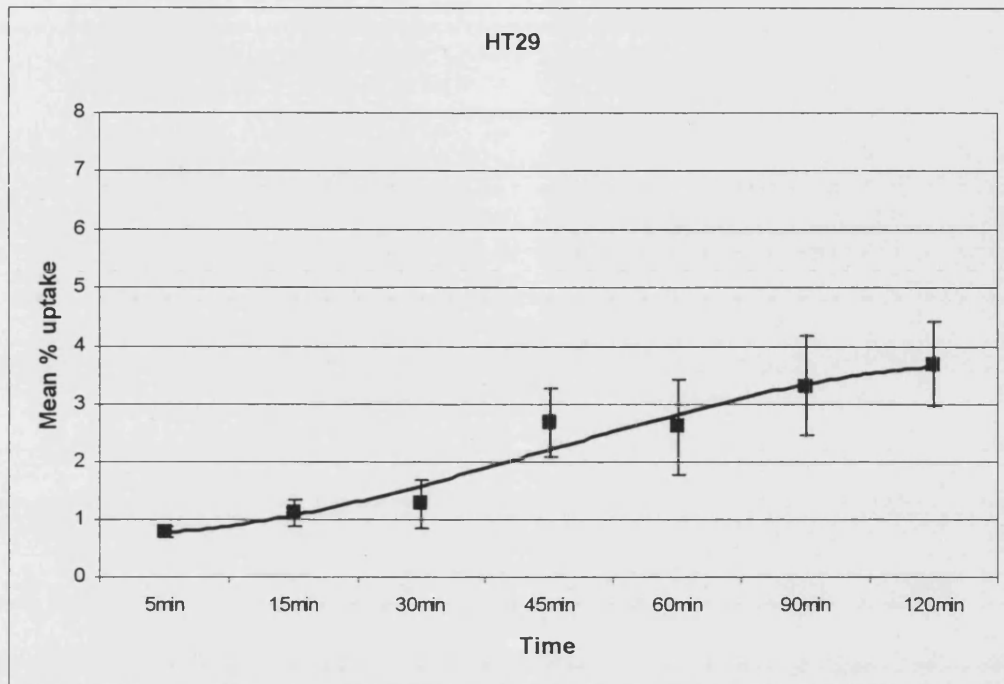
(a)
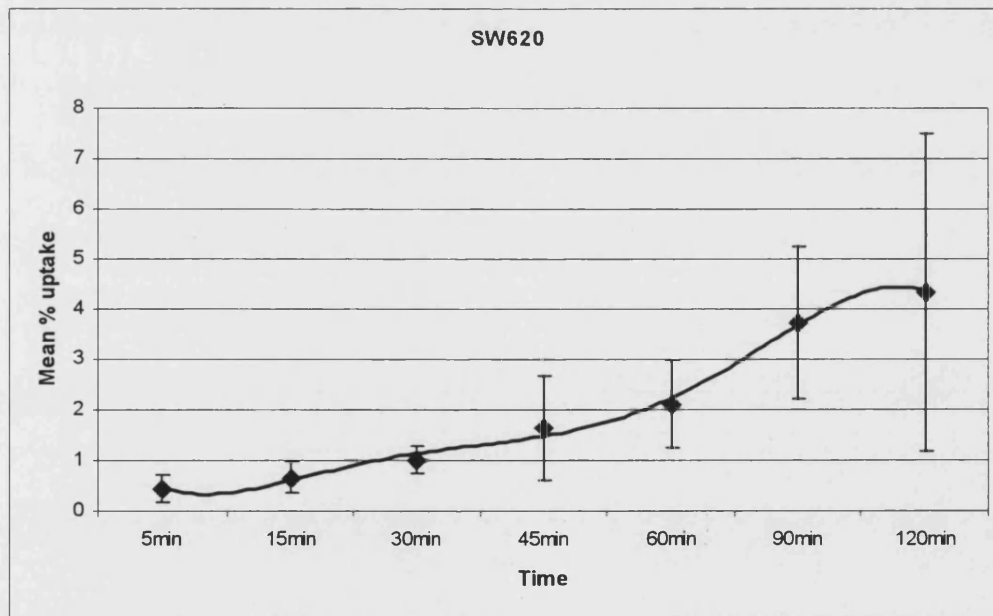
(b)

Figure 6.4 FLT uptake over time seen for both cell linesHT29 (a) and SW620 (b). Results are shown as means and SD of 5 experiments.

Before counting cell radioactivity, the wells had been washed three times to remove excess (figure 6.5). The largest percentage of radioactivity was present in the supernatant and of the remaining excess radiotracer, most was removed with subsequent washes.
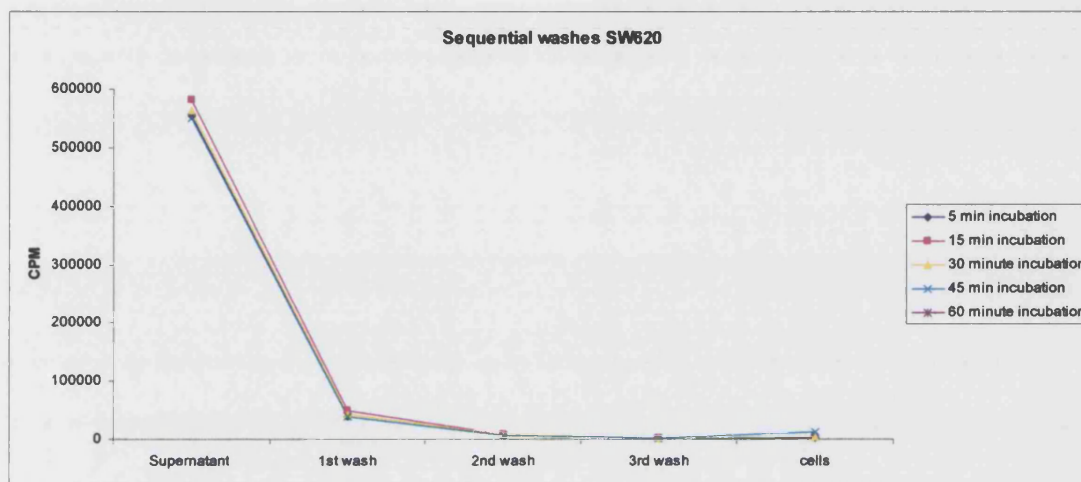
(a)
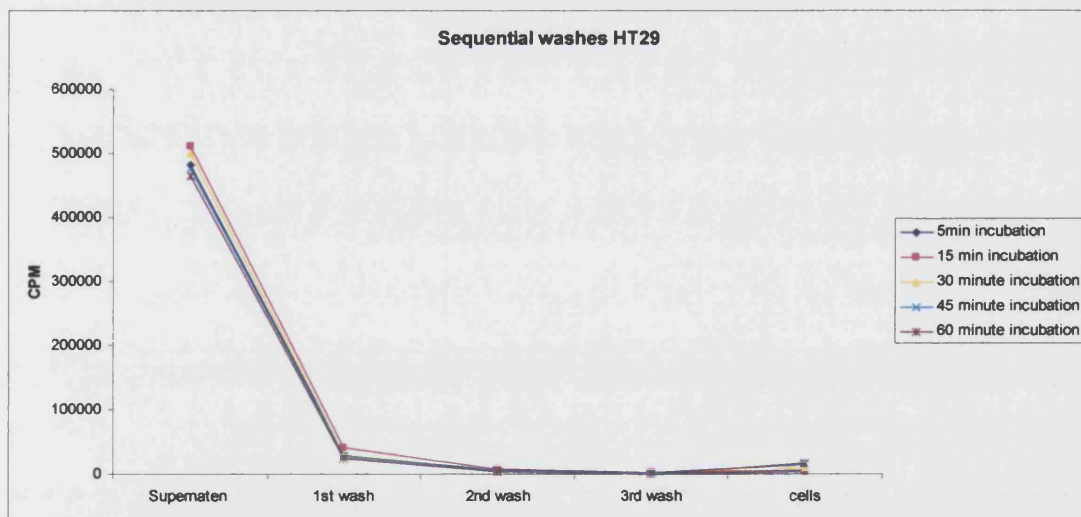
(b)

Figure 6.5 Example of amounts of radiotracer (counts per minute, CPM) present in supernatant, washes and cells, at 5 – 60 minutes of incubation. (a) HT29, (b) SW620.

6.4.4 FLT uptake in 5FU treated cells

Cells (SW620) were treated with 5FU (50μg/ml, 2 hours) and were given FLT either immediately after 5FU removal (day 0), or after 1 or 2 days. For meaningful comparisons, the radioactivity taken up by specific test and experimental cell populations was corrected for cell number. Although 5FU treated cell numbers compared to controls were unchanged on day 0, a median 4.7- fold increase in FLT uptake was observed (table 6.1).

	% cell killing		Fold increase in FLT uptake	
	Median	Range	Median	Range
Day 0	5	0 - 16	4.8	3.6 – 6.9
Day 1	47	26 – 54	8.3	6.5 – 10.2
Day 2	76	73 - 82	14.7	12.7 – 17.8

Table 6.1 % cell killing with corresponding increase in FLT uptake for days 0 – 2.

On day 1, 5FU produced 47% (26-54) killing, with a corresponding 8.3 fold increase in FLT uptake. On day 2, the drug killed 76% of cells and FLT uptake increased 14.7-fold. Therefore, as cell kill increased, there was a corresponding increase in FLT uptake which correlated well (R = 0.9) (figure 6.6)

193
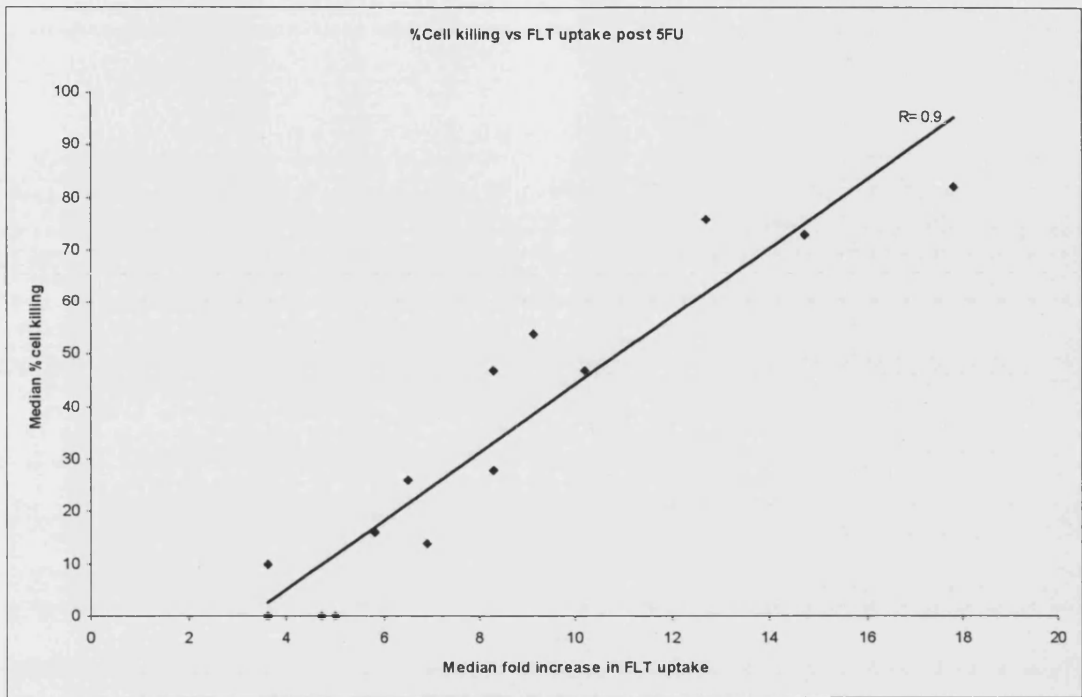
Figure 6.6 Correlation between cell killing and FLT uptake in the SW620 cell line.

6.4   Discussion

The study in this chapter represents the first *in vitro* work carried out assessing the effect on FLT uptake of 5FU, when administered to CRC cell lines. 5FU belongs to a group of anti-cancer drugs known as the "anti metabolites" which exert lethal toxicity only for cells that are synthesising DNA and is therefore an S phase specific drug. After killing all vulnerable cells, an increase in concentration of 5FU will have systemic deleterious effects.

The doses of 5FU chosen for the experiments described result in approximately 50% and 75% reduction in viable cell numbers at 1 and 2 days post treatment. The effect of 5FU seen here is comparable to previous research which found cells derived from the HT29 cell line to be most sensitive to 5FU from a total of six human epithelial cancer cell lines, including two colonic adenocarcinoma cell lines (Calabro-Jones et al., 1982).

In assessing response to chemotherapy using FDG-PET a decrease in the uptake of the tracer is taken as a indicator of a positive response (Young et al., 1999)The results of this study have demonstrated that *in vitro,* a dramatic increase in FLT uptake by CRC cells is seen, which corresponds to a positive response to 5FU therapy in terms of cell kill. This indicates that although increasing 5FU doses resulted in decreased absolute numbers of viable cells, the ability of these cells to take up FLT increased.

Dittmann et al have conducted the only *in vitro* study to date investigating the potential of FLT in monitoring the early response to chemotherapy (Dittmann et al., 2002). Oesphageal cell lines were used and the early changes in FLT uptake following chemotherapy were assessed. The effects of 5FU, methotrexate, cisplatin and gemcitabine on FLT accumulation 4, 24 and 72 hours following exposure were recorded. FLT uptake

was shown to increase 7-10 fold 24 hours following treatment with 5FU or methotrexate. A more moderate 5 fold increase in FLT accumulation was observed with gemcitabine. For the above drugs the total FLT uptake exceeded that of controls despite considerable reduction in cell counts due to cytostasis up to 72hr after treatment. In contrast, accumulation of FLT decreased in a dose related manner following exposure to cisplatin. This study suggests that tumour cell uptake of FLT reflects changes specific to the cytostatic drug used for treatment.

Both the study presented here and the results published by Dittmann et al highlight the significant increase in FLT uptake early after 5FU therapy. The implications of this dramatic increase can be partly explained by the mechanism by which FLT is sequestered by the cells. As has been previously discussed in section 1.10.3 FLT trapping is dependant on the S-phase specific enzyme thymidine kinase 1 (TK1). Recent *in vitro* work using pancreatic cell lines evaluated the expression of the pyrimidine metabolising enzymes in addition to the uptake of FLT (Seitz et al., 2002). TK activity was measured by Western blot analysis, immunofluoresence staining and flow cytometry. Quantitative DNA recovery was performed to assess FLT incorporation into DNA in addition to HPLC analysis of the FLT metabolites in cells. This study demonstrated the uptake, trapping and a 1.28% incorporation of FLT into the DNA. TK1 was validated as the rate limiting enzyme of FLT metabolism and its over expression in pancreatic cell lines and human pancreatic cancer led to it being thought of as a promising tracer in this disease. Furthermore in a recent study by Barthel et al, TK1 levels were significantly increased compared to controls 2 days post 5FU treatment. This is consistent with the possibility

arising from this study that increased FLT uptake may be partly the result of altered TK1 catalytic activity (Barthel et al., 2003).

Like any *in vitro* study, the present study is a simplified version of the *in vivo* situation. It does not account for important parameters like vascularisation and oxygenation, which often vary in different tumour regions and may also be modulated by treatment. Furthermore, tumours regularly contain non-uniform cell populations of which a proportion are not tumour cells but supporting stroma cells, endothelial cells and inflammatory cells. PET imaging of *in vivo* tumours represents a reflection of the average behaviour of the cell types present in the tumour mass. This needs to be taken into account when interpreting the results of this study.

If the 5FU mediated increase in FLT accumulation demonstrated in this study is also seen *in vivo* then persistent uptake after treatment of CRC with this agent would be non-diagnostic, since a drug induced increase might obscure effective proliferation inhibition by the drug. Barthel's study demonstrated FLT uptake by fibrosarcomas grown in mice was actually reduced following 5FU treatment. This corresponded to a decrease in tumour cell proliferation, detected by staining histological sections (Barthel et al., 2003). It would be interesting to carry out similar investigations in the clinical setting to determine the uses of FLT in mapping treatment response in CRC.

6.5 Conclusion

In response to the treatment of CRC cell lines to 5FU chemotherapy, FLT surprisingly demonstrated a dramatic increase in uptake. A likely explanation of this is through an increased activation of the salvage pathway of DNA synthesis and the cytostolic enzyme TK1. If a similar pattern is observed *in vivo* then the problem will be determining whether the drug has caused effective proliferative inhibition or indeed one is simply observing a drug induced increase in tracer accumulation.

CHAPTER 7

Conclusion

7.1 Summary of findings

The success of PET in oncological imaging is based on the knowledge that malignancy leads to an alteration in cellular biochemical reactions. Synthesis of positron-emitting analogues from molecules of organic matter can demonstrate these biochemical processes. The combination of PET and the glucose tracer FDG is an established imaging tool which has made a significant impact in CRC.

The recent development of the biologically stable thymidine analogue FLT has allowed PET to visualise a different biological process. This is achieved by targeting the salvage pathway of DNA synthesis, and hence the images are related to cellular proliferation.

This thesis has investigated various techniques for the characterization of FLT uptake *in vivo* in patients with primary and metastatic CRC. In chapter 3 when time activity curves were acquired using the gold standard oncological PET tracer FDG and compared to those acquired using FLT, there was lower uptake by FLT as a function of time. In terms of quantitative analysis the behaviour of FLT *in vivo* utilization was characterized by a 3k model for data up to 60 minutes p.i. In addition, a high correlation was demonstrated between the NLR(3k) and the simplified Patlak analysis with either measured or image derived input functions. The good correlation seen between SUVs and the quantitative measures of FLT utilization in terms of the net influx constant K_i suggests that non-invasive methodology may be used to assess the proliferation rates of CRC tumours with FLT. In view of these findings the quantification of the uptake of this

new tracer using SUVs represents a true reflection of rate of uptake of the tracer. It was therefore justified to use SUVs.

In chapter 4, FLT was shown to demonstrate considerably lower cellular trapping and hence lower SUVs in comparison with FDG. This lack of correlation between the retention of the two tracers gave further evidence to there being no direct relationship between glucose utilisation and the uptake of FLT in tumour cells. Unfortunately poor sensitivity was demonstrated in the detection of liver metastases which is a common site for metastatic spread. This makes FLT a poor candidate as a staging tool for CRC. Although lacking in sensitivity, FLT did display potential in improving the specificity for the detection of CRC, as in this study no FLT uptake was seen in the inflammatory lesions which displayed high avidity for FDG.

Chapter 5 demonstrated that FLT PET may be used as a non-invasive method of quantitating cellular proliferation in CRC. The tracer FDG, on the other hand, does not offer this. This might allow CRC to be imaged at a pre-treatment stage and define the population of patients who might benefit from neo-adjuvant therapy. In addition, it may also help in identifying a group of patients with recurrent disease who would not benefit from first line anti proliferative chemotherapy as a result of the low proliferation rate of the tumour as demonstrated by the low SUV on FLT PET imaging. The prognostic implications of the uptake of this new PET probe warrant further investigation in terms of response to chemoradiotherapy and ultimately survival.

The final results chapter of this thesis (chapter 6) attempted to assess the effect on FLT uptake of the most commonly used chemotherapeutic agent for CRC. The dramatic increase in FLT uptake demonstrated *in vitro* following 5FU administration most

probably reflected the activated salvage pathway of DNA synthesis, overshadowing the inhibition of proliferation caused by 5FU. This of course presents a potential problem trying to determine whether the drug has caused effective proliferative inhibition. However it was encouraging to see excellent correlation between the increase in FLT uptake and cell kill induced by the 5FU.

7.2 Future perspectives

`The development of FLT has raised the hope of a PET probe whose specific biological action has the potential to (a) determine tumour proliferation rates and therefore aggressiveness and (b) monitor response to chemoradiation therapy.

Work in this thesis demonstrated that FLT may be used as a non-invasive *in vivo* assessment of proliferation within CRC. Its potential to act as an indicator of tumour aggressiveness through this biological parameter has to be followed up in terms of patient outcome and ultimately survival. This would enable us to see if uptake of FLT indeed gave a true reflection of the future pathological disease process.

The effect on tracer uptake that 5FU chemotherapy has on CRC cell lines was also investigated in this thesis. This work has to be taken from the bench and assessed *in vivo*. If meaningful results are obtained FLT-PET might allow the clinician to overcome the inherent problems of tumour heterogeneity and tissue sampling in assessing a tumour's response to therapy.

Appendix A

PET components and image generation

i) Components of a PET facility

Cyclotron

The positron emitting radionuclides ^{15}O, ^{13}N, ^{11}C and ^{18}F are all produced by nuclear bombardment in a cyclotron. The cyclotron consists of two 'dee electrodes', which are about 1m in diameter. An ion source is located at the centre of the dees and produces negative ions. The application of an alternating voltage causes the ions to move from one dee to another. The ions are forced to travel in a circular orbit by a strong magnetic field at right angles to the plane of the dees. The diameter of orbit increases as the ions pick up energy from the electric field. As they approach the outer edge of the dees, the ions are passed through a thin carbon stripping foil which where electrons are stripped and the resulting H^+ ions move out of the magnetic field and directed towards a target to undergo a nuclear reaction with a specific target material needed to produce the radionuclide required.

The short half lives of the radionuclides ^{15}O ($T_{1/2} = 2.07$min), ^{13}N ($T_{1/2} = 9.96$min) and ^{11}C ($T_{1/2} = 20.4$min) necessitate that the scanner be sited close to the cyclotron. The most widely used clinical PET tracer is [18F]Fluoro-2-Deoxy-D-glucose (FDG) which uses the radionuclide ^{18}F incorporated into the biological compound FDG. This synthesis occurs in a radiochemistry laboratory. The $T_{1/2}$ of 109.8min allows for several hours transport time, therefore for centres without their own on-site cyclotron, a radiotracer distribution facility is used which supplies [18F]FDG once or twice daily. Prior to use or dispatch the PET tracer undergoes strict quality control and quality assurance eg, high performance liquid chromatography (HPLC) is employed to ensure adequate chemical, radiochemical and radionuclide purity.

FDG is the most commonly used PET tracer for CRC imaging and is described in detail in section 1.7.2. Another tracer which has been used with effect is [^{18}F]Fluorouracil. This is a ligand which is identical to the non- labelled fluorouracil chemotherapeutic agent used in CRC, has also been used in the assessment of CLM. A double tracer study using [^{18}F]Fluorouracil and [^{15}O]water identified the transport system of fluorouracil in the liver metastases and showed potential for the selection of those patients more likely to profit from intra-arterial chemotherapy (Dimitrakopoulou-Strauss et al., 1998).

PET scanners

There are a variety of detectors capable of imaging positron-emitting tracers. They can be broadly divided into four classes:

i) thallium doped sodium iodide gamma camera with lead collimators

ii) dual-head rotating sodium iodide camera with modified electronics for coincidence detection

iii) dedicated sodium iodide PET camera with ring detection system

iv) dedicated bismuth germinate oxide (BGO) PET camera with either a full or partial ring detection system.

It is not in the realms of this thesis to discuss the technology of each of these detectors as current dedicated PET scanners are high performance multi-slice devices usually employing discrete BGO scintillation crystals. The PET scanner used in this thesis is the Advance Scanner (Advance, General Electric Medical Systems, Milwaukee, W1). This consists of 12,096 bismuth germinate crystals constructed into a ring which surrounds the

patient. This is considered to be the gold standard because the BGO crystals are better suited to the 511KeV photons produced. Much higher count rate performance is achieved due to the multicrystal layout, allowing a higher injected dose and improved image quality.

ii) Annihilation coincidence detection

The average range of a positron in soft tissue is only a few millimetres following this journey it combines with a electron to produce two 511KeV γ rays which are emitted at almost 180° to each other. If these are detected within a certain time of each other (this is known as the *coincidence time window*) then it is assumed that they both originated from the same annihilation event, and the original disintegration occurred along a line joining the two detection positions and coincidence detection occurs. The BGO ring surrounding the patient is arranged in such a way that pairs of detectors are placed on opposite sides of the ring to allow them to operate in coincidence with each other and data can be reconstructed without the use of a collimator.

iii) Attenuation correction

The definition of "attenuation" is the process by which a beam of radiation is reduced in energy when passed through tissue or other material (Dorland.,1988).

The ability to directly measure and correct for photon attenuation makes PET an inherently quantitative procedure, enabling the rates of biochemical processes to be measured *in vivo*. Attenuation correction can be performed using an external (transmission) source. PET allows the fraction of the photon flux attenuated by tissue to

be independent of where along the line joining the detectors the radionuclide lies. Therefore accurate attenuation correction can be made. The correction factors are obtained by the calculation of the ratio between two additional scans, a blank scan and a transmission scan, which are performed with external positron emitting sources (Germanium rod sources). The introduction of the state of the art Discovery LS PET/CT scanner used in this thesis, utilises CT images for PET attenuation correction (CTAC). The advantages of this are that it produces less noisy transmission maps with shorter times of acquisition. Recent work by Visvikis et al has demonstrated that with FDG, CTAC is a viable alternative to rod sources for AC, reducing overall time of wholebody transmission acquisition from 15-20 min to 0.5-1.5 min (Visvikis D et al., 2002).

iv) Image reconstruction

The theory of reconstruction is very mathematical and is outside the scope of this thesis. Briefly two methods are commonly used. Filtered back projection (FBP) is the most common technique in use with gamma cameras as it is quick and provides acceptable results. The theory is that the acquired planar images are projections of the distribution of activity. These projections can subsequently be backprojected onto a matrix placed at the centre of the camera's field of view to produce an image. Simple back projection creates a very blurred image and a filter is applied to the data to remove this blurring and to control noise and artefacts at high spatial frequencies hence the term FBP.

Ordered Subsets Expectation Maximisation (OSEM) method is the most widely applied iterative reconstruction technique, which modifies the reconstructed data set until

projections formed from the reconstructed dataset match those measured from the patient. This type of reconstruction used to be much slower but courtesy of modern improved computer technology is in common use and able to include corrections for scattering, AC and variation in response with depth.

Appendix B

Ethical approval

UNIVERSITY COLLEGE LONDON HOSPITALS
THE MIDDLESEX HOSPITAL
Department of Surgery
2nd Floor, 67/73 Riding House Street
London, W1W 7EJ
Fax No: 020 7636 5176

HOSPITALS

Consultant:	**Professor I.Taylor**		
Personal Assistant:		**(020 7679 9312)**	
Research Fellow:	**Mr Daren Francis**	**(07976 396684)**	**e-mail: dlfrancis@ukonline.co.uk**

09.10.01

Dear Dr MacAllister

Study No: **00/0295**
Title: **A comparison of 2-F18 fluoro-2-deoxy-D-glucose (FDG) with F18-fluorothymidine PET for imaging patients with colorectal cancer.**

Thankyou for considering the amendments to our study. We have addressed the four issues raised as follows:

1. The information sheet now contains details of the risks associated with arterial line insertion. Pain, haemorrhage and thrombosis. (Please see highlighted section on the amended information sheet attached)

2. Local anaesthetic will be used for arterial cannulation.

3. The gauge of the cannula will be 20 gauge (1mm diameter).

4. Bilateral arterial supply to the hand will be confirmed and documented with hand held doppler and if there is any doubt of the presence of an Ulnar artery then the patient would be **excluded** from the study.

University College London Hospitals **NHS**

NHS Trust

The Joint UCL/UCLH Committees on the Ethics of
Human Research: Committee Alpha

Chairman:
Professor André McLean

Please address all correspondence to:
Iwona Nowicka
Research & Development Directorate
UCLH NHS Trust
1st floor, Vezey Strong Wing
112 Hampstead Road, LONDON NW1 2LT
Tel. 020 7380 9579   Fax 020 7380 9937
e-mail: iwona.nowicka@uclh.org

Professor PJ Ell
Institute of Nuclear Medicine
The Middlesex Hospital
Mortimer Street
London
W1N 8AA

06 February 2002

Dear Professor Ell

Study No: **02/0013** *(Please quote in all correspondence)*
Title: **Comparison of F-18-3-deoxy-3-fluoro-thymidine (FLT) and F-18-fluorodeoxyglucose (FDG) PET imaging in patients with metastatic or locally advanced cancer: A phase I pilot study.**

Thank you for letting us see the above application which was reviewed by the Chairman and agreed by Chairman's Action.   There are no objections on ethical grounds to this study going ahead on condition that the radiation dose is explained in the patient information sheet. Please supply a copy of an amended information sheet for completeness of our records.

Please ensure that you have obtained final approval from the Trust (via the R&D office) before proceeding with your research.

Please note that it is important that you notify the Committee of any adverse events or changes (name of investigator etc) relating to this project.   You should also notify the Committee on completion of the project, or indeed if the project is abandoned. **Please remember to quote the above number in any correspondence.**

Yours sincerely

Professor André McLean, BM BCh PhD FRC Path
Chairman

/comalpha/aml/ijn/06/02/02

University College London Hospitals **NHS**

NHS Trust

Committee A Co-Chairmen:
Mr Michael Harrison and Dr Raymond MacAllister

Please address all correspondence to:
Iwona Nowicka
Research & Development Directorate
UCLH NHS Trust
1st floor, Vezey Strong Wing
112 Hampstead Road, LONDON NW1 2LT
Tel. 020 7380 9579   Fax 020 7380 9937
e-mail: iwona.nowicka@uclh.org

Mr D Francis
Department of Surgery
67-73 Charles Bell House

3-Oct-01

Dear Mr Francis

Study No: **00/0295** *(Please quote in any correspondence)*
Title: **A comparison of 2-F18 fluoro-2-deoxy-D-glucose (FDG) with F18-fluorothymidine PET for imaging patients with colorectal cancer.**

Your amendment to the study was considered by Ethics Committee A and the following points raised:

1. The information sheet should contain details of the risks associated with arterial cannulation (pain, haemorrhage, thrombosis).
2. Local anaesthetic should be used for arterial cannulation.
3. What is the gauge of the cannula to be used?
4. Do you intend to confirm bilateral arterial supply to the hand via the ulnar artery prior to cannulation? If so, do you intend to cannulate the radial artery in patients who do not have an ulnar artery?

If you can address these issues then your study may proceed.

Yours sincerely

Dr R MacAllister
Chairman

Francis3oct/rmac/03/10/01

213

CONFIDENTIAL
Patient Information Sheet

A comparison of F18 –fluorothymidine (FLT) PET with routine PET in patients with colorectal cancer

You are invited to take part in a research project. You do not have to take part in this study if you do not want to. If you do decide to take part you may withdraw at any time without having to give any reason. Your decision whether to take part or not will not affect your care and management in any way. All proposals for research using human subjects are reviewed by an ethics committee before they can proceed. This proposal was reviewed by the joint UCL/UCLH Committees on Ethics of Human Research.

1. This study aims to establish if positron emission tomography (PET) scans using an alternative radioactive tracer, FLT, is more accurate than the conventional radioactive tracer, FDG for imaging bowel cancer.

2. It has been shown that FDG-PET is an accurate and safe means of imaging patients with bowel cancer. This allows the most appropriate treatment to deal with an individual patient's cancer to be chosen. The information, therefore, influences the extent of surgery performed and possibly the use of other treatments such as chemotherapy or radiotherapy.

3. The accuracy of FDG-PET, although extremely good, is not perfect. One method of improving this situation is to use an alternative radioactive substance to pinpoint the site of cancer cells in the body. FLT is such an alternative and it can be safely substituted for FDG for PET scanning.

Description of the research study:

In addition to a routine FDG-PET scan that patients with bowel cancer undergo at this hospital, you will have an FLT-PET scan. PET scans take place in the Institute of Nuclear Medicine at the Middlesex hospital, usually on separate days. The procedure will entail you having to fast for a period of four hours (so that glucose that you consume in your diet will not interfere with the FDG-PET scan). Once you are in the Institute of Nuclear Medicine you will be given an injection of FDG (chemically similar to glucose, but which has been labelled with a radioactive substance) through a cannula (plastic tube) in a vein. The radioactivity lasts approximately 90 minutes, therefore you do not have to wait for the scan. You will have to lie on a platform that moves you into the scanner. The scan itself takes one hour and you will need to lie still with minimum interaction with staff, as this interferes with the scan quality. The whole process takes between 2 to 4 hours. The procedure for the FLT scan is similar to that described above, but you will receive an injection of FLT instead of FDG. **Most importantly**, you will have a cannula inserted into an artery and a vein in your arm so that we can take blood (about 50 ml in total – 1/6 of the volume of a standard fizzy drinks can) in order to analyse it. Before inserting the arterial cannula the blood supply to your hand will be evaluated to assess if it is OK for you to take part in the study. We undertake this so that in the highly unlikely event that the artery should become damaged or clotted (thrombosed) there would be **no** adverse affects. Local anaesthetic will be used prior to inserting the arterial cannula to minimise any pain or discomfort. After removal of the cannula we will press on the artery so as to stop it bleeding. This all helps to increase the accuracy of the scan report we can give to the doctors looking after you. It will also help us develop a way of working out the distribution of FLT in the blood so that patients in the future may avoid the blood tests. The cannulae will remain in your arm for an hour. If you proceed to have an operation, the surgeon will make a thorough examination and document the findings. A tiny fragment of the cancer and surrounding tissue will be taken for examination by one of the doctors involved in the study. Cancers need growth promoting agents as well as a blood supply therefore particular attention will be

paid to the presence of these factors. The main part of the tissue, which is removed, will be sent for analysis by a pathologist, as is the usual practise. A comparison will be made between both types of PET scan to see if there is in fact any difference in the information gained. Both scan findings will then be related to the analysis of the tissue removed.

The Joint UCL/UCLH Committees on the Ethics of Human Research:
Committee Alpha and A
Research & Development Office
UCLH NHS Trust
1st floor Vezey Strong Wing
112 Hampstead Road
London NW1 2LT

ACKNOWLEDGEMENT

Study reference: **00/0295**	Principal Investigator's name: **Professor PJ Ell**

Study title: **A comparison of 2-F18 fluoro-2-deoxy-D-glucose (FDG) with F18-fluorothymidine PET for imaging patients with colorectal cancer.**

We acknowledge that Mr Francis has taken over from Mr T Arulampalam as Clinical Research Fellow to Professor Taylor and Professor Ell.

Opinion of Ethic Committee: (please indicate one of the following)

(i)   The contents have been noted and the study may continue   ☑

(ii)   Please supply more information about the serious adverse event(s)   ☐

Signature:........................ .... Date: **May 11, 2001**

Print Name: Iwona Nowicka

Position in Ethics Committee: Administrator

/Please continue on a separate page if necessary/

Appendix C

ARSAC approval

CERTIFICATE

FOR THE

ADMINISTRATION OF RADIOACTIVE MEDICINAL PRODUCTS

Certificate Reference Number RPC 141-790 (15381)

It is hereby certified for the purposes of the Medicines (Administration of Radioactive Substances) Regulations 1978, amended by the Medicines (Administration of Radioactive Substances) Amendment Regulations 1995, that

      Peter Josef ELL
      The Middlesex Hospital
      Institute of Nuclear Medicine
      Mortimer Street
      London
      W1T 3AA

may administer until 8 Jul 2003 the radioactive medicinal products specified in the Schedule to this certificate for the purpose(s) there specified.

for The Secretary of State for Health

....
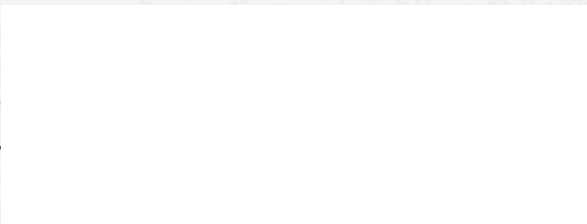
Health Care Directorate   9-Jul-2001
Specialist Clinical Services Division
Department of Health

Department of Health

MEDICINES CONTROL AGENCY

Market Towers   1 Nine Elms Lane   London SW8 5NQ
Telephone 020 7273 0220
Facsimile 020 7273 0443

Professor P J Ell
Institute of Nuclear Medicine
Mortimer Street
LONDON W1T 3AA

Our Ref: MF8000/11079

6 June 2001

Dear Professor Ell

THE MEDICINES (EXEMPTION FROM LICENCES) (SPECIAL CASES AND MISCELLANEOUS PROVISIONS) ORDER 1972
PRODUCT: (F-18) Fluorothymidine

I am writing in connection with your notification under the Medicines (Exemption from Licences) (Special Cases and Miscellaneous Provisions) Order 1972 which relates to a proposed trial using (F-18) Fluorothymidine supplied by Imaging Research Solutions Ltd.

This exemption is effective from 6 June 2001; the above-named supplier may lawfully supply the product for the purpose outlined in your notification: the Licensing Authority have decided not to issue a direction under article 4(2)(v) of the Order. There is no need for a marketing authorisation or for a clinical trial certificate for the purpose of the trial.

Please note that all serious unexpected adverse reactions occurring during the trial should be notified to the Licensing Authority.

In coming to its decision the Licensing Authority has not evaluated the safety, quality and efficacy of the product, and this notice should not be taken to imply approval of the product in terms of safety, quality or efficacy.

Remark:
* It is assumed that approval for this trial will be sought from the Administration of Radioactive Substances Advisory Committee.

We shall be pleased to see a copy of any report which is produced as a result of this trial.

Yours sincerely

Mrs O Olayinka
CLINICAL TRIALS UNIT
ddxappro

Appendix D

Dose calibrator QC

SOP:	PET_9	TITLE:	Dose Calibrator QC in PET			
Rev:	1.0		Date:	22/10/2001	Review:	Oct 2002
Group:	PET		Author:	CET / WW	Authorised:	PJE

OVERVIEW

The dose calibrator in the PET Suite needs to be calibrated every day that doses are measured in the calibrator. The calibration needs to be done before any doses are measured.

RELEVANT STAFF

INM practitioners and operators working in the PET Suite.

BACKGROUND

This SOP details how to perform daily QC testing on the PET Unit Veenstra VDC–404 Radioisotope Dose Calibrator. For further information regarding the calibrators' correct operation, refer to the Owner's Manual (copies are kept in the Dose Calibrator QC record file in the PET Unit and in the Physics Office).

The tests are designed to a) check the operation of the calibrator and b) its response to a standard ^{137}Cs source to eliminate the possibility of sudden equipment failure and incorrect readings. Additionally, as each radioisotope setting links to specific software and/or electronic circuitry, a reading must be obtained for the ^{137}Cs source for each radioisotope setting to be used that day. This policy is in line with current guidelines for the daily testing of dose calibrators, developed by the NPL and IPEM. The following tests must be performed each day for each calibrator to be used to assay dose preparations, and must be performed *before* that calibrator is used for the first time that day.

PROCEDURE

- Ensure that the LCD shows 'BGD On'. With no activity in the chamber or in the vicinity select **MODE** and then select **ZERO ADJUST.** Press **ENTER,** wait while the cycle completes (about 30-60 seconds) and then hit **ENTER** to continue.

- Select **BATTERY TEST**. Press **ENTER,** wait while the cycle completes (about 10 seconds).
  Check that the reading is greater than 135 volts, and enter this reading on the record sheet for Daily QC and Consistency Checking (see Appendix).
  NB   If the battery reading is less than 135 volts it must be replaced.

- Hit **ENTER** to continue, and select **MODE** to return to the measurement screen.

- Now use the Cs-137 standard source to record the activity measured in the Cs-137 channel and the F-18 channel. The source is kept in the locked isotope safe store, with the key is kept under the calibrator control panel. Remove the standard source and place it centrally in the dipper.

- To select the 137-Cs channel, hit the **SELECT ISOTOPE** key and use the arrow keys to locate CS-137. Press **ENTER** to measure. To select 18-F, locate F-18 using the arrows.

- Note the measured activity for both channels on the record sheet for Daily QC and Consistency Checking. **If the measured activity for either channel is outside the printed ± 5% limits shown on the record sheet, notify the Duty Physicist immediately.**

- Return the Cs-137 source to the safe and lock it.

NB Do not forget to select F-18 prior to measuring the patient's dose.

GLOSSARY

APPENDIX

Institute of Nuclear Medicine, UCL Hospitals NHS Trust
PET Unit   Veenstra VDC - 404   Dose Calibrator

Daily QC Check for Correct Operation and Consistency of Response

^{137}Caesium Dose Calibrator Standard Reference Source :	Month beginning :	Nov-01

Calibration Data	8.77 MBq on 23 Aug 2001
Serial No.	HT 778
Manufacturer	AEA Technology / QSA GmbH

Date	Operator Initials	Bkg Activity (MBq)	Ion Chamber Voltage (V)	^{137}Caesium Setting				^{18}Flourine Setting			
				-5%	Calculated Activity	+5%	Measured Activity	-5%	Calculated Activity	+5%	Measured Activity
01-Nov-01				8.295	8.731	9.168		4.956	5.217	5.478	
02-Nov-01				8.294	8.731	9.167		4.956	5.216	5.477	
03-Nov-01				8.294	8.730	9.167		4.955	5.216	5.477	
04-Nov-01				8.293	8.730	9.166		4.955	5.216	5.477	
05-Nov-01				8.293	8.729	9.165		4.955	5.216	5.476	
06-Nov-01				8.292	8.728	9.165		4.954	5.215	5.476	
07-Nov-01				8.292	8.728	9.164		4.954	5.215	5.476	
08-Nov-01				8.291	8.727	9.164		4.954	5.215	5.475	
09-Nov-01				8.290	8.727	9.163		4.953	5.214	5.475	
10-Nov-01				8.290	8.726	9.163		4.953	5.214	5.475	
11-Nov-01				8.289	8.726	9.162		4.953	5.214	5.474	
12-Nov-01				8.289	8.725	9.161		4.953	5.213	5.474	
13-Nov-01				8.288	8.725	9.161		4.952	5.213	5.474	
14-Nov-01				8.288	8.724	9.160		4.952	5.213	5.473	
15-Nov-01				8.287	8.724	9.160		4.952	5.212	5.473	
16-Nov-01				8.287	8.723	9.159		4.951	5.212	5.472	
17-Nov-01				8.286	8.722	9.159		4.951	5.212	5.472	
18-Nov-01				8.285	8.722	9.158		4.951	5.211	5.472	
19-Nov-01				8.285	8.721	9.157		4.950	5.211	5.471	
20-Nov-01	•			8.285	8.721	9.157		4.950	5.211	5.471	
21-Nov-01				8.284	8.720	9.156		4.950	5.210	5.471	
22-Nov-01				8.284	8.720	9.156		4.949	5.210	5.470	
23-Nov-01				8.283	8.719	9.155		4.949	5.210	5.470	
24-Nov-01				8.283	8.719	9.154		4.949	5.209	5.470	
25-Nov-01				8.282	8.718	9.154		4.948	5.209	5.469	
26-Nov-01				8.282	8.717	9.153		4.948	5.209	5.469	
27-Nov-01				8.281	8.717	9.153		4.948	5.208	5.469	
28-Nov-01				8.281	8.716	9.152		4.948	5.208	5.468	
29-Nov-01				8.280	8.716	9.152		4.947	5.208	5.468	
30-Nov-01				8.279	8.715	9.151		4.947	5.207	5.468	
01-Dec-01				8.279	8.715	9.150		4.947	5.207	5.467	

Appendix E

Record sheet of radiopharmaceutical holdings

INM PET Facility - Record Sheet of Current Radiopharmaceutical Holdings

Date : _____   Radiopharmaceutical Form : _____   Radiopharmaceutical QA Status (circle and initial) :   Pass   Fail

Consignor (tick) :   University of Cambridge   UMDS (Guy's and St. Thomas')   MRC Cyclotron Unit, Hammersmith

Activity Assay - Entire Shipment

	Stock Volume (mls)	Time of Assay	Assayed Activity (MBq)	Two Assays in Agreement ?
Consignor Activity Assay				(i.e. both agree within ± 10%)
Decay-Corrected Consignor Assay	_____	_____		circle below as appropriate
INM PET Unit Activity Assay				Yes / No

Activity Assay - Sub-dispensed Preparations

Time of Assay	Operator Initials	Stock Volume Diluted ?	Volume Removed (mls)	Assayed Activity (MBq)	Volume Remaining (mls)	Activity Remaining	Purpose

Consignment of Current Holdings to Waste

Time	Operator Initials	Volume Remaining (mls)	Estimated Max. Remaining Activity (MBq)	Purpose
				WASTE
				WASTE

SOP No: PET_7
Date of Issue: 22/10/2001

224

Version 1.0

Page of Pages 2

Measuring FDG upon arrival in the PET suite

Appendix F

Decay chart

^{18}Flourine - Decay Factors relative to Calibration Time

minutes	decay factor	minutes	decay factor	minutes	decay factor	minutes	decay factor	minutes	decay factor	minutes	decay factor	minutes	decay factor	minutes	decay factor
0	1.000														
1	0.994	61	0.680	121	0.466	181	0.319	241	0.218	301	0.149	361	0.102	421	0.070
2	0.987	62	0.676	122	0.463	182	0.317	242	0.217	302	0.148	362	0.102	422	0.070
3	0.981	63	0.672	123	0.460	183	0.315	243	0.215	303	0.148	363	0.101	423	0.069
4	0.975	64	0.667	124	0.457	184	0.313	244	0.214	304	0.147	364	0.100	424	0.069
5	0.969	65	0.663	125	0.454	185	0.311	245	0.213	305	0.146	365	0.100	425	0.068
6	0.963	66	0.659	126	0.451	186	0.309	246	0.211	306	0.145	366	0.099	426	0.068
7	0.957	67	0.655	127	0.448	187	0.307	247	0.210	307	0.144	367	0.098	427	0.067
8	0.951	68	0.651	128	0.446	188	0.305	248	0.209	308	0.143	368	0.098	428	0.067
9	0.945	69	0.647	129	0.443	189	0.303	249	0.207	309	0.142	369	0.097	429	0.067
10	0.939	70	0.643	130	0.440	190	0.301	250	0.206	310	0.141	370	0.097	430	0.066
11	0.933	71	0.639	131	0.437	191	0.299	251	0.205	311	0.140	371	0.096	431	0.066
12	0.927	72	0.635	132	0.434	192	0.297	252	0.204	312	0.139	372	0.095	432	0.065
13	0.921	73	0.631	133	0.432	193	0.296	253	0.202	313	0.138	373	0.095	433	0.065
14	0.915	74	0.627	134	0.429	194	0.294	254	0.201	314	0.138	374	0.094	434	0.064
15	0.910	75	0.623	135	0.426	195	0.292	255	0.200	315	0.137	375	0.094	435	0.064
16	0.904	76	0.619	136	0.424	196	0.290	256	0.199	316	0.136	376	0.093	436	0.064
17	0.898	77	0.615	137	0.421	197	0.288	257	0.197	317	0.135	377	0.092	437	0.063
18	0.893	78	0.611	138	0.418	198	0.286	258	0.196	318	0.134	378	0.092	438	0.063
19	0.887	79	0.607	139	0.416	199	0.285	259	0.195	319	0.133	379	0.091	439	0.062
20	0.881	80	0.603	140	0.413	200	0.283	260	0.194	320	0.132	380	0.091	440	0.062
21	0.876	81	0.600	141	0.410	201	0.281	261	0.192	321	0.132	381	0.090	441	0.062
22	0.870	82	0.596	142	0.408	202	0.279	262	0.191	322	0.131	382	0.090	442	0.061
23	0.865	83	0.592	143	0.405	203	0.277	263	0.190	323	0.130	383	0.089	443	0.061
24	0.859	84	0.588	144	0.403	204	0.276	264	0.189	324	0.129	384	0.088	444	0.061
25	0.854	85	0.585	145	0.400	205	0.274	265	0.188	325	0.128	385	0.088	445	0.060
26	0.849	86	0.581	146	0.398	206	0.272	266	0.186	326	0.128	386	0.087	446	0.060
27	0.843	87	0.577	147	0.395	207	0.271	267	0.185	327	0.127	387	0.087	447	0.059
28	0.838	88	0.574	148	0.393	208	0.269	268	0.184	328	0.126	388	0.086	448	0.059
29	0.833	89	0.570	149	0.390	209	0.267	269	0.183	329	0.125	389	0.086	449	0.059
30	0.827	90	0.566	150	0.388	210	0.265	270	0.182	330	0.124	390	0.085	450	0.058
31	0.822	91	0.563	151	0.385	211	0.264	271	0.181	331	0.124	391	0.085	451	0.058
32	0.817	92	0.559	152	0.383	212	0.262	272	0.179	332	0.123	392	0.084	452	0.058
33	0.812	93	0.556	153	0.380	213	0.260	273	0.178	333	0.122	393	0.084	453	0.057
34	0.807	94	0.552	154	0.378	214	0.259	274	0.177	334	0.121	394	0.083	454	0.057
35	0.802	95	0.549	155	0.376	215	0.257	275	0.176	335	0.121	395	0.083	455	0.056
36	0.797	96	0.545	156	0.373	216	0.256	276	0.175	336	0.120	396	0.082	456	0.056
37	0.792	97	0.542	157	0.371	217	0.254	277	0.174	337	0.119	397	0.081	457	0.056
38	0.787	98	0.538	158	0.369	218	0.252	278	0.173	338	0.118	398	0.081	458	0.055
39	0.782	99	0.535	159	0.366	219	0.251	279	0.172	339	0.118	399	0.080	459	0.055
40	0.777	100	0.532	160	0.364	220	0.249	280	0.171	340	0.117	400	0.080	460	0.055
41	0.772	101	0.528	161	0.362	221	0.248	281	0.170	341	0.116	401	0.079	461	0.054
42	0.767	102	0.525	162	0.359	222	0.246	282	0.168	342	0.115	402	0.079	462	0.054
43	0.762	103	0.522	163	0.357	223	0.245	283	0.167	343	0.115	403	0.078	463	0.054
44	0.757	104	0.518	164	0.355	224	0.243	284	0.166	344	0.114	404	0.078	464	0.053
45	0.753	105	0.515	165	0.353	225	0.241	285	0.165	345	0.113	405	0.077	465	0.053
46	0.748	106	0.512	166	0.350	226	0.240	286	0.164	346	0.112	406	0.077	466	0.053
47	0.743	107	0.509	167	0.348	227	0.238	287	0.163	347	0.112	407	0.076	467	0.052
48	0.738	108	0.506	168	0.346	228	0.237	288	0.162	348	0.111	408	0.076	468	0.052
49	0.734	109	0.502	169	0.344	229	0.235	289	0.161	349	0.110	409	0.076	469	0.052
50	0.729	110	0.499	170	0.342	230	0.234	290	0.160	350	0.110	410	0.075	470	0.051
51	0.725	111	0.496	171	0.340	231	0.232	291	0.159	351	0.109	411	0.075	471	0.051
52	0.720	112	0.493	172	0.337	232	0.231	292	0.158	352	0.108	412	0.074	472	0.051
53	0.716	113	0.490	173	0.335	233	0.230	293	0.157	353	0.108	413	0.074	473	0.050
54	0.711	114	0.487	174	0.333	234	0.228	294	0.156	354	0.107	414	0.073	474	0.050
55	0.707	115	0.484	175	0.331	235	0.227	295	0.155	355	0.106	415	0.073	475	0.050
56	0.702	116	0.481	176	0.329	236	0.225	296	0.154	356	0.106	416	0.072	476	0.049
57	0.698	117	0.478	177	0.327	237	0.224	297	0.153	357	0.105	417	0.072	477	0.049
58	0.693	118	0.475	178	0.325	238	0.222	298	0.152	358	0.104	418	0.071	478	0.049
59	0.689	119	0.472	179	0.323	239	0.221	299	0.151	359	0.104	419	0.071	479	0.049
60	0.685	120	0.469	180	0.321	240	0.220	300	0.150	360	0.103	420	0.070	480	0.048

Appendix G

Guidance to the clinical administration of radiopharmaceuticals

Part B: Diagnostic Procedures – PET

Radioactive medicinal product			Investigation	Route of adminis- tration	Diagnostic reference level (MBq)	Effective dose (mSv)	Dose to the uterus (mGy)
Serial	Radio- nuclide	Chemical form					
1	2	3	4	5	6	7	8
6b2i	^{11}C	L-methyl- methionine	Brain tumour imaging	IV	400	2	1
6b2ii	^{11}C	L-methyl- methionine	Parathyroid imaging	IV	400	2	1
7a22i	^{13}N	Ammonia	Myocardial blood flow imaging	IV	550	2	1
8a21i	^{15}O	Water (bolus)	Cerebral blood flow imaging	IV	2000	2	1
8a21ii	^{15}O	Water (bolus)	Myocardial blood flow imaging	IV	2000	2	1
9a21i	^{18}F	FDG	Tumour imaging	IV	400	10	7
9a22ii	^{18}F	FDG	Myocardial imaging	IV	400	10	7
9a23i	^{18}F	Fluoride	Bone Imaging	IV	250	7	5

Appendix H

FLT patient information and consent form

CONFIDENTIAL

Patient Information Sheet

A comparison of F18 –fluorothymidine (FLT) PET with routine PET in patients with colorectal cancer

Principal Investigators:

Professor P.J. Ell,
Institute of Nuclear Medicine,
Mortimer Street,
London W1N 8AA

Other Investigators:

Prof. I. Taylor	Department of Surgery
Mr. D. L. Francis	Department of Surgery / Institute of Nuclear Medicine
Dr. D.C. Costa	Institute of Nuclear Medicine

If you have any queries regarding this information sheet, please contact Mr D. L. Francis in the Department of Surgery on **07976 396684.**

CONFIDENTIAL
Patient Information Sheet

A comparison of F18 –fluorothymidine (FLT) PET with routine PET in patients with colorectal cancer

You are invited to take part in a research project. You do not have to take part in this study if you do not want to. If you do decide to take part you may withdraw at any time without having to give any reason. Your decision whether to take part or not will not affect your care and management in any way. All proposals for research using human subjects are reviewed by an ethics committee before they can proceed. This proposal was reviewed by the joint UCL/UCLH Committees on Ethics of Human Research.

1.   This study aims to establish if positron emission tomography (PET) scans using an alternative radioactive tracer, FLT, is more accurate than the conventional radioactive tracer, FDG for imaging bowel cancer.

2.   It has been shown that FDG-PET is an accurate and safe means of imaging patients with bowel cancer. This allows the most appropriate treatment to deal with an individual patient's cancer to be chosen. The information, therefore, influences the extent of surgery performed and possibly the use of other treatments such as chemotherapy or radiotherapy.

3.   The accuracy of FDG-PET, although extremely good, is not perfect. One method of improving this situation is to use an alternative radioactive substance to pinpoint the site of cancer cells in the body. FLT is such an alternative and it can be safely substituted for FDG for PET scanning.

Description of the research study:

In addition to a routine FDG-PET scan that patients with bowel cancer undergo at this hospital, you will have an FLT-PET scan. PET scans take place in the Institute of Nuclear Medicine at the Middlesex hospital, usually on separate days. The procedure will entail you having to fast for a period of four hours (so that glucose that you consume in your diet will not interfere with the FDG-PET scan). Once you are in the Institute of Nuclear Medicine you will be given an injection of FDG (chemically similar to glucose, but which has been labelled with a radioactive substance) through a cannula (plastic tube) in a vein. The radioactivity lasts approximately 90 minutes, therefore you do not have to wait for the scan. You will have to lie on a platform that moves you into the scanner. The scan itself takes one hour and you will need to lie still with minimum interaction with staff, as this interferes with the scan quality. The whole process takes between 2 to 4 hours. The procedure for the FLT scan is similar to that described above, but you will receive an injection of FLT instead of FDG. **Most importantly**, you will have a cannula inserted into an artery and a vein in your arm so that we can take blood (about 50 ml in total – 1/6 of the volume of a standard fizzy drinks can) in order to analyse it. Before inserting the arterial cannula the blood supply to your hand will be evaluated to assess if it is OK for you to take part in the study. We undertake this so that in the highly unlikely

event that the artery should become damaged or clotted (thrombosed) there would be **no** adverse affects. Local anaesthetic will be used prior to inserting the arterial cannula to minimise any pain or discomfort. After removal of the cannula we will press on the artery so as to stop it bleeding. This all helps to increase the accuracy of the scan report we can give to the doctors looking after you. It will also help us develop a way of working out the distribution of FLT in the blood so that patients in the future may avoid the blood tests. The cannulae will remain in your arm for an hour. If you proceed to have an operation, the surgeon will make a thorough examination and document the findings. A tiny fragment of the cancer and surrounding tissue will be taken for examination by one of the doctors involved in the study. Cancers need growth promoting agents as well as a blood supply therefore particular attention will be paid to the presence of these factors. The main part of the tissue, which is removed, will be sent for analysis by a pathologist, as is the usual practise. A comparison will be made between both types of PET scan to see if there is in fact any difference in the information gained. Both scan findings will then be related to the analysis of the tissue removed.

CONSENT FORM

STUDY TITLE: A comparison of F-18 fluorothymidine (FLT) PET with routine PET in patients with colorectal cancer

PATIENT NAME:

HOSPITAL NUMBER:

WARD/ ADDRESS:

By signing this form I agree that:

1.   I have read the patients information sheet and the procedure has been fully explained to me.

2.   I have had the opportunity to ask questions and I did receive satisfactory answers.

3.   I have been given a copy of the information sheet and the consent form to keep.

4.   I understand that I am participating in a research study and I understand the risks and benefits involved. I freely give my consent to participate in the research study outlined in the patient information sheet.

5.   I understand that I may withdraw from this research study at any time without giving a reason for withdrawing and such a decision would not affect the standard of care that I receive in any way.

Signature of participant……………………………………………….. Date………/………/……….

Name of participant (Block Capitals)………………………………………………………

Investigator Statement

I have carefully explained to the above named patient the nature of the research protocol. I hereby certify that to the best of my knowledge the subject signing this form understands the nature, demands, risks and benefits involved in participating in this study.

Signature of investigator…………………………….. Name of investigator (Block Capitals)…………………………………

Date…………/………/……….

Principal investigator : Prof. P.J. Ell (tel: **020-7380-9421**)

Appendix I

MIB-1 Immunohistochemistry

Citrate buffer recipe:

29.4g sodium citrate

54mls 1M HCL

10 litres distilled water

pH to 6.0 with 1M HCL

Appendix J

Publications arising from Thesis

Papers

Glucose utilisation and cell proliferation in colorectal cancer
Visvikis D, **Francis DL**, Costa DC, Mulligan R, Townsend C, Arulampalam
THA, Islam MS, Taylor I, Ell PJ
European Journal Nuclear Medicine 2002 Feb;29(2):280

Potential impact of [^{18}F]3'-deoxy-3'-fluorothymidine versus [^{18}F]fluoro-2-deoxy-D-glucose in positron emission tomography for colorectal cancer
D.L. Francis, D. Visvikis, D.C. Costa, T.H.A. Arulampalam, C. Townsend, S.K.
Luthra, I. Taylor, P.J. Ell
European Journal Nuclear Medicine 2003 Jul;30(7):988-94

***In vivo* imaging of cellular proliferation in colorectal cancer using Positron
Emission Tomography**
D.L. Francis, A. Freeman, D. Visvikis, D.C. Costa, S.K. Luthra, M. Novelli, I.
Taylor, P.J. Ell
GUT 2003 Nov;52(11):1602-6

**Comparison of methodologies for the *in vivo* assessment of ^{18}FLT utilization
in colorectal cancer**
D. Visvikis, **D. Francis**, R. Mulligan, D.C. Costa, I. Croasdale, S.K. Luthra, I.
Taylor, P.J. Ell
European Journal Nuclear Medicine 2003 (in press)

**Assessment of recurrent colorectal cancer following 5-Fluorouracil
chemotherapy using both ^{18}FDG and ^{18}FLT PET**
D.L. Francis, D. Visvikis, D.C. Costa, I. Croasdale, T. H. Arulampalam, S.K.
Luthra, I. Taylor, P.J.Ell
European Journal Nuclear Medicine 2003 (in press)

FDG-PET for the pre-operative evaluation of colorectal liver metastases
T.H. Arulampalam, **D.L. Francis**, D. Visvikis, P.J. Ell, I. Taylor
European Journal of Surgical Oncology 2004 (in press)

Book Chapters

Clinical Molecular Anatomic Imaging
Gustav K. von Schulthess, Lippincott Williams & Wilkins
**Chapter 45: PET and PET/CT of Cancers of the Esophagus, Stomach and
Large Intestine.**
Daren L Francis, Tan H A Arulampalam, Durval Campos Costa, Peter J Ell.

237

Nuclear Medicine in Clinical Diagnosis and Treatment
Gambhir and Ell, Elsevier 2003
Chapter 41: Atlas 1: PET and PET/CT.
Buck, G. Gorres, T. Hany, H. Ch. Steinert, K.D.M. Stumpe. G.K. von Schultess,
S. Hughes, **D. Francis**, D.Costa, P. Ell

Abstracts

Whole Body FDG-PET for Staging Colorectal Liver Metastases
Francis DL, Arulampalam THA, Costa DC, Loizidou M, Ell PJ, Taylor I.
Br. J. Surg. 2002;89:*58*

[^{18}F]FDG and [^{18}F]FLT in colorectal carcinoma: preliminary results of a comparative study
D. Visvikis, **D.L. Francis,** D.C. Costa, R. Mulligan, C. Townsend, M.S. Islam, I. Taylor.
Nuclear Medicine Communications 2002; **23**:386.

Quantitative comparison of 18FDG and 18FLT in colorectal cancer
D. Visvikis, **D.L. Francis,** D.C. Costa, R. Mulligan, C. Townsend, I.Taylor, P.J. Ell.
European Journal of Nuclear Medicine 2002; **29**:S79.

Glucose utilisation (^{18}FDG) versus cellular proliferation (^{18}FLT) using PET scanning in patients with colorectal carcinoma
D. Francis, D. Visvikis, D.C. Costa, R.S. Mulligan, C. Townsend, S.K. Luthra, I. Taylor, P.J. Ell.
European Jouranl of Surgical Oncology 2002; **28**:766.

Evaluating proliferative activity in colorectal cancer using ^{18}F-FLT-PET
Francis **D.L.,** Visvikis D, Freeman A, Costa DC, Luthra SK, Novelli M, Taylor I, Ell PJ.
Nuclear Medicine Communications 2003; **24**:458.

Positron Emission Tomography in colorectal cancer: A comparison between 18FDG and a new tracer 18FLT
DL Francis, D Visvikis, DC Costa, TH Arulampalam, C Townsend, SK Luthra, I Taylor, PJ Ell.
British Journal of Surgery 2003; **90**:8.

Quantifying cellular proliferation in colorectal cancer: A comparison between Positron Emission Tomography and MIB-1 Immunohistochemistry
DL Francis, A Freeman, D Visvikis, DC Costa, SK Luthra, M Novelli, I Taylor, PJ Ell.
British Journal of Surgery 2003; **90**:78.

A comparison of [18]FDG and [18]FLT-PET in quantifying cellular proliferation in colorectal cancer
DL Francis, D Visvikis, A Freeman, , DC Costa, SK Luthra, M Novelli, I Taylor, PJ Ell
The Journal of Nuclear Medicine 2003; 44:25

Can Positron Emission Tomography quantify cellular proliferation in colorectal cancer? A comparative study using MIB-1 and a new PET tracer [18]FLT.
DL Francis, A Freeman, D Visvikis, DC Costa, SK Luthra, M Novelli, I Taylor and PJ Ell.
Colorectal Disease 2003; 5;29

[18F] 3'-deoxy-3-fluorothymidine: A new Positron Emission Tomography tracer for imaging colorectal cancer.
DL Francis, D Visvikis, DC Costa, TH Arulampalam,C Townsend, SK Luthra, I Taylor and PJ Ell.
Colorectal Disease 2003; 5;76

Moitoring 5-Fluorouracil chemotherapy response in colorectal cancer using Positron Emission Tomography
Francis DL, Loizidou M, Visvikis D, De Vos S, Luthra S, Taylor I, Ell PJ
European Journal of Surgical Oncology 2003; 29;789

Bibliography

Abdel-Nabi,H., Doerr,R.J., Lamonica,D.M., Cronin,V.R., Galantowicz,P.J., Carbone,G.M., and Spaulding,M.B. (1998). Staging of primary colorectal carcinomas with fluorine-18 fluorodeoxyglucose whole-body PET: correlation with histopathologic and CT findings. Radiology *206*, 755-760.

Adam,R., Avisar,E., Ariche,A., Giachetti,S., Azoulay,D., Castaing,D., Kunstlinger,F., Levi,F., and Bismuth,F. (2001). Five-year survival following hepatic resection after neoadjuvant therapy for nonresectable colorectal. Ann. Surg. Oncol. *8*, 347-353.

Adson,M.A. (1987). Resection of liver metastases--when is it worthwhile? World J. Surg. *11*, 511-520.

Ahnen,D.J., Feigl,P., Quan,G., Fenoglio-Preiser,C., Lovato,L.C., Bunn,P.A., Jr., Stemmerman,G., Wells,J.D., Macdonald,J.S., and Meyskens,F.L., Jr. (1998). Ki-ras mutation and p53 overexpression predict the clinical behavior of colorectal cancer: a Southwest Oncology Group study. Cancer Res. *58*, 1149-1158.

Alberts,D.S., Martinez,M.E., Roe,D.J., Guillen-Rodriguez,J.M., Marshall,J.R., van Leeuwen,J.B., Reid,M.E., Ritenbaugh,C., Vargas,P.A., Bhattacharyya,A.B., Earnest,D.L., and Sampliner,R.E. (2000). Lack of effect of a high-fiber cereal supplement on the recurrence of colorectal adenomas. Phoenix Colon Cancer Prevention Physicians' Network. N. Engl. J. Med. *342*, 1156-1162.

Allegra,C.J., Paik,S., Colangelo,L.H., Parr,A.L., Kirsch,I., Kim,G., Klein,P., Johnston,P.G., Wolmark,N., and Wieand,H.S. (2003). Prognostic value of thymidylate synthase, Ki-67, and p53 in patients with Dukes' B and C colon cancer: a National Cancer Institute-National Surgical Adjuvant Breast and Bowel Project collaborative study. J. Clin. Oncol. *21*, 241-250.

American Joint Commmittee on Cancer (2002). Purposes and Principles of Staging. In AJCC Cancer Staging Handbook, Greene FL, Page DL, Fleming ID, Fritz AG, Balch CM, Haller DG, and Morrow M, eds. (New York: Springer), pp. 3-14.

Arulampalam,T., Costa,D., Visvikis,D., Boulos,P., Taylor,I., and Ell,P. (2001). The impact of FDG-PET on the management algorithm for recurrent colorectal cancer. Eur. J. Nucl. Med. *28*, 1758-1765.

Arulampalam,T., Francis,D.L., Visvikis,D., Taylor,I., and Ell,P. (2004). FDG-PET for the pre-operative evaluation of colorectal liver metastases. Eur. J. Surg Oncology (in press)

Astler,V.B. and Coller,F.A. (1954). The prognostic significance of direct extension of carcinomas of the colon and rectum. Ann. Surg. *139*, 846-852.

Azoulay,D., Castaing,D., Smail,A., Adam,R., Cailliez,V., Laurent,A., Lemoine,A., and Bismuth,H. (2000). Resection of nonresectable liver metastases from colorectal cancer after percutaneous portal vein embolization. Ann. Surg. *231*, 480-486.

Bading,J.R., Shahinian,A.H., Bathija,P., and Conti,P.S. (2000). Pharmacokinetics of the thymidine analog 2'-fluoro-5-[(14)C]-methyl-1-beta-D-arabinofuranosyluracil ([(14)C]FMAU) in rat prostate tumor cells. Nucl. Med. Biol. *27*, 361-368.

Balthazar,E.J. (1991). CT of the gastrointestinal tract: principles and interpretation. AJR Am. J. Roentgenol. *156*, 23-32.

Barbier,O., Turgeon,D., Girard,C., Green,M.D., Tephly,T.R., Hum,D.W., and Belanger,A. (2000). 3'-azido-3'-deoxythimidine (AZT) is glucuronidated by human UDP-glucuronosyltransferase 2B7 (UGT2B7). Drug Metab Dispos. *28*, 497-502.

Barthel,H., Cleij,M.C., Collingridge,D.R., Hutchinson,O.C., Osman,S., He,Q., Luthra,S.K., Brady,F., Price,P.M., and Aboagye,E.O. (2003). 3'-deoxy-3'-[18F]fluorothymidine as a new marker for monitoring tumor response to antiproliferative therapy in vivo with positron emission tomography. Cancer Res. *63*, 3791-3798.

Beets-Tan,R.G., Beets,G.L., Vliegen,R.F., Kessels,A.G., Van Boven,H., De Bruine,A., von Meyenfeldt,M.F., Baeten,C.G., and van Engelshoven,J.M. (2001). Accuracy of magnetic resonance imaging in prediction of tumour-free resection margin in rectal cancer surgery. Lancet *357*, 497-504.

Belluco,C., Esposito,G., Bertorelle,R., Del Mistro,A., Fassina,A., Vieceli,G., Chieco-Bianchi,L., Nitti,D., and Lise,M. (1999). Absence of the cell cycle inhibitor p27Kip1 protein predicts poor outcome in patients with stage I-III colorectal cancer. Ann. Surg. Oncol. *6*, 19-25.

Belt,J.A., Marina,N.M., Phelps,D.A., and Crawford,C.R. (1993). Nucleoside transport in normal and neoplastic cells. Adv. Enzyme Regul. *33*, 235-252.

Bettinardi,V., Pagani,E., Gilardi,M.C., Landoni,C., Riddell,C., Rizzo,G., Castiglioni,I., Belluzzo,D., Lucignani,G., Schubert,S., and Fazio,F. (1999). An automatic classification technique for attenuation correction in positron emission tomography. Eur. J. Nucl. Med. *26*, 447-458.

Beynon,J. (1989). An evaluation of the role of rectal endosonography in rectal cancer. Ann. R. Coll. Surg. Engl. *71*, 131-139.

Bird,R.P. (1987). Observation and quantification of aberrant crypts in the murine colon treated with a colon carcinogen: preliminary findings. Cancer Lett. *37*, 147-151.

Blasberg,R.G., Roelcke,U., Weinreich,R., Beattie,B., von Ammon,K., Yonekawa,Y., Landolt,H., Guenther,I., Crompton,N.E., Vontobel,P., Missimer,J., Maguire,R.P., Koziorowski,J., Knust,E.J., Finn,R.D., and Leenders,K.L. (2000). Imaging brain tumor proliferative activity with [124I]iododeoxyuridine. Cancer Res. *60*, 624-635.

Blomqvist,L., Holm,T., Rubio,C., and Hindmarsh,T. (1997). Rectal tumours--MR imaging with endorectal and/or phased-array coils, and histopathological staging on giant sections. A comparative study. Acta Radiol. *38*, 437-444.

Bodmer,W.F., Bailey,C.J., Bodmer,J., Bussey,H.J., Ellis,A., Gorman,P., Lucibello,F.C., Murday,V.A., Rider,S.H., Scambler,P., and . (1987). Localization of the gene for familial adenomatous polyposis on chromosome 5. Nature *328*, 614-616.

Boland,C.R., Thibodeau,S.N., Hamilton,S.R., Sidransky,D., Eshleman,J.R., Burt,R.W., Meltzer,S.J., Rodriguez-Bigas,M.A., Fodde,R., Ranzani,G.N., and Srivastava,S. (1998). A National Cancer Institute Workshop on Microsatellite Instability for cancer detection and familial predisposition: development of international criteria for the determination of microsatellite instability in colorectal cancer. Cancer Res. *58*, 5248-5257.

Broet,P., Romain,S., Daver,A., Ricolleau,G., Quillien,V., Rallet,A., Asselain,B., Martin,P.M., and Spyratos,F. (2001). Thymidine kinase as a proliferative marker: clinical relevance in 1,692 primary breast cancer patients. J Clin. Oncol. *19*, 2778-2787.

Brown,D.C. and Gatter,K.C. (1990). Monoclonal antibody Ki-67: its use in histopathology. Histopathology *17*, 489-503.

Brown,G., Radcliffe,A.G., Newcombe,R.G., Dallimore,N.S., Bourne,M.W., and Williams,G.T. (2003a). Preoperative assessment of prognostic factors in rectal cancer using high-resolution magnetic resonance imaging. Br. J. Surg. *90*, 355-364.

Brown,G., Richards,C.J., Bourne,M.W., Newcombe,R.G., Radcliffe,A.G., Dallimore,N.S., and Williams,G.T. (2003b). Morphologic predictors of lymph node status in rectal cancer with use of high-spatial-resolution MR imaging with histopathologic comparison. Radiology *227*, 371-377.

Buck,A.C., Schirrmeister,H.H., Guhlmann,C.A., Diederichs,C.G., Shen,C., Buchmann,I., Kotzerke,J., Birk,D., Mattfeldt,T., and Reske,S.N. (2001). Ki-67 immunostaining in pancreatic cancer and chronic active pancreatitis: does in vivo FDG uptake correlate with proliferative activity? J Nucl Med. *42*, 721-725.

Buck,A.K., Schirrmeister,H., Hetzel,M., Von Der,H.M., Halter,G., Glatting,G., Mattfeldt,T., Liewald,F., Reske,S.N., and Neumaier,B. (2002). 3-deoxy-3-[(18)F]fluorothymidine-positron emission tomography for noninvasive assessment of proliferation in pulmonary nodules. Cancer Res. *62*, 3331-3334.

Burger,C. and Buck,A. (1997). Requirements and implementation of a flexible kinetic modeling tool. J. Nucl. Med. *38*, 1818-1823.

Calabro-Jones,P.M., Byfield,J.E., Ward,J.F., and Sharp,T.R. (1982). Time-dose relationships for 5-fluorouracil cytotoxicity against human epithelial cancer cells in vitro. Cancer Res. *42*, 4413-4420.

Cascinu,S., Ligi,M., Graziano,F., Del Ferro,E., Valentini,M., Grianti,C., Bartolucci,M., and Catalano,G. (1998). S-phase fraction can predict event free survival in patients with pT2-T3N0M0 colorectal carcinoma: implications for adjuvant chemotherapy. Cancer *83*, 1081-1085.

Cattoretti,G., Becker,M.H., Key,G., Duchrow,M., Schluter,C., Galle,J., and Gerdes,J. (1992). Monoclonal antibodies against recombinant parts of the Ki-67 antigen (MIB 1 and MIB 3) detect proliferating cells in microwave-processed formalin-fixed paraffin sections. J. Pathol. *168*, 357-363.

Cheng,H., Bjerknes,M., Amar,J., and Gardiner,G. (1986). Crypt production in normal and diseased human colonic epithelium. Anat. Rec. *216*, 44-48.

Christman,D., Crawford,E.J., Friedkin,M., and Wolf,A.P. (1972). Detection of DNA synthesis in intact organisms with positron-emitting (methyl- 11 C)thymidine. Proc. Natl. Acad. Sci. U. S. A *69*, 988-992.

Cleij MC, Steel CJ, Brady F, Ell PJ, Pike VW, and Luthra SK (2001). An improved synthesis of 3-Deoxy-3-[18F]Fluorothymidine. J Lab Comp Radioph , *44*, S871.

Cocconi,G., Cunningham,D., Van Cutsem,E., Francois,E., Gustavsson,B., van Hazel,G., Kerr,D., Possinger,K., and Hietschold,S.M. (1998). Open, randomized, multicenter trial of raltitrexed versus fluorouracil plus high-dose leucovorin in patients with advanced colorectal cancer. Tomudex Colorectal Cancer Study Group. J. Clin. Oncol. *16*, 2943-2952.

Compton,C., Fenoglio-Preiser,C.M., Pettigrew,N., and Fielding,L.P. (2000). American Joint Committee on Cancer Prognostic Factors Consensus Conference: Colorectal Working Group. Cancer *88*, 1739-1757.

Conti,P.S., Alauddin,M.M., Fissekis,J.R., Schmall,B., and Watanabe,K.A. (1995). Synthesis of 2'-fluoro-5-[11C]-methyl-1-beta-D-arabinofuranosyluracil ([11C]-FMAU): a potential nucleoside analog for in vivo study of cellular proliferation with PET. Nucl. Med. Biol. *22*, 783-789.

Conti,P.S., Hilton,J., Wong,D.F., Alauddin,M.M., Dannals,R.F., Ravert,H.T., Wilson,A.A., and Anderson,J.H. (1994). High performance liquid chromatography of carbon-11 labeled thymidine and its major catabolites for clinical PET studies. Nucl. Med. Biol. *21*, 1045-1051.

Culy,C.R., Clemett,D., and Wiseman,L.R. (2000). Oxaliplatin. A review of its pharmacological properties and clinical efficacy in metastatic colorectal cancer and its potential in other malignancies. Drugs *60*, 895-924.

Cunningham,D., Pyrhonen,S., James,R.D., Punt,C.J., Hickish,T.F., Heikkila,R., Johannesen,T.B., Starkhammar,H., Topham,C.A., Awad,L., Jacques,C., and Herait,P. (1998). Randomised trial of irinotecan plus supportive care versus supportive care alone

after fluorouracil failure for patients with metastatic colorectal cancer. Lancet *352*, 1413-1418.

Cunningham,D., Zalcberg,J.R., Rath,U., Oliver,I., Van Cutsem,E., Svensson,C., Seitz,J.F., Harper,P., Kerr,D., and Perez-Manga,G. (1996). Final results of a randomised trial comparing 'Tomudex' (raltitrexed) with 5-fluorouracil plus leucovorin in advanced colorectal cancer. "Tomudex" Colorectal Cancer Study Group. Ann. Oncol. *7*, 961-965.

Davison,A.J. and Stern,H.S. (1995). Additional specific management problems. In Cancer of the colon, rectum and anus, Cohen AM, Winawer SJ, Friedman SJ, and Gunderson, eds. (New York: McGraw Hill), pp. 477-489.

de Gramont,A., Figer,A., Seymour,M., Homerin,M., Hmissi,A., Cassidy,J., Boni,C., Cortes-Funes,H., Cervantes,A., Freyer,G., Papamichael,D., Le Bail,N., Louvet,C., Hendler,D., de Braud,F., Wilson,C., Morvan,F., and Bonetti,A. (2000). Leucovorin and fluorouracil with or without oxaliplatin as first-line treatment in advanced colorectal cancer. J. Clin. Oncol. *18*, 2938-2947.

de Lange,E.E., Fechner,R.E., and Wanebo,H.J. (1989). Suspected recurrent rectosigmoid carcinoma after abdominoperineal resection: MR imaging and histopathologic findings. Radiology *170*, 323-328.

de Zwart,I.M., Griffioen,G., Shaw,M.P., Lamers,C.B., and de Roos,A. (2001). Barium enema and endoscopy for the detection of colorectal neoplasia: sensitivity, specificity, complications and its determinants. Clin. Radiol. *56*, 401-409.

Delbeke,D., Vitola,J.V., Sandler,M.P., Arildsen,R.C., Powers,T.A., Wright,J.K., Jr., Chapman,W.C., and Pinson,C.W. (1997). Staging recurrent metastatic colorectal carcinoma with PET. J. Nucl. Med. *38*, 1196-1201.

Deschner,E.E., Godbold,J., and Lynch,H.T. (1988). Rectal epithelial cell proliferation in a group of young adults. Influence of age and genetic risk for colon cancer. Cancer *61*, 2286-2290.

Dimitrakopoulou-Strauss,A., Strauss,L.G., Schlag,P., Hohenberger,P., Irngartinger,G., Oberdorfer,F., Doll,J., and van Kaick,G. (1998). Intravenous and intra-arterial oxygen-15-labeled water and fluorine-18- labeled fluorouracil in patients with liver metastases from colorectal carcinoma. J. Nucl. Med. *39*, 465-473.

Dittmann,H., Dohmen,B.M., Kehlbach,R., Bartusek,G., Pritzkow,M., Sarbia,M., and Bares,R. (2002). Early changes in [(18)F]FLT uptake after chemotherapy: an experimental study. Eur. J. Nucl. Med. Mol. Imaging *29*, 1462-1469.

Doerr,R.J., Abdel-Nabi,H., Krag,D., and Mitchell,E. (1991). Radiolabeled antibody imaging in the management of colorectal cancer. Results of a multicenter clinical study. Ann. Surg. *214*, 118-124.

Dorland's illustrated Medical Dictionary. (1988) Taylor EJ, ed. (Philadelphia: WB Saunders Company).

Douillard,J.Y., Cunningham,D., Roth,A.D., Navarro,M., James,R.D., Karasek,P., Jandik,P., Iveson,T., Carmichael,J., Alakl,M., Gruia,G., Awad,L., and Rougier,P. (2000). Irinotecan combined with fluorouracil compared with fluorouracil alone as first-line treatment for metastatic colorectal cancer: a multicentre randomised trial. Lancet *355*, 1041-1047.

Drenth,J.P., Nagengast,F.M., and Oyen,W.J. (2001). Evaluation of (pre-)malignant colonic abnormalities: endoscopic validation of FDG-PET findings. Eur. J. Nucl. Med. *28*, 1766-1769.

Dukes,C.E. (1932). The classification of cancer of the rectum. J Pathol *35*, 323.

Eary,J.F. (1999). Nuclear medicine in cancer diagnosis. Lancet *354*, 853-857.

Eary,J.F. and Mankoff,D.A. (1998). Tumor metabolic rates in sarcoma using FDG PET. J. Nucl. Med. *39*, 250-254.

Eary,J.F., Mankoff,D.A., Spence,A.M., Berger,M.S., Olshen,A., Link,J.M., O'Sullivan,F., and Krohn,K.A. (1999). 2-[C-11]thymidine imaging of malignant brain tumors. Cancer Res. *59*, 615-621.

Edgren,M., Westlin,J.E., and Ahlstrom,H. (1995). Positron emission tomography in the management of metastatic renal cell carcinoma. Antibody Immunoconjugates and Radiopharmaceuticals *8*, 215-226.

Erlichman,C., O'Connell,M., Kahn,M., Marsoni,S., Torri,V., Tardio,B., Zaniboni,A., Pancera,G., Martignoni,G., Labianca,R., Barni,A., Seitz,J.F., Milan,C., Bedenne,L., and Giovannini,M. (1999). Efficacy of adjuvant fluorouracil and folinic acid in B2 colon cancer. International Multicentre Pooled Analysis of B2 Colon Cancer Trials (IMPACT B2) Investigators. J. Clin. Oncol. *17*, 1356-1363.

Evan,G.I. and Vousden,K.H. (2001). Proliferation, cell cycle and apoptosis in cancer. Nature *411*, 342-348.

Falk,P.M., Gupta,N.C., Thorson,A.G., Frick,M.P., Boman,B.M., Christensen,M.A., and Blatchford,G.J. (1994). Positron emission tomography for preoperative staging of colorectal carcinoma. Dis. Colon Rectum *37*, 153-156.

Fearon,E.R. and Vogelstein,B. (1990). A genetic model for colorectal tumorigenesis. Cell *61*, 759-767.

Fenoglio-Preiser,C.M. and Hutter,R.V. (1985). Colorectal polyps: pathologic diagnosis and clinical significance. CA Cancer J. Clin. *35*, 322-344.

245

Ferrucci,J.T. (1990). Liver tumor imaging: current concepts [see comments]. AJR Am. J. Roentgenol. *155*, 473-484.

Findlay,M., Young,H., Cunningham,D., Iveson,A., Cronin,B., Hickish,T., Pratt,B., Husband,J., Flower,M., and Ott,R. (1996). Noninvasive monitoring of tumor metabolism using fluorodeoxyglucose and positron emission tomography in colorectal cancer liver metastases: correlation with tumor response to fluorouracil [see comments]. J. Clin. Oncol. *14*, 700-708.

Flamen,P., Hoekstra,O.S., Homans,F., Van Cutsem,E., Maes,A., Stroobants,S., Peeters,M., Penninckx,F., Filez,L., Bleichrodt,R.P., and Mortelmans,L. (2001). Unexplained rising carcinoembryonic antigen (CEA) in the postoperative surveillance of colorectal cancer: the utility of positron emission tomography (PET). Eur. J. Cancer *37*, 862-869.

Flamen,P., Stroobants,S., Van Cutsem,E., Dupont,P., Bormans,G., De Vadder,N., Penninckx,F., Van Hoe,L., and Mortelmans,L. (1999). Additional value of whole-body positron emission tomography with fluorine-18-2-fluoro-2-deoxy-D-glucose in recurrent colorectal cancer. J. Clin. Oncol. *17*, 894-901.

Flanagan,F.L., Dehdashti,F., Ogunbiyi,O.A., Kodner,I.J., and Siegel,B.A. (1998). Utility of FDG-PET for investigating unexplained plasma CEA elevation in patients with colorectal cancer. Ann. Surg. *227*, 319-323.

Flexner,C., van der,H.C., Jacobson,M.A., Powderly,W., Duncanson,F., Ganes,D., Barditch-Crovo,P.A., Petty,B.G., Baron,P.A., Armstrong,D., and . (1994). Relationship between plasma concentrations of 3'-deoxy-3'-fluorothymidine (alovudine) and antiretroviral activity in two concentration-controlled trials. J. Infect. Dis. *170*, 1394-1403.

Flier,J.S., Mueckler,M.M., Usher,P., and Lodish,H.F. (1987). Elevated levels of glucose transport and transporter messenger RNA are induced by ras or src oncogenes. Science *235*, 1492-1495.

Fong,Y., Saldinger,P.F., Akhurst,T., Macapinlac,H., Yeung,H., Finn,R.D., Cohen,A., Kemeny,N., Blumgart,L.H., and Larson,S.M. (1999). Utility of 18F-FDG positron emission tomography scanning on selection of patients for resection of hepatic colorectal metastases. Am. J. Surg. *178*, 282-287.

Freeny,P.C., Marks,W.M., Ryan,J.A., and Bolen,J.W. (1986). Colorectal carcinoma evaluation with CT: preoperative staging and detection of postoperative recurrence. Radiology *158*, 347-353.

Fuchs,C.S., Giovannucci,E.L., Colditz,G.A., Hunter,D.J., Stampfer,M.J., Rosner,B., Speizer,F.E., and Willett,W.C. (1999). Dietary fiber and the risk of colorectal cancer and adenoma in women. N. Engl. J. Med. *340*, 169-176.

Fusai,G. and Davidson,B.R. (2003). Management of colorectal liver metastases. Colorectal Dis. *5*, 2-23.

Gelfand,D.W. (1997). Colorectal cancer. Screening strategies. Radiol. Clin. North Am. *35*, 431-438.

Gerace,A.P. and Foisner,F. (1994). Integral membrane proteins and dynamic organisation of the nuclear envelope. Trends Cell Biol *4*, 127-131.

Gerdes,H., Gillin,J.S., Zimbalist,E., Urmacher,C., Lipkin,M., and Winawer,S.J. (1993). Expansion of the epithelial cell proliferative compartment and frequency of adenomatous polyps in the colon correlate with the strength of family history of colorectal cancer. Cancer Res. *53*, 279-282.

Germano,G., Chen,B.C., Huang,S.C., Gambhir,S.S., Hoffman,E.J., and Phelps,M.E. (1992). Use of the abdominal aorta for arterial input function determination in hepatic and renal PET studies. J. Nucl. Med. *33*, 613-620.

Giacchetti,S., Perpoint,B., Zidani,R., Le Bail,N., Faggiuolo,R., Focan,C., Chollet,P., Llory,J.F., Letourneau,Y., Coudert,B., Bertheaut-Cvitkovic,F., Larregain-Fournier,D., Le Rol,A., Walter,S., Adam,R., Misset,J.L., and Levi,F. (2000). Phase III multicenter randomized trial of oxaliplatin added to chronomodulated fluorouracil-leucovorin as first-line treatment of metastatic colorectal cancer. J. Clin. Oncol. *18*, 136-147.

Giardiello,F.M., Hamilton,S.R., Krush,A.J., Piantadosi,S., Hylind,L.M., Celano,P., Booker,S.V., Robinson,C.R., and Offerhaus,G.J. (1993). Treatment of colonic and rectal adenomas with sulindac in familial adenomatous polyposis. N. Engl. J. Med. *328*, 1313-1316.

Glazer,R.I. and Lloyd,L.S. (1982). Association of cell lethality with incorporation of 5-fluorouracil and 5-fluorouridine into nuclear RNA in human colon carcinoma cells in culture. Mol. Pharmacol. *21*, 468-473.

Glotzer,M., Murray,A.W., and Kirschner,M.W. (1991). Cyclin is degraded by the ubiquitin pathway. Nature *349*, 132-138.

Goethals,P., van Eijkeren,M., Lodewyck,W., and Dams,R. (1995). Measurement of [methyl-carbon-11]thymidine and its metabolites in head and neck tumors. J. Nucl. Med. *36*, 880-882.

Good,S.S., Koble,C.S., Crouch,R., Johnson,R.L., Rideout,J.L., and de Miranda,P. (1990). Isolation and characterization of an ether glucuronide of zidovudine, a major metabolite in monkeys and humans. Drug Metab Dispos. *18*, 321-326.

Graham,M.M., Peterson,L.M., and Hayward,R.M. (2000). Comparison of simplified quantitative analyses of FDG uptake. Nucl. Med. Biol. *27*, 647-655.

Gray,R.G., Kerr,D.J., McConkey,C.C., Williams,N.S., and Hills,R.K. (2000). Comparison of flourouracil with additional levamisole, higher-dose folinic acid, or both, as adjuvant chemotherapy for colorectal cancer: a randomised trial. QUASAR Collaborative Group. Lancet *355*, 1588-1596.

Grierson,J.R. and Shields,A.F. (2000). Radiosynthesis of 3'-deoxy-3'-[(18)F]fluorothymidine: [(18)F]FLT for imaging of cellular proliferation in vivo. Nucl. Med. Biol. *27*, 143-156.

Guillem,J.G., Puig-La Calle,J., Jr., Akhurst,T., Tickoo,S., Ruo,L., Minsky,B.D., Gollub,M.J., Klimstra,D.S., Mazumdar,M., Paty,P.B., Macapinlac,H., Yeung,H., Saltz,L., Finn,R.D., Erdi,Y., Humm,J., Cohen,A.M., and Larson,S. (2000). Prospective assessment of primary rectal cancer response to preoperative radiation and chemotherapy using 18-fluorodeoxyglucose positron emission tomography. Dis. Colon Rectum *43*, 18-24.

Guinet,C., Buy,J.N., Sezeur,A., Mosnier,H., Ghossain,M., Malafosse,M., Guivarc'h,M., Vadrot,D., and Ecoiffier,J. (1988). Preoperative assessment of the extension of rectal carcinoma: correlation of MR, surgical, and histopathologic findings. J. Comput. Assist. Tomogr. *12*, 209-214.

Haberkorn,U., Strauss,L.G., Dimitrakopoulou,A., Engenhart,R., Oberdorfer,F., Ostertag,H., Romahn,J., and van Kaick,G. (1991). PET studies of fluorodeoxyglucose metabolism in patients with recurrent colorectal tumors receiving radiotherapy. J. Nucl. Med. *32*, 1485-1490.

Hall,P.A. and Levison,D.A. (1990). Review: assessment of cell proliferation in histological material. J. Clin. Pathol. *43*, 184-192.

Hall,P.A. and Woods,A.L. (1990). Immunohistochemical markers of cellular proliferation: achievements, problems and prospects. Cell Tissue Kinet. *23*, 505-522.

Harvey,C.J., Amin,Z., Hare,C.M., Gillams,A.R., Novelli,M.R., Boulos,P.B., and Lees,W.R. (1998). Helical CT pneumocolon to assess colonic tumors: radiologic-pathologic correlation. AJR Am. J. Roentgenol. *170*, 1439-1443.

Hatanaka,M. (1974). Transport of sugars in tumor cell membranes. Biochim. Biophys. Acta *355*, 77-104.

Heald,R.J. and Ryall,R.D. (1986). Recurrence and survival after total mesorectal excision for rectal cancer. Lancet *1*, 1479-1482.

Heriot,A.G., Grundy,A., and Kumar,D. (1999). Preoperative staging of rectal carcinoma. Br. J. Surg. *86*, 17-28.

Herzfeld,A., Legg,M.A., and Greengard,O. (1978). Human colon tumors: enzymic and histological characteristics. Cancer *42*, 1280-1283.

Higashi,K., Clavo,A.C., and Wahl,R.L. (1993). Does FDG uptake measure proliferative activity of human cancer cells? In vitro comparison with DNA flow cytometry and tritiated thymidine uptake. J Nucl Med. *34*, 414-419.

Hildebrandt,U. and Feifel,G. (1995). Importance of endoscopic ultrasonography staging for treatment of rectal cancer. Gastrointest. Endosc. Clin. N. Am. *5*, 843-849.

Hiraki,Y., Rosen,O.M., and Birnbaum,M.J. (1988). Growth factors rapidly induce expression of the glucose transporter gene. J. Biol. Chem. *263*, 13655-13662.

Hoff,P.M., Ansari,R., Batist,G., Cox,J., Kocha,W., Kuperminc,M., Maroun,J., Walde,D., Weaver,C., Harrison,E., Burger,H.U., Osterwalder,B., Wong,A.O., and Wong,R. (2001). Comparison of oral capecitabine versus intravenous fluorouracil plus leucovorin as first-line treatment in 605 patients with metastatic colorectal cancer: results of a randomized phase III study. J. Clin. Oncol. *19*, 2282-2292.

Hoff,P.M. and Pazdur,R. (1998). UFT Plus Oral Leucovorin: A New Oral Treatment for Colorectal Cancer. Oncologist. *3*, 155-164.

Holzer,B., Urban,M., Holbling,N., Feil,W., Novi,G., Hruby,W., Rosen,H.R., and Schiessel,R. (2003). Magnetic resonance imaging predicts sphincter invasion of low rectal cancer and influences selection of operation. Surgery *133*, 656-661.

Hounsfield,G.N. (1995). Computerized transverse axial scanning (tomography): Part I. Description of system. 1973. Br. J. Radiol. *68*, H166-H172.

Howard,A. and Pelc,S.R. (1951). Nuclear incorporation of P32 as demonstrated by autoradiographs. Exp Cell Res *2*, 178-187.

Howe,G.R., Benito,E., Castelleto,R., Cornee,J., Esteve,J., Gallagher,R.P., Iscovich,J.M., Deng-ao,J., Kaaks,R., Kune,G.A., and . (1992). Dietary intake of fiber and decreased risk of cancers of the colon and rectum: evidence from the combined analysis of 13 case-control studies. J. Natl. Cancer Inst. *84*, 1887-1896.

Huang,S.C., Phelps,M.E., Hoffman,E.J., Sideris,K., Selin,C.J., and Kuhl,D.E. (1980). Noninvasive determination of local cerebral metabolic rate of glucose in man. Am. J. Physiol *238*, E69-E82.

Huebner,R.H., Park,K.C., Shepherd,J.E., Schwimmer,J., Czernin,J., Phelps,M.E., and Gambhir,S.S. (2000). A meta-analysis of the literature for whole-body FDG PET detection of recurrent colorectal cancer. J. Nucl. Med. *41*, 1177-1189.

Hughes,W.L., Bond,V.P., Brecher,G., Cronkite,E.P., Painter,R.B., Quastler,H., and Sherman,F.G. (1958). Cellular proliferation in the mouse as revealed by autoradiography with tritiated thymidine. Proc Natl Acad Sci *44*, 476-483.

Ito,K., Nakata,K., Watanabe,T., Hibi,K., Kasai,Y., Akiyama,S., and Takagi,H. (1997). [Diagnosis of local recurrence of colorectal cancer, using PET and immunoscintigraphy

by means of 131I or 111In anti-CEA monoclonal antibody]. Nippon Geka Gakkai Zasshi *98*, 373-379.

Jass,J.R. and Sobin,L.H. (1989). Histological typing of intestinal tumours. In WHO international histological classification of tumours, (Berlin-New York: Springr-Verlag).

Kalender,W.A., Seissler,W., Klotz,E., and Vock,P. (1990). Spiral volumetric CT with single-breath-hold technique, continuous transport, and continuous scanner rotation. Radiology *176*, 181-183.

Kalff,V., Hicks,R.J., Ware,R.E., Hogg,A., Binns,D., and McKenzie,A.F. (2002). The clinical impact of (18)F-FDG PET in patients with suspected or confirmed recurrence of colorectal cancer: a prospective study. J. Nucl. Med. *43*, 492-499.

Kemeny,N.E. and Ron,I.G. (1999). Hepatic arterial chemotherapy in metastatic colorectal patients. Semin. Oncol. *26*, 524-535.

Khosraviani,K., Weir,H.P., Hamilton,P., Moorehead,J., and Williamson,K. (2002). Effect of folate supplementation on mucosal cell proliferation in high risk patients for colon cancer. Gut *51*, 195-199.

Kiffer,J.D., Berlangieri,S.U., Scott,A.M., Quong,G., Feigen,M., Schumer,W., Clarke,C.P., Knight,S.R., and Daniel,F.J. (1998). The contribution of 18F-fluoro-2-deoxy-glucose positron emission tomographic imaging to radiotherapy planning in lung cancer. Lung Cancer *19*, 167-177.

Kimura,T., Tanaka,S., Haruma,K., Sumii,K., Kajiyama,G., Shimamoto,F., and Kohno,N. (2000). Clinical significance of MUC1 and E-cadherin expression, cellular proliferation, and angiogenesis at the deepest invasive portion of colorectal cancer. Int. J. Oncol. *16*, 55-64.

Kinkel,K., Lu,Y., Both,M., Warren,R.S., and Thoeni,R.F. (2002). Detection of hepatic metastases from cancers of the gastrointestinal tract by using noninvasive imaging methods (US, CT, MR imaging, PET): a meta-analysis. Radiology *224*, 748-756.

Kinzler,K.W., Nilbert,M.C., Su,L.K., Vogelstein,B., Bryan,T.M., Levy,D.B., Smith,K.J., Preisinger,A.C., Hedge,P., McKechnie,D., and . (1991). Identification of FAP locus genes from chromosome 5q21. Science *253*, 661-665.

Kubota,Y., Petras,R.E., Easley,K.A., Bauer,T.W., Tubbs,R.R., and Fazio,V.W. (1992). Ki-67-determined growth fraction versus standard staging and grading parameters in colorectal carcinoma. A multivariate analysis. Cancer *70*, 2602-2609.

Kyzer,S. and Gordon,P.H. (1997). Determination of proliferative activity in colorectal carcinoma using monoclonal antibody Ki67. Dis. Colon Rectum *40*, 322-325.

Labayle,D., Fischer,D., Vielh,P., Drouhin,F., Pariente,A., Bories,C., Duhamel,O., Trousset,M., and Attali,P. (1991). Sulindac causes regression of rectal polyps in familial adenomatous polyposis. Gastroenterology *101*, 635-639.

Labianca,R., Marsoni,S., Pancera,G., Torri,V., Zaniboni,A., Erlichman,C., Pater,J., and Zeitoun,P. (1995). Efficacy of adjuvant fluorouracil and folinic acid in colon cancer. International Multicentre Pooled Analysis of Colon Cancer Trials (IMPACT) investigators. Lancet *345*, 939-944.

Lai,D.T., Fulham,M., Stephen,M.S., Chu,K.M., Solomon,M., Thompson,J.F., Sheldon,D.M., and Storey,D.W. (1996). The role of whole-body positron emission tomography with [18F]fluorodeoxyglucose in identifying operable colorectal cancer metastases to the liver. Arch. Surg. *131*, 703-707.

Larson, S. M. Cohen A. M. Cascade M. B. A. Clinical application and economic implications of PET in the assessment of colorectal cancer recurrence: a retrospective study. Abstract from the 1994 ICP Meeting, Institute for Clinical PET, Fairfax, Virginia. 1994.

Levine,M.S., Rubesin,S.E., Laufer,I., and Herlinger,H. (2000). Diagnosis of colorectal neoplasms at double-contrast barium enema examination. Radiology *216*, 11-18.

Libutti,S.K., Alexander,H.R., Jr., Choyke,P., Bartlett,D.L., Bacharach,S.L., Whatley,M., Jousse,F., Eckelman,W.C., Kranda,K., Neumann,R.D., and Carrasquillo,J.A. (2001). A prospective study of 2-[18F] fluoro-2-deoxy-D-glucose/positron emission tomography scan, 99mTc-labeled arcitumomab (CEA-scan), and blind second-look laparotomy for detecting colon cancer recurrence in patients with increasing carcinoembryonic antigen levels. Ann. Surg. Oncol. *8*, 779-786.

Lipkin,M., Enker,W.E., and Winawer,S.J. (1987). Tritiated-thymidine labeling of rectal epithelial cells in 'non-prep' biopsies of individuals at increased risk for colonic neoplasia. Cancer Lett. *37*, 153-161.

Loda,M., Cukor,B., Tam,S.W., Lavin,P., Fiorentino,M., Draetta,G.F., Jessup,J.M., and Pagano,M. (1997). Increased proteasome-dependent degradation of the cyclin-dependent kinase inhibitor p27 in aggressive colorectal carcinomas. Nat. Med. *3*, 231-234.

Lodge,M.A., Lucas,J.D., Marsden,P.K., Cronin,B.F., O'Doherty,M.J., and Smith,M.A. (1999). A PET study of 18FDG uptake in soft tissue masses. Eur. J. Nucl. Med. *26*, 22-30.

Lu,L., Samuelsson,L., Bergstrom,M., Sato,K., Fasth,K.J., and Langstrom,B. (2002). Rat studies comparing 11C-FMAU, 18F-FLT, and 76Br-BFU as proliferation markers. J. Nucl. Med. *43*, 1688-1698.

Lunniss,P.J., Skinner,S., Britton,K.E., Granowska,M., Morris,G., and Northover,J.M. (1999). Effect of radioimmunoscintigraphy on the management of recurrent colorectal cancer. Br. J. Surg. *86*, 244-249.

Lynch,H.T. (1996). Is there a role for prophylactic subtotal colectomy among hereditary nonpolyposis colorectal cancer germline mutation carriers? Dis. Colon Rectum *39*, 109-110.

Lynch,H.T. and Krush,A.J. (1971). Cancer family "G" revisited: 1895-1970. Cancer *27*, 1505-1511.

Lynch,H.T., Shaw,M.W., Magnuson,C.W., Larsen,A.L., and Krush,A.J. (1966). Hereditary factors in cancer. Study of two large midwestern kindreds. Arch. Intern. Med. *117*, 206-212.

Machulla HJ, Blocher A, Kuntzch M, Piert M, Wei R, and Grierson JR (2000). Simplified labeling approach for synthesing 3'-deoxy-3-[18F]fluorothymidine ([18F]FLT). J Radioanal Nucl Chem *243*, 843-846.

Mamounas,E., Wieand,S., Wolmark,N., Bear,H.D., Atkins,J.N., Song,K., Jones,J., and Rockette,H. (1999). Comparative efficacy of adjuvant chemotherapy in patients with Dukes' B versus Dukes' C colon cancer: results from four National Surgical Adjuvant Breast and Bowel Project adjuvant studies (C-01, C-02, C-03, and C-04). J. Clin. Oncol. *17*, 1349-1355.

Mazia,D. (1961). Mitosis and physiology of cell division. In The Cell, (New York: Academic Press).

McCormick,D., Chong,H., Hobbs,C., Datta,C., and Hall,P.A. (1993). Detection of the Ki-67 antigen in fixed and wax-embedded sections with the monoclonal antibody MIB1. Histopathology *22*, 355-360.

Mendelsohn ML (1962). Autoradiographic analysis of cell proliferation in spontaneous breast cancer of C3H mouse. The growth fraction. J Natl Cancer Inst *28*, 1015-1029.

Mendez,R.J., Rodriguez,R., Kovacevich,T., Martinez,S., Moreno,G., and Cerdan,J. (1993). CT in local recurrence of rectal carcinoma. J. Comput. Assist. Tomogr. *17*, 741-744.

Midgley,R. and Kerr,D. (1999). Colorectal cancer. Lancet *353*, 391-399.

Mier,W., Haberkorn,U., and Eisenhut,M. (2002). [18F]FLT; portrait of a proliferation marker. Eur. J. Nucl. Med. Mol. Imaging *29*, 165-169.

Moehler,M., Dimitrakopoulou-Strauss,A., Gutzler,F., Raeth,U., Strauss,L.G., and Stremmel,W. (1998). 18F-labeled fluorouracil positron emission tomography and the prognoses of colorectal carcinoma patients with metastases to the liver treated with 5-fluorouracil. Cancer *83*, 245-253.

Moore,K.H., Raasch,R.H., Brouwer,K.L., Opheim,K., Cheeseman,S.H., Eyster,E., Lemon,S.M., and van der Horst,C.M. (1995). Pharmacokinetics and bioavailability of zidovudine and its glucuronidated metabolite in patients with human immunodeficiency

virus infection and hepatic disease (AIDS Clinical Trials Group protocol 062). Antimicrob. Agents Chemother. *39*, 2732-2737.

Mukai,M., Sadahiro,S., Yasuda,S., Ishida,H., Tokunaga,N., Tajima,T., and Makuuchi,H. (2000). Preoperative evaluation by whole-body 18F-fluorodeoxyglucose positron emission tomography in patients with primary colorectal cancer. Oncol. Rep. *7*, 85-87.

Munch-Petersen,B., Cloos,L., Jensen,H.K., and Tyrsted,G. (1995). Human thymidine kinase 1. Regulation in normal and malignant cells. Adv. Enzyme Regul. *35*, 69-89.

Muto,T., Bussey,H.J., and Morson,B.C. (1975). The evolution of cancer of the colon and rectum. Cancer *36*, 2251-2270.

Nakata,B., Chung,Y.S., Nishimura,S., Nishihara,T., Sakurai,Y., Sawada,T., Okamura,T., Kawabe,J., Ochi,H., and Sowa,M. (1997). 18F-fluorodeoxyglucose positron emission tomography and the prognosis of patients with pancreatic adenocarcinoma. Cancer *79*, 695-699.

Napoleon,B., Pujol,B., Berger,F., Valette,P.J., Gerard,J.P., and Souquet,J.C. (1991). Accuracy of endosonography in the staging of rectal cancer treated by radiotherapy. Br. J. Surg. *78*, 785-788.

Newland,R.C., Chapuis,P.H., Pheils,M.T., and MacPherson,J.G. (1981). The relationship of survival to staging and grading of colorectal carcinoma: a prospective study of 503 cases. Cancer *47*, 1424-1429.

NICE (2002). Guidance on the use of irinotecan, oxaliplatin and raltitrexed for the treatment of advanced colorectal cancer. In National Institute for clinical excellence.

Nicolas,F., De Sousa,G., Thomas,P., Placidi,M., Lorenzon,G., and Rahmani,R. (1995). Comparative metabolism of 3'-azido-3'-deoxythymidine in cultured hepatocytes from rats, dogs, monkeys, and humans. Drug Metab Dispos. *23*, 308-313.

Ogunbiyi,O.A., Flanagan,F.L., Dehdashti,F., Siegel,B.A., Trask,D.D., Birnbaum,E.H., Fleshman,J.W., Read,T.E., Philpott,G.W., and Kodner,I.J. (1997a). Detection of recurrent and metastatic colorectal cancer: comparison of positron emission tomography and computed tomography. Ann. Surg. Oncol. *4*, 613-620.

Ogunbiyi,O.A., McKenna,K., Birnbaum,E.H., Fleshman,J.W., and Kodner,I.J. (1997b). Aggressive surgical management of recurrent rectal cancer--is it worthwhile? Dis. Colon Rectum *40*, 150-155.

Ohtake,T., Kosaka,N., Watanabe,T., Yokoyama,I., Moritan,T., Masuo,M., Iizuka,M., Kozeni,K., Momose,T., Oku,S., and . (1991). Noninvasive method to obtain input function for measuring tissue glucose utilization of thoracic and abdominal organs. J. Nucl. Med. *32*, 1432-1438.

Okada,J., Yoshikawa,K., Imazeki,K., Minoshima,S., Uno,K., Itami,J., Kuyama,J., Maruno,H., and Arimizu,N. (1991). The use of FDG-PET in the detection and management of malignant lymphoma: correlation of uptake with prognosis. J. Nucl. Med. *32*, 686-691.

Oku,S., Nakagawa,K., Momose,T., Kumakura,Y., Abe,A., Watanabe,T., and Ohtomo,K. (2002). FDG-PET after radiotherapy is a good prognostic indicator of rectal cancer. Ann. Nucl. Med. *16*, 409-416.

Oshowo,A., Gillams,A.R., Lees,W.R., and Taylor,I. (2003). Radiofrequency ablation extends the scope of surgery in colorectal liver metastases. Eur. J. Surg. Oncol. *29*, 244-247.

Ott,D.J. (2000). Accuracy of double-contrast barium enema in diagnosing colorectal polyps and cancer. Semin. Roentgenol. *35*, 333-341.

Padhani,A.R. and Husband,J.E. (2000). Commentary. Are current tumour response criteria relevant for the 21st century? Br. J. Radiol. *73*, 1031-1033.

Paganelli,G.M., Santucci,R., Biasco,G., Miglioli,M., and Barbara,L. (1990). Effect of sex and age on rectal cell renewal in humans. Cancer Lett. *53*, 117-121.

Palmqvist,R., Sellberg,P., Oberg,A., Tavelin,B., Rutegard,J.N., and Stenling,R. (1999). Low tumour cell proliferation at the invasive margin is associated with a poor prognosis in Dukes' stage B colorectal cancers. Br. J. Cancer *79*, 577-581.

Patlak,C.S., Blasberg,R.G., and Fenstermacher,J.D. (1983). Graphical evaluation of blood-to-brain transfer constants from multiple-time uptake data. J. Cereb. Blood Flow Metab *3*, 1-7.

Patt,Y.Z., Lamki,L.M., Shanken,J., Jessup,J.M., Charnsangavej,C., Ajani,J.A., Levin,B., Merchant,B., Halverson,C., and Murray,J.L. (1990). Imaging with indium111-labeled anticarcinoembryonic antigen monoclonal antibody ZCE-025 of recurrent colorectal or carcinoembryonic antigen- producing cancer in patients with rising serum carcinoembryonic antigen levels and occult metastases. J. Clin. Oncol. *8*, 1246-1254.

Paul,M.A., Mulder,L.S., Cuesta,M.A., Sikkenk,A.C., Lyesen,G.K., and Meijer,S. (1994). Impact of intraoperative ultrasonography on treatment strategy for colorectal cancer. Br. J. Surg. *81*, 1660-1663.

Piazza,G.A., Rahm,A.L., Krutzsch,M., Sperl,G., Paranka,N.S., Gross,P.H., Brendel,K., Burt,R.W., Alberts,D.S., and Pamukcu,R. (1995). Antineoplastic drugs sulindac sulfide and sulfone inhibit cell growth by inducing apoptosis. Cancer Res. *55*, 3110-3116.

Piedbois,P., Buyse,M., Rustum,Y., Machover,D., Erlichman,C., Carlson,R.W., Valone,F., Labianca,R., Doroshow,J.H., and Petrellin,N. (1992). Modulation of fluorouracil by leucovorin in patients with advanced colorectal cancer: evidence in terms of response rate. Advanced Colorectal Cancer Meta-Analysis Project. J. Clin. Oncol. *10*, 896-903.

Pijl,M.E., Chaoui,A.S., Wahl,R.L., and van Oostayen,J.A. (2002). Radiology of colorectal cancer. Eur. J. Cancer *38*, 887-898.

Pin,C.A., Grigolon,M.V., Etchebehere,E.C., Santos,A.O., Lima,M.C., Ramos,C.D., and Camargo,E.E. (2000). Detection of synchronous carcinomas of the colon with F-18 fluorodeoxyglucose: a case report. Clin. Nucl. Med. *25*, 370-371.

Potter,J.D. (1999). Colorectal cancer: molecules and populations. J. Natl. Cancer Inst. *91*, 916-932.

Pretlow,T.P., Barrow,B.J., Ashton,W.S., O'Riordan,M.A., Pretlow,T.G., Jurcisek,J.A., and Stellato,T.A. (1991). Aberrant crypts: putative preneoplastic foci in human colonic mucosa. Cancer Res. *51*, 1564-1567.

Pretlow,T.P., Roukhadze,E.V., O'Riordan,M.A., Chan,J.C., Amini,S.B., and Stellato,T.A. (1994). Carcinoembryonic antigen in human colonic aberrant crypt foci. Gastroenterology *107*, 1719-1725.

Price,P. and Jones,T. (1995). Can positron emission tomography (PET) be used to detect subclinical response to cancer therapy? The EC PET Oncology Concerted Action and the EORTC PET Study Group. Eur. J. Cancer *31A*, 1924-1927.

Rasey,J.S., Grierson,J.R., Wiens,L.W., Kolb,P.D., and Schwartz,J.L. (2002). Validation of FLT uptake as a measure of thymidine kinase-1 activity in A549 carcinoma cells. J. Nucl. Med. *43*, 1210-1217.

Reivich,M., Kuhl,D., Wolf,A., Greenberg,J., Phelps,M., Ido,T., Casella,V., Fowler,J., Hoffman,E., Alavi,A., Som,P., and Sokoloff,L. (1979). The [18F]fluorodeoxyglucose method for the measurement of local cerebral glucose utilization in man. Circ. Res. *44*, 127-137.

Rifkin,M.D., Ehrlich,S.M., and Marks,G. (1989). Staging of rectal carcinoma: prospective comparison of endorectal US and CT. Radiology *170*, 319-322.

Risio,M., Coverlizza,S., Ferrari,A., Candelaresi,G.L., and Rossini,F.P. (1988). Immunohistochemical study of epithelial cell proliferation in hyperplastic polyps, adenomas, and adenocarcinomas of the large bowel. Gastroenterology *94*, 899-906.

Risio,M. and Rossini,F.P. (1993). Cell proliferation in colorectal adenomas containing invasive carcinoma. Anticancer Res. *13*, 43-47.

Rodriguez-Bigas,M.A., Maamoun,S., Weber,T.K., Penetrante,R.B., Blumenson,L.E., and Petrelli,N.J. (1996). Clinical significance of colorectal cancer: metastases in lymph nodes < 5 mm in size. Ann. Surg. Oncol. *3*, 124-130.

Roncucci,L., Ponz,d.L., Scalmati,A., Malagoli,G., Pratissoli,S., Perini,M., and Chahin,N.J. (1988). The influence of age on colonic epithelial cell proliferation. Cancer *62*, 2373-2377.

Rosenman,J. (2001). Incorporating functional imaging information into radiation treatment. Semin. Radiat. Oncol. *11*, 83-92.

Rozen,P., Fireman,Z., Fine,N., Chetrit,A., and Lubin,F. (1990). Rectal epithelial proliferation characteristics of first degree relatives of sporadic colon cancer patients. Cancer Lett. *51*, 127-132.

Rummeny,E.J., Wernecke,K., Saini,S., Vassallo,P., Wiesmann,W., Oestmann,J.W., Kivelitz,D., Reers,B., Reiser,M.F., and Peters,P.E. (1992). Comparison between high-field-strength MR imaging and CT for screening of hepatic metastases: a receiver operating characteristic analysis. Radiology *182*, 879-886.

Sakamoto,S., Kasahara,N., Kudo,H., and Iwama,T. (1992). Effects of carcinogenesis on colonic thymidine kinase activity in familial adenomatous polyposis. Carcinogenesis *13*, 873-876.

Sakamoto,S., Sagara,T., Iwama,T., Kawasaki,T., and Okamoto,R. (1985). Increased activities of thymidine kinase isozymes in human colon polyp and carcinoma. Carcinogenesis *6*, 917-919.

Saltz,L.B., Cox,J.V., Blanke,C., Rosen,L.S., Fehrenbacher,L., Moore,M.J., Maroun,J.A., Ackland,S.P., Locker,P.K., Pirotta,N., Elfring,G.L., and Miller,L.L. (2000). Irinotecan plus fluorouracil and leucovorin for metastatic colorectal cancer. Irinotecan Study Group. N. Engl. J. Med. *343*, 905-914.

Sandler,R.S., Baron,J.A., Tosteson,T.D., Mandel,J.S., and Haile,R.W. (2000). Rectal mucosal proliferation and risk of colorectal adenomas: results from a randomized controlled trial. Cancer Epidemiol. Biomarkers Prev. *9*, 653-656.

Sano,H., Kawahito,Y., Wilder,R.L., Hashiramoto,A., Mukai,S., Asai,K., Kimura,S., Kato,H., Kondo,M., and Hla,T. (1995). Expression of cyclooxygenase-1 and -2 in human colorectal cancer. Cancer Res. *55*, 3785-3789.

Saunders,M.P. and Valle,J.W. (2002). Why hasn't the National Institute been 'NICE' to patients with colorectal cancer? National Institute of Clinical Excellence. Br. J. Cancer *86*, 1667-1669.

Schatzkin,A., Lanza,E., Corle,D., Lance,P., Iber,F., Caan,B., Shike,M., Weissfeld,J., Burt,R., Cooper,M.R., Kikendall,J.W., and Cahill,J. (2000). Lack of effect of a low-fat, high-fiber diet on the recurrence of colorectal adenomas. Polyp Prevention Trial Study Group. N. Engl. J. Med. *342*, 1149-1155.

Schiepers,C., Penninck,F., De Vadder,N., Merck,E., Mortelmans,L., Bormans,G., Marchal,G., Filez,L., and Aerts,R. (1995). Contribution of PET in the diagnosis of recurrent colorectal cancer: comparison with conventional imaging. Eur. J. Surg. Oncol. *21*, 517-522.

Schlag,P., Lehner,B., Strauss,L.G., Georgi,P., and Herfarth,C. (1989). Scar or recurrent rectal cancer. Positron emission tomography is more helpful for diagnosis than immunoscintigraphy. Arch. Surg. *124*, 197-200.

Schluter,C., Duchrow,M., Wohlenberg,C., Becker,M.H., Key,G., Flad,H.D., and Gerdes,J. (1993). The cell proliferation-associated antigen of antibody Ki-67: a very large, ubiquitous nuclear protein with numerous repeated elements, representing a new kind of cell cycle-maintaining proteins. J. Cell Biol. *123*, 513-522.

Seitz,U., Wagner,M., Neumaier,B., Wawra,E., Glatting,G., Leder,G., Schmid,R.M., and Reske,S.N. (2002). Evaluation of pyrimidine metabolising enzymes and in vitro uptake of 3'-[(18)F]fluoro-3'-deoxythymidine ([(18)F]FLT) in pancreatic cancer cell lines. Eur. J. Nucl. Med. Mol. Imaging *29*, 1174-1181.

Shani,J., Young,D., Schlesinger,T., Siemsen,J.K., Chlebowski,R.T., Bateman,J.R., and Wolf,W. (1982). Dosimetry and preliminary human studies of 18F-5-fluorouracil. Int. J. Nucl. Med. Biol. *9*, 25-35.

Sherley,J.L. and Kelly,T.J. (1988). Regulation of human thymidine kinase during the cell cycle. J. Biol. Chem. *263*, 8350-8358.

Shields,A.F., Grierson,J.R., Muzik,O., Stayanoff,J.C., Lawhorn-Crews,J.M., Obradovitch,J.E., and Mangner,T.J. (2002). Kinetics of 3'-deoxy-3'-[F-18]Fluorothymidine uptake and retention in dogs. Molecular Imaging and Biology *4*, 83-89.

Shields,A.F., Dohmen,B.M., Manger,T.J., Kuntzsch,M., Bares,R., Stayanoff,J., Muzik,O., Machulla,H.J. (2000). Metabolism of ^{18}F-FLT in patients. J. Nucl. Med. *41*, 36P.

Shields,A.F., Graham,M.M., Kozawa,S.M., Kozell,L.B., Link,J.M., Swenson,E.R., Spence,A.M., Bassingthwaighte,J.B., and Krohn,K.A. (1992). Contribution of labeled carbon dioxide to PET imaging of carbon-11-labeled compounds. J. Nucl. Med. *33*, 581-584.

Shields,A.F., Mankoff,D.A., Link,J.M., Graham,M.M., Eary,J.F., Kozawa,S.M., Zheng,M., Lewellen,B., Lewellen,T.K., Grierson,J.R., and Krohn,K.A. (1998a). Carbon-11-thymidine and FDG to measure therapy response. J. Nucl. Med. *39*, 1757-1762.

Shields,A.F., Grierson,J.R., Dohmen,B.M., Machulla,H.J., Stayanoff,J.C., Lawhorn-Crews,J.M., Obradovich,J.E., Muzik,O., and Mangner,T.J. (1998b). Imaging proliferation in vivo with [F-18]FLT and positron emission tomography. Nat. Med. *4*, 1334-1336.

Shields,A.F., Grierson,J.R., Kozawa,S.M., and Zheng,M. (1996). Development of labeled thymidine analogs for imaging tumor proliferation. Nucl. Med. Biol. *23*, 17-22.

Shpitz,B., Bomstein,Y., Mekori,Y., Cohen,R., Kaufman,Z., Grankin,M., and Bernheim,J. (1997). Proliferating cell nuclear antigen as a marker of cell kinetics in aberrant crypt

foci, hyperplastic polyps, adenomas, and adenocarcinomas of the human colon. Am. J. Surg. *174*, 425-430.

Simmonds,P.C. (2000). Palliative chemotherapy for advanced colorectal cancer: systematic review and meta-analysis. Colorectal Cancer Collaborative Group. BMJ *321*, 531-535.

Simo,M., Lomena,F., Setoain,J., Perez,G., Castellucci,P., Costansa,J.M., Setoain-Quinquer,J., Domenech-Torne,F., and Carrio,I. (2002). FDG-PET improves the management of patients with suspected recurrence of colorectal cancer. Nucl. Med. Commun. *23*, 975-982.

Slattery,M.L., Potter,J., Caan,B., Edwards,S., Coates,A., Ma,K.N., and Berry,T.D. (1997). Energy balance and colon cancer--beyond physical activity. Cancer Res. *57*, 75-80.

Slingerland,J.M. and Tannock,I.F. (1998). Cell proliferation and cell death. In The Basic Science of Oncology, Tannock IF and Hill RP, eds. McGraw-Hill), pp. 134-165.

Smith,C. (1997). Colorectal cancer. Radiologic diagnosis. Radiol. Clin. North Am. *35*, 439-456.

Sokoloff,L., Reivich,M., Kennedy,C., Des Rosiers,M.H., Patlak,C.S., Pettigrew,K.D., Sakurada,O., and Shinohara,M. (1977). The [14C]deoxyglucose method for the measurement of local cerebral glucose utilization: theory, procedure, and normal values in the conscious and anesthetized albino rat. J. Neurochem. *28*, 897-916.

Srivastava,S., Verma,M., and Henson,D.E. (2001). Biomarkers for early detection of colon cancer. Clin. Cancer Res. *7*, 1118-1126.

Steele,G., Jr., Bleday,R., Mayer,R.J., Lindblad,A., Petrelli,N., and Weaver,D. (1991). A prospective evaluation of hepatic resection for colorectal carcinoma metastases to the liver: Gastrointestinal Tumor Study Group Protocol 6584 [see comments]. J. Clin. Oncol. *9*, 1105-1112.

Strauss,L.G., Clorius,J.H., Schlag,P., Lehner,B., Kimmig,B., Engenhart,R., Marin-Grez,M., Helus,F., Oberdorfer,F., and Schmidlin,P. (1989). Recurrence of colorectal tumors: PET evaluation. Radiology *170*, 329-332.

Strauss,L.G. and Conti,P.S. (1991). The applications of PET in clinical oncology. J. Nucl. Med. *32*, 623-648.

Sugarbaker,P.H. and Corlew,S. (1982). Influence of surgical techniques on survival in patients with colorectal cancer. Dis. Colon Rectum *25*, 545-557.

Sundoro-Wu,B.M., Schmall,B., Conti,P.S., Dahl,J.R., Drumm,P., and Jacobsen,J.K. (1984). Selective alkylation of pyrimidyldianions: synthesis and purification of 11C

labeled thymidine for tumor visualization using positron emission tomography. Int. J. Appl. Radiat. Isot. *35*, 705-708.

Taal,B.G., Van Tinteren,H., and Zoetmulder,F.A. (2001). Adjuvant 5FU plus levamisole in colonic or rectal cancer: improved survival in stage II and III. Br. J. Cancer *85*, 1437-1443.

Takenoue,T., Nagawa,H., Matsuda,K., Fujii,S., Nita,M.E., Hatano,K., Kitayama,J., Tsuruo,T., and Muto,T. (2000). Relation between thymidylate synthase expression and survival in colon carcinoma, and determination of appropriate application of 5-fluorouracil by immunohistochemical method. Ann. Surg. Oncol. *7*, 193-198.

Takeuchi,O., Saito,N., Koda,K., Sarashina,H., and Nakajima,N. (1999). Clinical assessment of positron emission tomography for the diagnosis of local recurrence in colorectal cancer. Br. J. Surg. *86*, 932-937.

Talbot,I.C., Ritchie,S., Leighton,M.H., Hughes,A.O., Bussey,H.J., and Morson,B.C. (1981). Spread of rectal cancer within veins. Histologic features and clinical significance. Am. J. Surg. *141*, 15-17.

Tanaka,T., Kawai,Y., Kanai,M., Taki,Y., Nakamoto,Y., and Takabayashi,A. (2002). Usefulness of FDG-positron emission tomography in diagnosing peritoneal recurrence of colorectal cancer. Am. J. Surg. *184*, 433-436.

Tatlidil,R., Jadvar,H., Bading,J.R., and Conti,P.S. (2002). Incidental colonic fluorodeoxyglucose uptake: correlation with colonoscopic and histopathologic findings. Radiology *224*, 783-787.

Therasse,P., Arbuck,S.G., Eisenhauer,E.A., Wanders,J., Kaplan,R.S., Rubinstein,L., Verweij,J., Van Glabbeke,M., van Oosterom,A.T., Christian,M.C., and Gwyther,S.G. (2000). New guidelines to evaluate the response to treatment in solid tumors. European Organization for Research and Treatment of Cancer, National Cancer Institute of the United States, National Cancer Institute of Canada. J. Natl. Cancer Inst. *92*, 205-216.

Thompson,W.M., Halvorsen,R.A., Foster,W.L., Jr., Roberts,L., and Gibbons,R. (1986). Preoperative and postoperative CT staging of rectosigmoid carcinoma. AJR Am. J. Roentgenol. *146*, 703-710.

Topal,B. (2001). Clinical value of whole-body emission tomography in potentially curable colorectal liver metastases. Eur. J. Surg. Oncol. *27*, 175-179.

Toyohara,J., Waki,A., Takamatsu,S., Yonekura,Y., Magata,Y., and Fujibayashi,Y. (2002). Basis of FLT as a cell proliferation marker: comparative uptake studies with [3H]thymidine and [3H]arabinothymidine, and cell-analysis in 22 asynchronously growing tumor cell lines. Nucl. Med. Biol. *29*, 281-287.

Tudek,B., Bird,R.P., and Bruce,W.R. (1989). Foci of aberrant crypts in the colons of mice and rats exposed to carcinogens associated with foods. Cancer Res. *49*, 1236-1240.

Turk,P.S. (1993). Resection of pelvic recurrence. In Colorectal Cancer, Wanebo, ed. (St Louis: CV Mosby), pp. 443-463.

Valk,P.E., Abella-Columna,E., Haseman,M.K., Pounds,T.R., Tesar,R.D., Myers,R.W., Greiss,H.B., and Hofer,G.A. (1999). Whole-body PET imaging with [18F]fluorodeoxyglucose in management of recurrent colorectal cancer. Arch. Surg. *134*, 503-511.

Van Cutsem,E., Twelves,C., Cassidy,J., Allman,D., Bajetta,E., Boyer,M., Bugat,R., Findlay,M., Frings,S., Jahn,M., McKendrick,J., Osterwalder,B., Perez-Manga,G., Rosso,R., Rougier,P., Schmiegel,W.H., Seitz,J.F., Thompson,P., Vieitez,J.M., Weitzel,C., and Harper,P. (2001). Oral capecitabine compared with intravenous fluorouracil plus leucovorin in patients with metastatic colorectal cancer: results of a large phase III study. J. Clin. Oncol. *19*, 4097-4106.

van der Weerdt,A.P., Klein,L.J., Boellaard,R., Visser,C.A., Visser,F.C., and Lammertsma,A.A. (2001). Image-derived input functions for determination of MRGlu in cardiac (18)F-FDG PET scans. J. Nucl. Med. *42*, 1622-1629.

van Eijkeren,M.E., De Schryver,A., Goethals,P., Poupeye,E., Schelstraete,K., Lemahieu,I., and De Potter,C.R. (1992). Measurement of short-term 11C-thymidine activity in human head and neck tumours using positron emission tomography (PET). Acta Oncol. *31*, 539-543.

Veal,G.J. and Back,D.J. (1995). Metabolism of Zidovudine. Gen. Pharmacol. *26*, 1469-1475.

Venkatesh,K.S., Weingart,D.J., and Ramanujam,P.J. (1994). Comparison of double and single parameters in DNA analysis for staging and as a prognostic indicator in patients with colon and rectal carcinoma. Dis. Colon Rectum *37*, 1142-1147.

Veroux,G., Nicosia,A.S., Veroux,P., Cardillo,P., Veroux,M., and Amodeo,C. (1999). Radioimmunoguided surgery. Hepatogastroenterology *46*, 3099-3108.

Vesselle,H., Grierson,J., Muzi,M., Pugsley,J.M., Schmidt,R.A., Rabinowitz,P., Peterson,L.M., Vallieres,E., and Wood,D.E. (2002). In Vivo Validation of 3'deoxy-3'-[(18)F]fluorothymidine ([(18)F]FLT) as a Proliferation Imaging Tracer in Humans: Correlation of [(18)F]FLT Uptake by Positron Emission Tomography with Ki-67 Immunohistochemistry and Flow Cytometry in Human Lung Tumors. Clin. Cancer Res. *8*, 3315-3323.

Vijayalakshmi,D. and Belt,J.A. (1988). Sodium-dependent nucleoside transport in mouse intestinal epithelial cells. Two transport systems with differing substrate specificities. J Biol. Chem *263*, 19419-19423.

Visvikis,D., Cheze-LeRest,C., Costa,D.C., Bomanji,J., Gacinovic,S., and Ell,P.J. (2001). Influence of OSEM and segmented attenuation correction in the calculation of standardised uptake values for [18F]FDG PET. Eur. J. Nucl. Med. *28*, 1326-1335.

260

Visvikis,D., Costa,D.C., Croasdale,I., Lonn,A.H., Bomanji,J., Gacinovic,S., and Ell,P.J. (2003). CT-based attenuation correction in the calculation of semi-quantitative indices of [(18)F]FDG uptake in PET. Eur. J. Nucl. Med. Mol. Imaging *30*, 344-353.

Vitola,J.V., Delbeke,D., Sandler,M.P., Campbell,M.G., Powers,T.A., Wright,J.K., Chapman,W.C., and Pinson,C.W. (1996). Positron emission tomography to stage suspected metastatic colorectal carcinoma to the liver. Am. J. Surg. *171*, 21-26.

Vogelstein,B., Fearon,E.R., Hamilton,S.R., Kern,S.E., Preisinger,A.C., Leppert,M., Nakamura,Y., White,R., Smits,A.M., and Bos,J.L. (1988). Genetic alterations during colorectal-tumor development. N. Engl. J. Med. *319*, 525-532.

Wagner,M., Seitz,U., Buck,A., Neumaier,B., Schultheiss,S., Bangerter,M., Bommer,M., Leithauser,F., Wawra,E., Munzert,G., and Reske,S.N. (2003). 3'-[18F]fluoro-3'-deoxythymidine ([18F]-FLT) as positron emission tomography tracer for imaging proliferation in a murine B-Cell lymphoma model and in the human disease. Cancer Res. *63*, 2681-2687.

Wahl,R.L., Harney,J., Hutchins,G., and Grossman,H.B. (1991). Imaging of renal cancer using positron emission tomography with 2-deoxy-2-(18F)-fluoro-D-glucose: pilot animal and human studies. J. Urol. *146*, 1470-1474.

Warburg, O. The metabolism of tumours. 129-169. 1931. New York, Smith RR.

Weber,G. (1977a). Enzymology of cancer cells (first of two parts). N. Engl. J. Med. *296*, 486-492.

Weber,G. (1977b). Enzymology of cancer cells (second of two parts). N. Engl. J. Med. *296*, 541-551.

Weber,G., Hager,J.C., Lui,M.S., Prajda,N., Tzeng,D.Y., Jackson,R.C., Takeda,E., and Eble,J.N. (1981). Biochemical programs of slowly and rapidly growing human colon carcinoma xenografts. Cancer Res. *41*, 854-859.

Wells,P., Gunn,R.N., Alison,M., Steel,C., Golding,M., Ranicar,A.S., Brady,F., Osman,S., Jones,T., and Price,P. (2002). Assessment of proliferation in vivo using 2-[(11)C]thymidine positron emission tomography in advanced intra-abdominal malignancies. Cancer Res. *62*, 5698-5702.

Whiteford,M.H., Whiteford,H.M., Yee,L.F., Ogunbiyi,O.A., Dehdashti,F., Siegel,B.A., Birnbaum,E.H., Fleshman,J.W., Kodner,I.J., and Read,T.E. (2000). Usefulness of FDG-PET scan in the assessment of suspected metastatic or recurrent adenocarcinoma of the colon and rectum. Dis. Colon Rectum *43*, 759-767.

Wiggers,T., Jeekel,J., Arends,J.W., Brinkhorst,A.P., Kluck,H.M., Luyk,C.I., Munting,J.D., Povel,J.A., Rutten,A.P., Volovics,A., and . (1988). No-touch isolation technique in colon cancer: a controlled prospective trial. Br. J. Surg. *75*, 409-415.

261

Williams,C.S., Mann,M., and DuBois,R.N. (1999). The role of cyclooxygenases in inflammation, cancer, and development. Oncogene *18*, 7908-7916.

Wilson IK, Chatterjee S, and Wolf W (1991). Synthesis of 3'-fluoro-3'-deoxythymidine and studies of its 18F-radiolabeling, as a tracer for the non invasive monitoring of the biodistribution of drugs against AIDS. Journal of Fluorine chemistry *55*, 283-289.

Witzig,T.E., Loprinzi,C.L., Gonchoroff,N.J., Reiman,H.M., Cha,S.S., Wieand,H.S., Katzmann,J.A., Paulsen,J.K., and Moertel,C.G. (1991). DNA ploidy and cell kinetic measurements as predictors of recurrence and survival in stages B2 and C colorectal adenocarcinoma. Cancer *68*, 879-888.

Woolmark,N., Piedbois,P., Rougier,P., Buyse,M., Pignon,J.P., Ryan,L., Hansen,R., Zee,B., Weinerman,B., Pater,J., Leichman,C., Macdonald,J., Benedetti,J., Lokich,J., and Fryer,J. (1998). Efficacy of intravenous continuous infusion of fluorouracil compared with bolus administration in advanced colorectal cancer. Meta-analysis Group In Cancer. J. Clin. Oncol. *16*, 301-308.

Wong,W.M., Mandir,N., Goodlad,R.A., Wong,B.C., Garcia,S.B., Lam,S.K., and Wright,N.A. (2002). Histogenesis of human colorectal adenomas and hyperplastic polyps: the role of cell proliferation and crypt fission. Gut *50*, 212-217.

Wright,C.M., Dent,O.F., Barker,M., Newland,R.C., Chapuis,P.H., Bokey,E.L., Young,J.P., Leggett,B.A., Jass,J.R., and Macdonald,G.A. (2000). Prognostic significance of extensive microsatellite instability in sporadic clinicopathological stage C colorectal cancer. Br. J. Surg. *87*, 1197-1202.

Wynder,E.L. and Reddy,B.S. (1974). The epidemiology of cancer of the large bowel. Am. J. Dig. Dis. *19*, 937-946.

Yasuda,S., Ide,M., Fujii,H., Nakahara,T., Mochizuki,Y., Takahashi,W., and Shohtsu,A. (2000). Application of positron emission tomography imaging to cancer screening. Br. J. Cancer *83*, 1607-1611.

Young,H., Baum,R., Cremerius,U., Herholz,K., Hoekstra,O., Lammertsma,A.A., Pruim,J., and Price,P. (1999). Measurement of clinical and subclinical tumour response using [18F]-fluorodeoxyglucose and positron emission tomography: review and 1999 EORTC recommendations. European Organization for Research and Treatment of Cancer (EORTC) PET Study Group. Eur. J. Cancer *35*, 1773-1782.

Zerhouni,E.A., Rutter,C., Hamilton,S.R., Balfe,D.M., Megibow,A.J., Francis,I.R., Moss,A.A., Heiken,J.P., Tempany,C.M., Aisen,A.M., Weinreb,J.C., Gatsonis,C., and McNeil,B.J. (1996). CT and MR imaging in the staging of colorectal carcinoma: report of the Radiology Diagnostic Oncology Group II. Radiology *200*, 443-451.

Zervos,E.E., Badgwell,B.D., Burak,W.E., Jr., Arnold,M.W., and Martin,E.W. (2001). Fluorodeoxyglucose positron emission tomography as an adjunct to carcinoembryonic

antigen in the management of patients with presumed recurrent colorectal cancer and nondiagnostic radiologic workup. Surgery *130*, 636-643.

Zhuang,H., Sinha,P., Pourdehnad,M., Duarte,P.S., Yamamoto,A.J., and Alavi,A. (2000). The role of positron emission tomography with fluorine-18-deoxyglucose in identifying colorectal cancer metastases to liver. Nucl. Med. Commun. *21*, 793-798.